THE INTERACTION OF BONE POROSITY AND CROSS-SECTIONAL GEOMETRY FOR THE CONSERVATION OF BONE STRENGTH

by

Richard Allan Lazenby

B.A. (Hons.), Simon Fraser University, 1981

THESIS SUBMITTED IN PARTIAL FULFILLMENT OF

THE REQUIREMENTS FOR THE DEGREE OF

MASTER OF ARTS

in the Department

of

Archaeology

SIMON FRASER UNIVERSITY

April 1986

APPROVAL

Name: Richard A. Lazenby

Degree: Master of Arts

Title of thesis: The Interaction of Bone Porosity and Cross-Sectional Geometry For The Conservation of Bone Strength

Examining Committee:

Chairman: Prof. P.M. Hobler

Dr. Mark Skinner
Senior Supervisor

Dr. Jack D. Nance

Dr. John M. Gosline
External Examiner
Dept. of Zoology
University of British Columbia

Date Approved: APRIL 17, 1986.

Title of Thesis/Dissertation:

The Interaction of Bone Porosity and Cross-Sectional Geometry for the Conservation of Bone Strength

Author: ______________________

(signature)

Richard Allen Lazenby

(name)

April 23, 1986

(date)

ABSTRACT

The study of bone strength is important in the study of aging populations. This fact is attested to by the great expenditure of time and energy devoted to understanding osteoporosis. Two aspects of morphology underlie the structural strength of bone: its physical properties (especially porosity), and its geometric properties. Few studies have attempted to examine interrelationships between these properties. This study examines whether or not the degree and distribution of cortical bone porosity reflects geometric parameters of femoral cross-sections.

A model stating that strength-reducing porosity should occur to a greater degree in the direction of maximum bending strength is proposed. In keeping with the underlying principles of functional adaptation (implicit in all analyses of bone morphology), it is argued that the interaction between porosity and geometry should result in a more uniform porosity distribution as cross-sections become more circular. The study also examines the contention that continuous periosteal apposition mechanically compensates for endosteal resorption.

Data collected from a series of human femoral cross-sections obtained from subjects of known sex and age are used to test the model. Geometric parameters are estimated using stereological methods and appropriate formulae derived from the literature. Cortical porosity is quantified from radiographs of the same sections using automated image analysis, and is evaluated in the anterior and lateral cortices, relative to the axes of maximum and minimum geometric bending strength. The data are analyzed using bivariate and multivariate statistical techniques.

The results of this study support a model that emphasizes conservation of bone strength. The analysis suggests that the overall degree of cortical porosity is independent of cross-sectional geometry, but that porosity distribution is not. Greater porosity occurs along the axis of maximum geometric resistance to bending. As cross-section geometry approaches

circularity, porosity becomes more equally distributed between axes. Finally, mechanical compensation occurs only in the axial direction of least bending strength, achieved through endosteal resorption and not periosteal apposition as generally accepted.

The results of this study suggest that the processes of internal and external remodeling of human bone do not proceed independently. It is likely that the same ultimate stimulus mediates both processes. The nature of this stimulus is thought to be aspects of the strain environment, in keeping with current theoretical models based on *in vivo* studies of non-human bone.

QUOTATION

A substance like bone, so universally abounding, possessing such great strength, and considerable flexibility, ought to be restored to its proper place in the scale of bodies, applicable to so many purposes in the arts (B. Bevan (1826) On The Strength of Bone *Philosophical Magazine* 68:181)

ACKNOWLEDGEMENTS

This thesis has benefitted greatly through the course of its development from the authors association with many people. They are to be thanked for their candour in sharing comments and criticisms with regard to ideas expressed herein. I would like to thank my committee, Dr. Mark Skinner and Dr. Jack Nance. They were placed in the difficult position of supervising a thesis topic of a very esoteric nature for an archaeology department, and were able to provide cogent and timely advice. Their efforts are truely appreciated. I am especially pleased to have had Dr. John Gosline, Department of Zoology, University of British Columbia, serve as External Examiner.

Many individuals contributed materially to this work. Radiographs were prepared through the kind assistance of Les Josza and technicians at Forintek, Inc., Vancouver; and the automated image analysis system was provided by Infrascan, Inc., Richmond, for which I thank Les Hooten and Brian Vanderlinden. I would also like to acknowledge Dr. K. Donnelly, Department of Anatomy, University of British Columbia for his assistance in sample collection. Others who have contributed directly or indirectly include Dr. Bill Cave, Royal Columbian Hospital; Dr. Susan Pfieffer, University of Guelph; and Dr. David Burr, West Virginia University. My sincere thanks to them all.

A number of people have made my tenure at Simon Fraser more than just a learning experience. Ingrid Bell deservedly achieves eminent status on the Acknowledgement page of most, if not all, archaeology theses. She is truely surrogate mother to us all. I also thank my fellow graduate students, in particular Joanna Casey, Dr. Gerry Conaty, Larry Titus, Brian Chisholm and Dorothy Godfrey-Smith, for providing diversians (academic and otherwise), and for reminding me that not all anthropology is physical.

Two individuals deserve special credit. In the course of my nine years as an undergraduate and graduate student, Mark Skinner has become more than an academic supervisor. It is a privilage for me that we have become personal friends as well as colleagues over this time. Finally, I thank my wife Joanna Casey, a scholar in her own right who has saved me more than once from the perils of pomposity. Without her indulgence, this thesis would have been a much more difficult exercise.

TABLE OF CONTENTS

Approval ii

Abstract iii

Quotation v

Acknowledgements vi

List of Tables x

List of Figures xi

I. Introduction 1

Introductory Remarks 1

Aim and Scope of the Research 1

II. Functionally Adaptive Remodeling 9

Functional Adaptation and Wolff's Law 9

Remodeling: Cellular Mechanisms and Theoretical Models 10

Integrating Internal and External Remodeling 20

Summary 23

III. Remodeling in Biological Context 25

Introduction 25

Biomechanical Referents and Norms 25

Geometric, Physical and Material Properties 39

Age, Sex and Side Factors 46

Summary 58

IV. The Interaction of Geometry and Porosity: Hypotheses 59

Introduction 59

Functional Strain and Remodeling 60

A Conservancy Model for Geometry/Porosity Interaction 63

V. Materials and Methods 69

Sample Collection and Preparation 69

Data Collection 74

VI. Results and Discussion 91

Results 91

Discussion 109

VII. Summary and Conclusion 117

Appendix I 120

Appendix II 121

References Cited 125

LIST OF TABLES

Table | Page

1 Technical Elastic Moduli for Compact Bone. 32

2 Orientation Differences in Human Bone Strength. 46

3 Aging Bone Loss in Different Populations. 50

4 Age-Related Increase in Cortical Bone Parameters. 55

5 Geometric Variables Used in This Study. 86

6 The Data Set for This Study. 92

7 Pearson Product-Moment Correlation Matrix: All Variables. 94

8 Quartimax Rotated Factor Matrix. 99

9 Cortical Thickness and Moment Arm (mm); Ratios - Age-Ranked. 105

10 Correlation and Significance For Apparent Density Versus Age. 106

LIST OF FIGURES

Figure		Page
1	Remodeling of long bones by the V-Principle.	13
2	Remodeling by the Flexure-Drift tenet.	15
3	Characteristic cross-section of human bone showing variation in microstructure.	17
4	Models of the bone turnover system.	22
5	Forces and their resulting deformations.	27
6	A generalized stress-strain curve.	29
7	Stress distribution in three-point bending.	37
8	The relationship of cross-sectional shape to predominant bending force direction.	40
9	The relationship between section shape and the area moment of inertia.	42
10	Primary orientations in a long bone.	45
11	Scenarios for porosity/geometry interaction.	66
12	Section location and block technique for removal.	72
13	Locating the section centroid by point-count technique.	77
14	A typical cross-section depicting reference and principal moment axes.	80
15	The relationship of area and polar moment axes.	82
16	Geometric variables used in this study.	85
17	Quartimax rotated factor axes.	101
18	A scatterplot of porosity and moment ratios.	103
19	Scattergrams of apparent density versus age.	107
20	TMRX and CTX versus AGE in logarithmic space.	110
21	The primary results of this study.	113

CHAPTER I

INTRODUCTION

> It is not the shape either of the body or its parts, which gives rise to the habits of animals and their mode of life; but it is, on the contrary, the habits, mode of life, and all the other influences of the environment, which have in course of time built up the shape of the body and of the parts of animals [Lamarck, 1809, *Philosophie Zoologique* cited in Gould 1985:17].

Introductory Remarks

The ability of physical anthropologists to provide valid interpretations of morphological variability in human skeletal populations is ultimately determined by their understanding of bone biology. This requires a fundamental comprehension of normal and pathological growth, development and remodeling variability of bone as a tissue; and of individual bones as elements in a skeletal system. Furthermore, bone tissue must be interpreted as an adaptation to a complex physical, behavioral and cultural environment. Such an understanding of bone biology would integrate the several levels of bone tissue organization, from the molecular level to the complete element (and ultimately to the whole skeleton or even population) with the metabolic and structural functions performed by bone tissue.

Aim and Scope of the Research

This thesis reports the results of an investigation into the relationship between two specific aspects of bone structure and function. These are the cross-sectional geometry of the human femur and its internal remodeling dynamics. A bone's cross-sectional geometry specifies the two-dimensional distribution of matrix perpendicular to its longitudinal neutral axis (Ruff and Hayes 1983a; Martin and Atkinson 1977). Internal remodeling refers to the removal and replacement of small volumes of bone substance within the cortex, producing secondary osteons (Currey 1982b), or Haversian systems. This internal remodeling process is quite distinct from external remodeling, both conceptually (Cowin 1981, 1983; Currey 1984b) and possibly in terms of the sequence of events which comprise the process (O'Conner et al. 1982). Frost (1964, 1976a, 1980) and Jaworski (1984) have in the past distinguished the two as remodeling (internal) and modeling (external). Recently, Frost (1985) has refined (or at least made more explicit) the distinction between the two processes. Modeling is limited to organismic growth, and remodeling distinguishes all bone turnover which occurs after the skeleton has 'matured'. This convention will be followed in this thesis.

The vertebrate skeleton serves two purposes. First, it is the major reservoir for calcium and phosphorus in the body (Bronner 1982). Approximately 98–99% of total body calcium (Chestnut et al. 1973) and 80–90% of phosphorus (Fleisch 1980; Dabek et al. 1977) is retained in bone as hydroxyapatite. Actual serum concentrations of these minerals available for metabolic work are low. According to Neuman (1980:85) the normal concentration for free ionic calcium in serum is 1.25 mM (milliMoles) "irrespective of species, time of day, diet, sex or persuasion". (Vaughn (1976:124), however, notes that there "are considerable diurnal variations in any one individual".) The relative invariance in the concentration of calcium is understandable considering its multifunctional role in normal physiology: in muscle contraction, nerve conduction, synaptic transmission, hormonal response, and various secretory processes (Neuman 1980). Plasma phosphate concentration, on the other hand, is highly variable between individuals and species. It is highest in certain fishes and lowest in adult humans; and is known to follow a definite circadian rhythm (Fleisch 1980; Dabek et al. 1977).

The second function of the skeleton is to provide the structural framework within which organs are protected and supported, and against which muscles act synergistically and antagonistically to provide a characteristic range of locomotory and manipulatory versatility. The ability of individual bones to fulfill this latter purpose is termed 'mechanical competence'. Ultimately, mechanical competence will be a function of the geometric, material and physical properties of bone. Geometric properties derive from size and shape, whereas physical properties are determined primarily by the mineral density and porosity of the cortex (Burr 1980; Currey 1969a, 1975, 1984c). Material properties, on the other hand, are in part extrinsic to the bone. For any given bone type (e.g., Haversian, circumferential lamellar) these properties are determined by characteristics of the particular loading situation to which the bone (or specimen) is subjected. Examples of material properties include 'stiffness', 'ultimate strain' and others. Factors such as load direction and magnitude, and the rate (i.e., fast or slow) and frequency (i.e., static/dynamic; continuous/intermittent) of load application, all affect the material strength of the specimen (Nordin and Frankel 1980). The success of the interaction among these extrinsic and intrinsic properties may be considered in relation to the normal conditions of life under which the bone is expected to perform (Currey 1981a). In actuality, mechanical competence is viewed in terms of bone strength (which simply defined is the amount of force per unit area required to cause the specimen to fail), as well as in terms of resistance to deformation (Currey 1984e).

In the last two decades a considerable volume of work has been published which describes the behavior both of whole bones and bone samples under various mechanical testing conditions (reviewed by Welch 1970; Currey 1970, 1981b, 1984e; Evans 1973, 1976, 1980; Reilly and Burstein 1974; Burr 1980). Several researchers have examined the relationship of material strength to variation in bone structure at the microscopic level (e.g., Carter et al. 1976; Saha and Hayes 1977; Carter and Hayes 1977; Carter and Spengler 1978) and at the submicroscopic, or ultrastructural, level (e.g., Evans and Vincentelli 1969; Vincentelli and Evans 1971; Currey 1969a,b, 1975, 1984c; Minns et al. 1983). Variables such as the proportion and distribution of secondary osteons; the arrangement of the collagen fraction of matrix within osteons (relative to the long axis of the bone); and the degree of mineralization of the tissue have been considered. These studies were concerned primarily with the material and physical property components of bone strength.

On the other hand, relatively few studies have investigated quantitatively the contribution of geometric properties to overall mechanical competence. Martin and Atkinson (1977) investigated age-related changes in the cross-sectional geometry of male and female femora in light of recognized age-deterioration in the physical properties of bone (Mazess 1982). They found that a geometric compensation occurred only in males, and suggested that this was one reason why aged women were more at risk to bone failure than males. Lovejoy et al. (1976) analyzed cross-sectional geometry as an indicator of relative bone strength. Their study was motivated by a desire to find a technique which would permit reliable assessment of archaeological and fossil bone strength, which could not be achieved using direct mechanical testing procedures, since the latter are appropriate only for fresh bone (Kimura and Takahashi 1982). Lovejoy et al. (1976) assumed a constant stress and normalized their data for bone size. Under these conditions cross-sectional geometry could be considered an indirect measure of relative bone strength. As a test case, a sample of platycnemic and eurycnemic tibiae were compared. Their results showed platycnemic tibiae to have greater antero-posterior bending strength, as well as greater torsional strength; eurycnemic tibiae have greater medio-lateral bending strength. Cortical areas in both cases were not significantly different, leading to the conclusion that the shape variation in these tibiae reflected qualitatively different adaptive mechanical histories: "the eurycnemic tibia is more equally adapted to all-strain inducing modes" (Lovejoy et al. 1976:505).

One reason why such studies have been lacking is the great amount of time which must be invested in order to quantify the geometry of irregularly-shaped bone sections (Martin 1975; Ruff and Hayes 1983a). Consequently, studies have been restricted to very small samples. Recently, however, computer programs have been written which are able to estimate these properties with a high degree of accuracy and precision. Programs such as SLICE (Nagurka and Hayes 1980) have proven useful in analyses of cross-sectional geometric variability in several prehistoric populations, leading to inferences regarding both behavioral and subsistence activities (Ruff and Hayes 1983a,b; Ruff et al. 1984; Brock 1985). These studies did not, however, relate observed geometric variation to physical properties of the bone, nor to any relative measure of material strength.

Ruff and Hayes (1984a,b) have also investigated the relationship between cross-sectional geometry and bone mineral content, measured at five equi-distant locations in femoral and tibial diaphyses, and at the femoral neck, using photon absorptiometry. They found that variation in **bone** density was determined primarily by bone volume at the sampling site, with actual **mineral** density accounting for relatively little variation. They concluded that "the most critical age-related changes in the skeleton may be those that occur in bone geometry" (Ruff and Hayes 1984a:1030). A similar conclusion was reached by Hoyer et al. (1983) who characterized remodeling frequency and endosteal expansion of the femoral cortex with age. Recently, a study of archaeological tibiae from Alaskan Eskimo groups (Martin et al. 1985), related cross-sectional geometric variation to bone mineral content using photon absorptiometry. Again, the observed age and sex differences were interpreted in terms of behavioral variation within the groups studied, with the female sample showing evidence of greater sedentary behavior than males.

Several studies by Lanyon and associates over the past few years (Lanyon et al. 1979, 1982; Lanyon and Rubin 1980; O'Conner et al. 1982; Lanyon 1984) have considered limited aspects of geometry (i.e., areas) in their investigation of the *in vivo* remodeling response of bone from various non-human animals exposed to altered mechanical environments. Bone area increased in full compensation for the experimentally-imposed increased load. Similar studies are those of Simon et al. (1984, 1985a-c) who exposed rats to hypergravic environments. They found that the increased load created by centrifugation (producing up to a 100 per cent body weight increase) enhanced limb bone growth and bone mineral content in normal and hypophysectomized rats. That is, both geometric and physical properties responded positively when subjected to increased mechanical load.

A question which has not been adequately addressed is how internal remodeling processes, particularly the development of intracortical porosity, relate to specific geometric properties of bone cross-sections. Both have been shown to affect bone strength, but in opposite ways. Geometric changes act to enhance the mechanical competence of bones (e.g., Martin and Atkinson 1977; Lanyon 1984). Numerous studies have shown that Haversian remodeling and increased porosity act to reduce bone strength (Carter and Hayes 1977; Saha and Hayes 1977; Currey 1981a, 1984c; Martin 1984). The decreased mechanical competence of bone as a result of internal remodeling has been reported in both human (Reilly and Burstein 1974) and non-human (mainly cow) bone (Katz et al. 1984; Lanyon et al. 1979; Currey 1975; Lipson and Katz 1984).

The aim of the present study is to investigate the relationship between bone cross-sectional geometry and the development of intracortical porosity. a product of Haversian remodeling. Such a study is of interest for two reasons. First, porosity is the most significant physical property of bone, as mineral density has been shown to be more or less constant through life (Wall et al. 1979; Ruff and Hayes 1984b). Second, of the three components which comprise mechanical competence, only geometric and physical properties vary significantly. Material properties have been shown to be more of less constant across species of similar and vastly different body sizes (Rubin 1984; Rubin and Lanyon 1984; Biewener 1982). Bone of the same histological character from different mammals behaves similarly when tested (i.e., loaded) in a similar way.

The manner in which geometric properties vary will be a function of external remodeling of the bone (Cowin 1983). Removing or adding bone at either the periosteal or endosteal surfaces will result in a change in cross-sectional shape. In humans, the most rapid changes in bone geometry occur during growth (Enlow 1976), as would be expected. Throughout adulthood, however, cross-sectional geometry (e.g., in femora) continues to change, albeit slowly. This occurs as a result of a continuous apposition of bone on the periosteal surface coupled with a progressive involution of bone endosteally (Ruff and Hayes 1983b; Ericksen 1979; Garn et al. 1967; 1968; Garn and Shaw 1976; Martin and Atkinson 1977). These changes produce increased diameters of both the medullary cavity and periosteal margin.

Variation in the physical properties of bone with increasing age has also been reported. Although an optimal mineral density (Currey 1969a,b; 1984a) is more or less maintained throughout life (Ruff and Hayes 1984a,b; Wall et al. 1979), considerable topographic variation in mineral density and porosity exists within bones (Martin and Burr 1984, Martin 1984; Atkinson 1969; Atkinson and Weatherell 1967). From a purely clinical perspective, the most significant age-related alteration of the physical properties of bones occurs through the net bone loss associated with osteoporosis. Primary osteoporosis, both Type I (post-menopausal) and Type II (senile) (Sutton and Cameron 1985) is manifested as medullary involution and increased porosity, particularly of the endosteal cortex. It is characteristic of women beyond the age of 45 and men over 65 (Mazess 1982).

Cowin (1983) has suggested that changes in bone geometry can occur independent of changes in 'bulk density' (a measure of mineralization and porosity). A recent study by Martin and Burr (1984) found, however, that the distribution of porosity in the cortices of several limb bones was not random. They evaluated porosity by point-counting at each of eight microscope fields equally spaced around both the periosteal and endosteal margins of cross-sections of femur, tibia, humerus, radius and second metacarpal. Their results suggested that areas of bone perpendicular to the axis of predominant bending were more porous than areas occurring along this axis. This non-uniform distribution of porosity produced up to an 18 per cent increase in bone stiffness relative to that calculated for a uniform porosity distribution. The broad implication is that internal remodeling does not occur independently of external remodeling. The alteration of the physical properties of a bone should occur with particular regard to previous geometric remodeling activity.

The specific goal of this thesis is to investigate further the relationship of cross-sectional geometry and remodeling, with particular regard to the net bone volume loss associated with aging, that is, increased intracortical porosity and endosteal resorption. A theoretical relationship which implicates internal and external remodeling as separate, yet interrelated, processes having a common goal must be established before specific hypotheses can be formulated. This is developed in the following chapter.

CHAPTER II

FUNCTIONALLY ADAPTIVE REMODELING

Functional Adaptation and Wolff's Law

Adaptation is the central theme in the natural history of all living things. Diminished performance (maladaptation) results in decreased net reproductive success. A traditional approach to understanding adaptation in the analysis of prehistoric fossil forms has been through the study of form-function relationships; that is, functional adaptation. Regardless of whether the perspective brought to the analysis is phylogenetic or ontogenetic (Oxnard 1975), paleobiologists agree that morphology can be related directly to the manner of use. As defined by Cowin

> Functional adaptation is the term used to describe the ability of organisms to increase their capacity to accomplish their function with increased demand and to decrease their capacity with lesser demand [Cowin 1983:275].

In other words, functional adaptation refers to the fit of a thing for its use, with the capacity to modify structure in light of modified need.

The concept of functional adaptation in biological systems was developed explicitly by Roux (1880, cited in Roesler 1981). Applied to skeletal structure, functional adaptation is implicit in the work of Bell (1834), Ward (1838), Ludwig (1852) and Meyer (1867)(all cited in Treharne 1981). It was not explicitly formulated, however, until Julius Wolff published his Law of Bone Transformation in the late nineteeth century (Roesler 1981). Keith (1919, cited in Treharne 1981) has translated Wolff's Law (as it came to be known) thusly: "Every change in the ... function of a bone ... is followed by certain definite changes in ... internal architecture and external comformation in accordance with mathematical laws" (Treharne 1981:35). Implied within Wolff's Law is the premise that an optimal distribution of bone material with respect to its function is achieved with a minimum of material.

Wolff formulated his law of bone transformation with specific reference to the architecture of the trabecular bone of the human proximal femur. Trabecular orientation was seen to correspond to the principal stress trajectories operating within this region. Although Roesler (1981) has identified several inconsistencies underlying Wolff's formulation, the general tenets of the law remain valid (Hayes and Snyder 1981; Takahashi 1982; Woo 1981). That is, the form and distribution of bone should provide maximum utility per unit quantity, relative to the normal demands placed upon the bone. Furthermore, Wolff's Law not only applies to trabecular bone, but to cortical bone as well - the "external conformation" in Keith's translation quoted above.

Wolff's Law describes the processes of remodeling as homeostatic responses. Inasmuch as they determine the geometric and physical properties of a bone, these processes are able to respond to any destabilizing input (e.g., altered function) which reduces the mechanical competence of the existing configuration of properties. This is accomplished by modifying the distribution of bone quantity and quality (Lanyon 1984; Rubin 1984; Hart et al. 1984; Jaworski 1981). The outcome of the response is functional adaptation. Should survival and reproduction rest upon the outcome, the success of the response would be determined by natural selection (Currey 1981a).

Remodeling: Cellular Mechanisms and Theoretical Models

Alteration in the form of a substance can only be produced by the removal of some quantity at point A and the addition of some (not necessarily equal) quantity at point B, where A and B are topographically distinct (Saunders 1985). In bone, this result is achieved through the processes of resorption and deposition.

In bone remodeling, resorption is carried out by a population of multinucleated cells called osteoclasts, and deposition by mononucleated osteoblasts (though Ries et al. (1985) argue for the existence of multinucleate osteoblast-like cells whose small size and orientation account for their having gone previously undetected). Both processes are surface phenomena, and may occur on any of the four surfaces - periosteal, endosteal, trabecular or Haversian - defined for bone (Frost 1980, 1985).

Though identical cellular mechanisms operate in both internal and external remodeling, the two processes do differ. Topographically, external remodeling is restricted to the periosteal, endosteal and trabecular surfaces; while internal remodeling takes place within bone cortex resulting in the production of new Haversian systems. In Haversian remodeling, the sequence of cellular events is activation, followed by resorption, then by formation (Frost 1980, 1985; Jaworski 1981). The sequence is preceded by a period of cellular quiescence; and the resorptive and depositional phases are interrupted by a reversal event which witnesses smoothing over of the rough erosion surface with an inorganically rich cement (Parfitt 1984a). On the other hand, external remodeling may result from the complete sequence as listed; activation and resorption alone; or activation and formation alone (Frost 1980). The occurrence of one phase in the absence of the counterpart constitutes a cortical drift (Frost 1980, 1982, 1985).

The effect of external remodeling is to change the shape and size of the cortical and trabecular architecture, while at the same time conserving mass, whereas Haversian remodeling alters mass without outwardly effecting changes in size and shape (Cowin 1981; 1983). In reality, with increasing age, external remodeling is accompanied by a net bone volume loss due to a large negative bone balance at the endosteal and trabecular surfaces (Frost 1980). Bone balance refers to the sum of the resorptive and depositional events, considered in volumetric terms. When more bone is resorbed overall (or at any given site), a negative bone balance exists for the bone (or site) in question. By logical extension, zero and positive bone balance refer to equal and greater net depositional activity, respectively. A fuller discussion of these processes is found in Chapter Three.

External Remodeling

External remodeling is particularly characteristic of the growing skeleton (Frost 1980, 1982), since with allometric growth the mechanical arrangement of bones to one another, to adhering muscles and other tissues, and to the external environment, demands continual alteration of bone size and shape in order to maintain an optimal design for the whole system. Two fundamental principles of bone remodeling account for the changes that occur during growth (Saunders 1985). These are the V-principle (Enlow 1976), descriptive of bone elongation; and the Flexure-Drift tenet (Frost 1964, 1980, 1982) by which bones may alter shape and position relative to their mechanical arrangement.

The V-principle operates in all cases where elongation of a bone occurs as a result of the activity of one (or two) endochondral growth plates. Examples are the long and short bones, such as femur, tibia and metacarpals. With length increase, bone material which comprises the wide metaphyseal ends must be 'relocated' into the narrower diaphysis. This entails localized resorption periosteally accompanied by deposition endosteally (Figure 1). In this manner, bone size increases while shape is preserved (Enlow 1976). However, the maintenence of shape with size increase is precluded if the optimal design of the musculo-skeletal system is compromised. In such cases the bone must change shape and/or be repositioned. Such alterations are achieved through cortical drift.

When any substance is bent, compressed or pulled, the various surfaces change in a manner that can be described in terms of increasing or decreasing concavity (or convexity). Given this observation, Frost (1964, 1980, 1982) proposed that bone resorption and deposition occur in response to "repeated non-trivial and uniformly oriented flexural strains", the consequence of which is that "all bone surfaces drift toward the direction of increasing concavity as flexural strain develops" (Frost 1980:220). In other words, should the characteristic loading situation of any element be altered, either through growth or function,

Figure 1.
Remodeling of long bones by the V–Principle.
Arrows indicate direction of surface movement which produces size increase.
(From D. Enlow (1976), used with permission.)

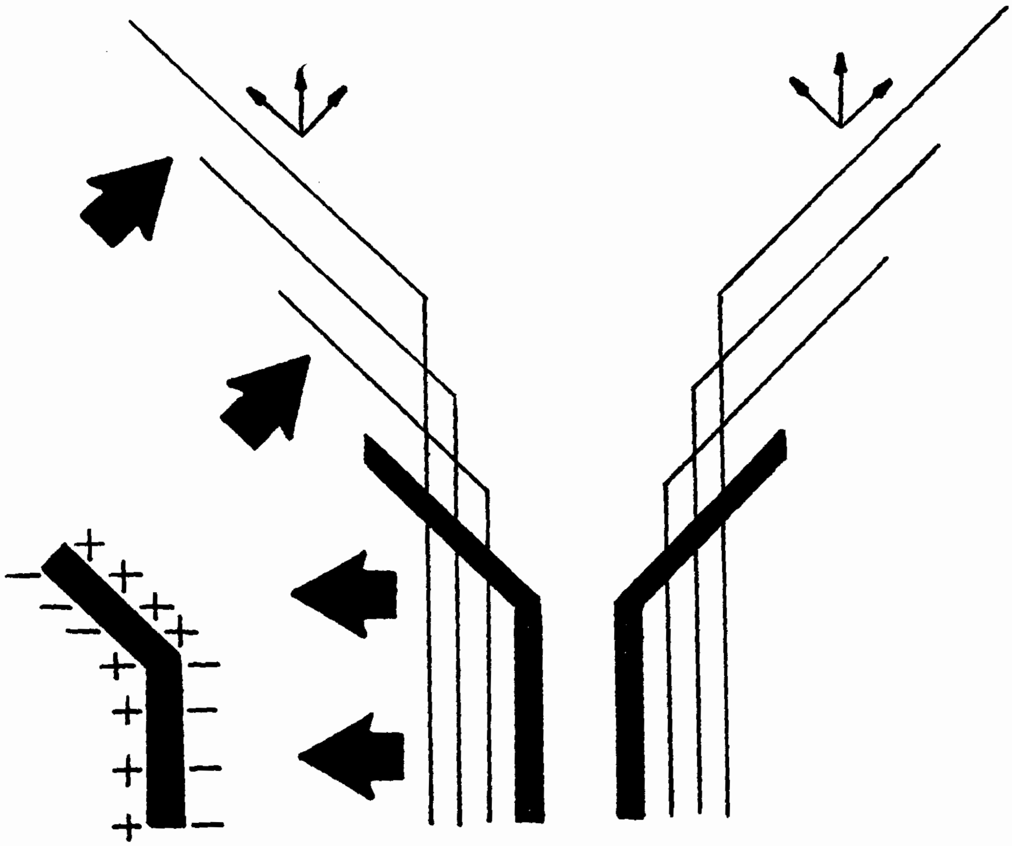

+ = deposition

− = resorption

such that the element is repeatedly deformed in a new, albeit consistent manner, remodeling will ensue with the aim of altering bone shape so as to minimize future similar deformations. Bone will be deposited upon concave surfaces and resorbed from convex surfaces (Figure 2).

Currey (1968, 1984e, and in Wainwright et al. 1976) has observed that Frost's model, while appearing to describe accurately the process of external remodeling, fails to do so if the bone is loaded in **net** compression or **net** tension. That is, both compressive and tensile surfaces must exist as a result of the deforming event for Frost's model to operate. In response to this difficulty, Currey has suggested that appropriate cell systems do not respond so much to changes in surface curvature as to gradients of compression measured at increasing distance from the bone surface. With increasing depth, compression increases if the surface becomes more convex, and decreases if it becomes more concave. Currey argues that the in situ osteocyte network and nerves contained within anastomosing Haversian systems would provide a method of transmitting this information to the appropriate cell systems, and of directing remodeling events. (Regarding the probability of a bony structure coming under net tension, refer to Oxnard (1971) who discusses the unlikelihood of this event; and to recent work by Hayes and Snyder (1981) who provide some experimental/theoretical evidence for the existence of net tension in the human patella. Currey (1984e:141–2) discusses this subject at length.)

Internal Remodeling

Following growth cessation, fully 95% of bone turnover is a consequence of internal remodeling activity (Frost 1980). This involves the removal and replacement of a discrete volume of bone within existing cortex, resulting in the production of Haversian systems (otherwise known as secondary osteons) (Currey 1982a). Katz has aptly defined the Haversian system as

Figure 2.
Remodeling by the Flexure-Drift tenet.

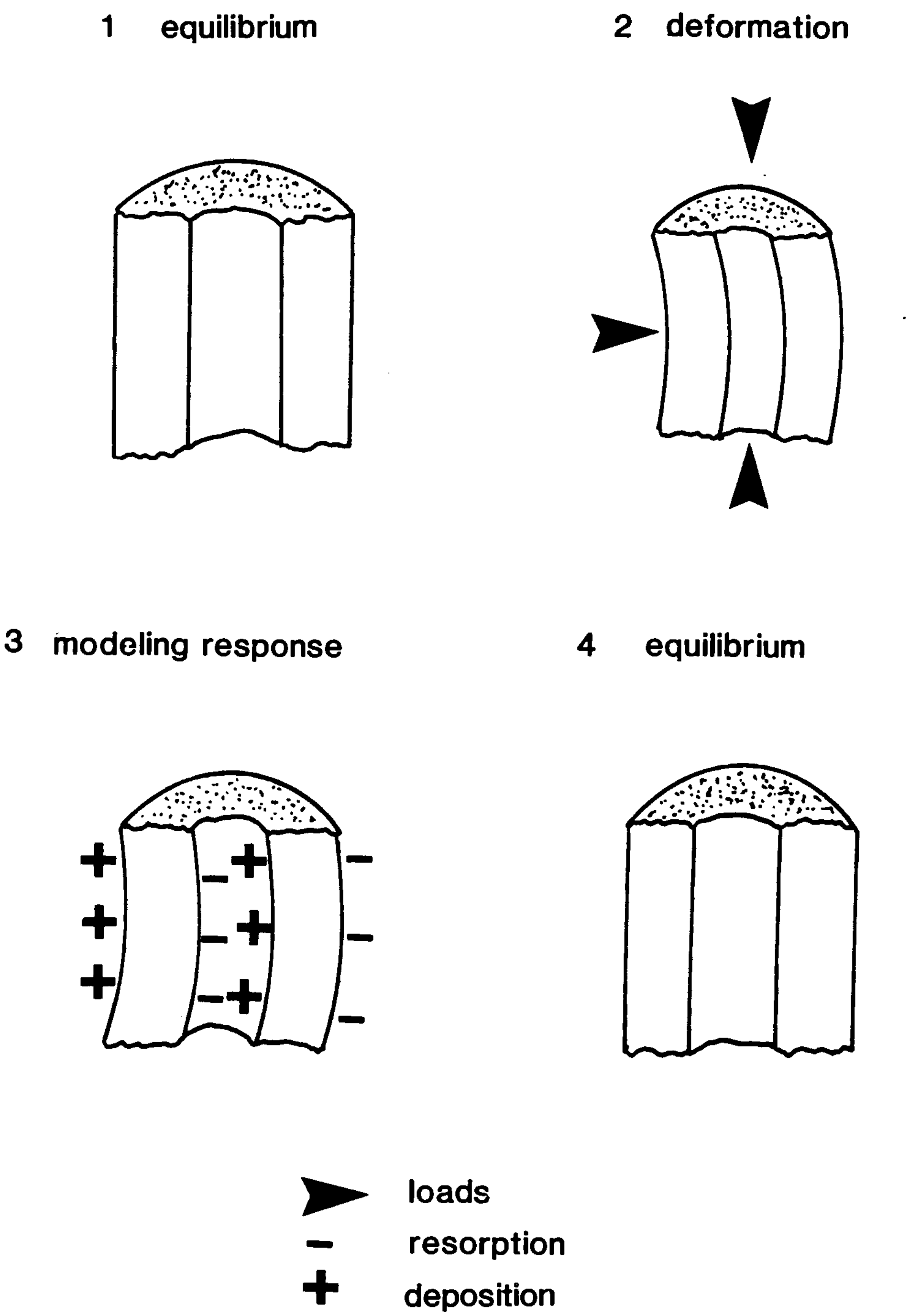
1 equilibrium
2 deformation
3 modeling response
4 equilibrium
loads
resorption
deposition

> a nearly cylindrical body, generally coursing almost parallel with the long axis of the bone, comprised of concentric lamellae about a central vascular canal (Haversian canal) demarked by a clear external boundary (cement line) [Katz 1981:173].

Haversian remodeling activity creates a characteristic picture of bone cortex when viewed microscopically in cross-section (Figure 3). In that the process is progressive with age (Currey 1964; Jowsey 1966, 1968; Enlow 1962a,b, 1966, 1976; Burr 1980; Kerley 1965; Singh and Gunberg 1970; Ahlqvist and Damsten 1969; Thompson 1979; Hoyer et al. 1983) the microscopic picture changes from few secondary osteons surrounded by primary circumferential lamellar bone characteristic of young children, to the almost totally remodeled adult cortex which sees whole secondary osteons surrounded by fragments of previously remodeled bone.

Various explanations for the existence and function of Haversian systems have been proposed. The idea that bone microstructure could be classified along a scale from primitive to advanced, and subsequently be used as taxonomic criteria for fossil forms, can be found in some early work (Quekett 1849; Foote 1916; Crawford 1940). Following 'The Great Chain of Being', human Haversian bone with its regular and highly organized cellular structure qualified as the advanced form, with lower orders showing progressively less organization of microscopic minutiae. Crawford, in fact, attempted to apply the Biogenetic Law to bone structure:

> During development of the mammalian long bones there are stages in which the arrangement of cells is directly comparable with that found in the adults of more primitive species [Crawford 1940:296].

Considerable differences in the microstructural appearance of bone from different organisms (e.g., fish to mammal) do exist (Enlow and Brown 1956, 1957, 1958). The differences, however, are with respect to the arrangement of certain fundamental components (such as circumferential and concentric lamellae, osteocytes and primary osteons) and not to a scale of developmental complexity within individual components (Enlow and Brown 1958).

Figure 3.
Characteristic cross-section of human bone showing variation in microstructure.

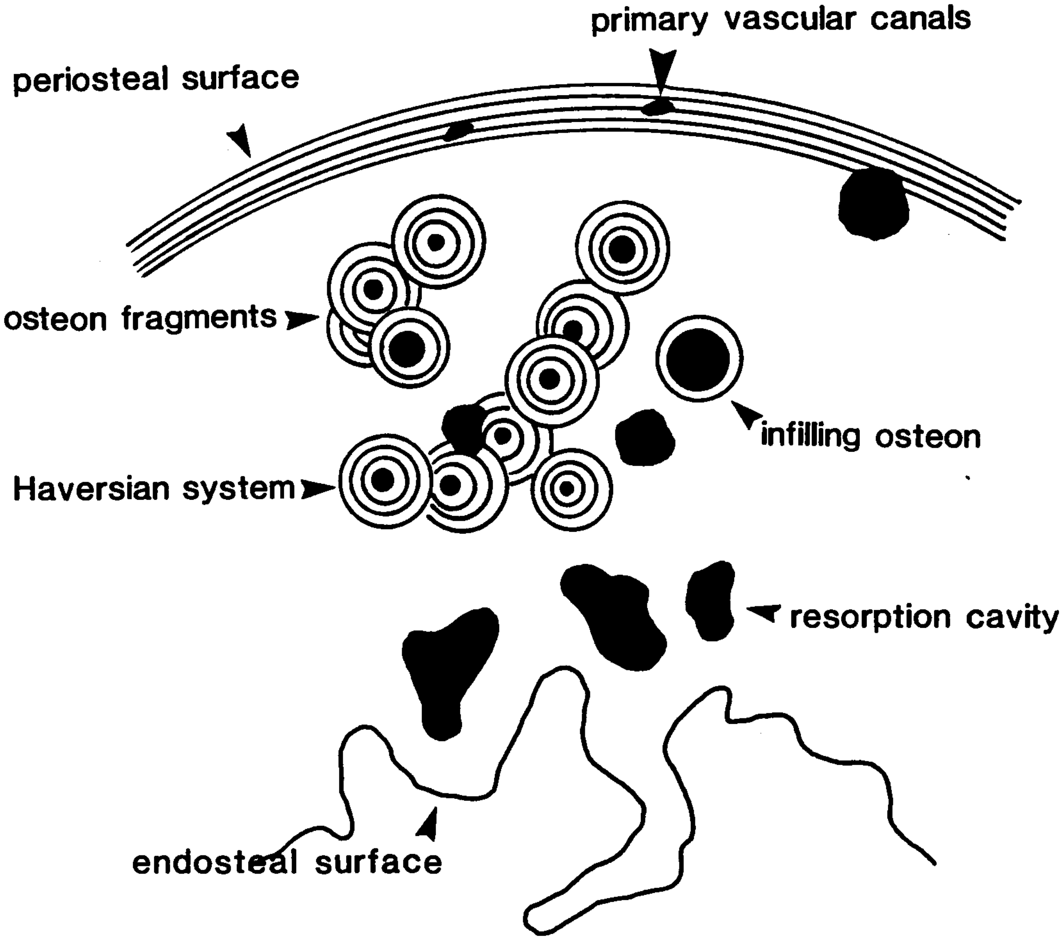

NB. DARK AREAS REPRESENT POROSITY

At present there are two contending, though not necessarily mutually exclusive, bodies of theory which attempt to provide a functional explanation for Haversian remodeling. These are: (1) mechanically-based models, in which remodeling has been viewed as either enhancing bone strength and/or repairing bone damage; and (2) physiologically-based models, in which Haversian remodeling is directed towards mineral homeostasis.

The idea that Haversian remodeling serves to enhance bone strength (e.g., Gebhardt 1901-1906, cited in Amprino 1948) has generally fallen into disfavour, since a large body of experimental work has demonstrated the mechanical inferiority of remodeled compared to primary compact bone. Hert et al. (1965) have shown bovine Haversian bone to be weaker in axial, radial and tangential compression. Currey (1959), Evans and Bang (1967), Evans (1976, 1980), Saha and Hayes (1977) and Vincentelli and Grigorov (1985) have demonstrated decreased tensile strength (in static and/or impact loading) for human/bovine remodeled bone when compared to primary lamellar/plexiform bone. Katz et al. (1984) and Lipson and Katz (1984), using ultrasonic wave velocity, have shown bovine plexiform bone to possess elastic properties superior to that of Haversian bone in all three orthogonal directions. Prior to these studies, Amprino's (1948) observation that the replacement of primary tissue by Haversian systems within the ossified tendons of birds created a structure "less resistent on the whole to traction" (p. 298) lead him to propose that osteonal remodeling served first and foremost to mobilize mineral salts (i.e., calcium) for metabolic work. Amprino (1967) further argues this point, citing some of the experimental data referred to above, as do Amtmann and Doden (1981) more recently. This 'metabolic function' argument is not supported by Schaffler and Burr's (1984) examination of the per cent distribution of Haversian bone in femoral mid-shaft cross-sections of several species of primates, including man. In spite of the fact that no significant differences in calcium metabolism exist between primate species studied, significant differences in per cent osteonal bone were found, which Shaffler and Burr argue reflects locomotory behavior (i.e., arboreal and terrestrial quadrupedality, suspension, bipedality).

The most widely accepted mechanically-based theory for the existence of Haversian remodeling suggests that osteons serve to repair and replace damaged and necrotic bone tissue (Enlow 1962b, 1976; Currey 1962, 1964; Martin and Burr 1982; Burr et al. 1985; Carter and Hayes 1977; Carter and Spengler 1978; Lipson and Katz 1984) with the effect of increasing the fatigue life of the bone. Fatigue is taken to be the decrease in strength associated with repetitive loading (Carter and Hayes 1976; Carter and Spengler 1978; Nordin and Frankel 1980), and is likely the most significant cause of bone failure under physiological conditions. Fatigue life is simply the time elapsed between onset of the cyclic loading situation and failure of the element, the value of which will be a function of load magnitude and frequency as well as the bone's physical properties. It is generally believed that Haversian remodeling extends the fatigue life of bone in two ways. The first is by repairing accumulated microscopic damage within the cortex (e.g., microcracks (Frost 1960) and debonded osteons which have slipped in position along their cementline interface) or by replacing tissue necrotized through local osteocyte death. Secondly, the circular shape of osteons permits them to act as 'crackstoppers'. Microcrack propagation will tend to follow cement lines and lamellar boundaries along the tensile side of a strained element (Martin and Burr 1982) and it has been suggested that the concentric organization of Haversian lamellae acts to limit the progression of an initial microcrack (Currey 1962; Saha and Hayes 1977; Martin and Burr 1982). Extending fatigue life through Haversian remodeling is considerably more efficient metabolically than the alternative of dramatically increasing cross-sectional area (i.e., bone thickness) (Lipson and Katz 1984).

It should be noted that mechanically- and metabolically-based theories for Haversian remodeling are likely not mutually exclusive (Ascenzi 1980). *In vivo* experiments involving dynamic loading of sheep radii (Lanyon et al. 1982) witnessed rapid remodeling of **newly deposited** lamellar bone on the caudal surface. This remodeling occurred at a rate too rapid for the sole causal factor to have been fatigue microdamage, and the authors suggest that a metabolic factor may have been involved (though see Burr et al. (1985) who suggest that fatigue alone could well have produced the observed repair). Furthermore, in that as much as fifty per cent of plasma calcium is skeletally-derived (Bronner 1982), the responsibilites of bone resorption (primarily) and deposition in conjunction with intestinal uptake and nephritic output cannot be ignored. It is possible that Haversian remodeling is activated in the main by mechanical considerations under normal circumstances, while the calcium net bone balance may in part be regulated by metabolic requirements. This interplay is suggested in Jaworski's (1981, 1984) Lamellar Bone Turnover System where the spatial organization of Haversian systems is mechanically controlled, while bone balance is metabolically regulated. This would produce characteristic patterns of remodeling consistent with particular loading situations (cf. Schaffler and Burr's (1984) correlation of 'per cent remodeled bone' with locomotory behavior) with the possibility of regulating remodeling rate (i.e., the duration of the resorptive and depositional phases) vis-à-vis the metabolic state of the individual at that particular point in time.

Integrating Internal and External Remodeling

Whether one is studying internal or external remodeling phenomena in bone, the same cell system is being considered. Since it is difficult to imagine separate control systems operating at the cellular level (Frost 1985), it would be reasonable to presume that the two processes do not proceed independently. At both the gross and microscopic level it should be possible to derive continuum models for bone morphology.

Cowin (1981, 1983, 1984) views bone form as the product of two interrelated remodeling systems: (1) a global, or whole bone level system and (2) a local, or bone tissue level system. Both systems possess three similar components: (1) a control surface, to which the bone cells are directed and upon which they operate, and at which the initial stimulus is measured; (2) the state of stress at, or the mechanical forces acting upon, the control surface, and (3) the matter which flows across the control surface, the result of which is either a build-up or break-down of the bone's organic and inorganic constituents. For modeling purposes, at the local level a control surface can be defined as any point in the bone, and the sum of all tissue level systems equals the global level system. The two systems are related by the theory of elasticity, under the assumption of linear elasticity. (This and other concepts introduced above are discussed in detail in Chapter Three.) It is sufficient now to recognize that normal internal and external remodeling does not proceed independently, and although this seems intuitively reasonable, models integrating the two processes have only recently been constructed.

Two such models are those provided by Hart et al. (1984) and Jaworski (1981), which both view internal remodeling as a special case of the external process. Figure 4 gives a schematic comparison of their models. The term 'transducer' refers to the specific chemical, electrochemical or physical messenger responsible for cellular activation and direction, a broad and controversial topic. Davidovitch et al. (1984) and Binderman et al. (1984) provide interesting, though complex, discussion along these lines. Note that Hart et al. (1984) consider 'material properties' to include both material and physical properties, as defined here. Generally, 'material properties' embraces both the intrinsic physical and geometric properties of the tissue together with the extrinsic characteristics of the particular loading situation employed. The material properties possessed by bones and bone tissue can only be evaluated in light of the manner of loading, and in this regard they differ from physical and geometric properties which can be measured and compared independently. Unfortunately, this distinction is seldom drawn in the biomechanical literature, which can make for some confusion as to what is being tested and what is being controlled.

Two things are apparent in these models which make them appealing given the existing state of knowledge. First, the remodeling potential is determined in light of both mechanical

Figure 4.
Models of the bone turnover system.
Model (a) is modified from Hart et al. (1984) and (b) from Jaworski (1981). The end result of any remodeling sequence is an alteration of bone size, shape or mass. The outcome is always constrained by the physiological status of the organism.

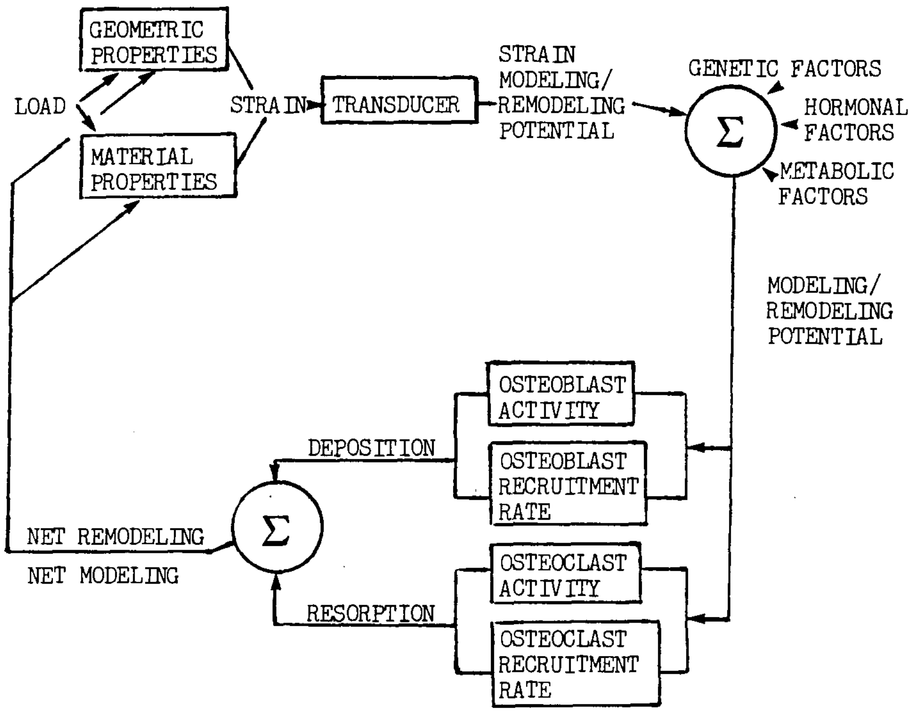

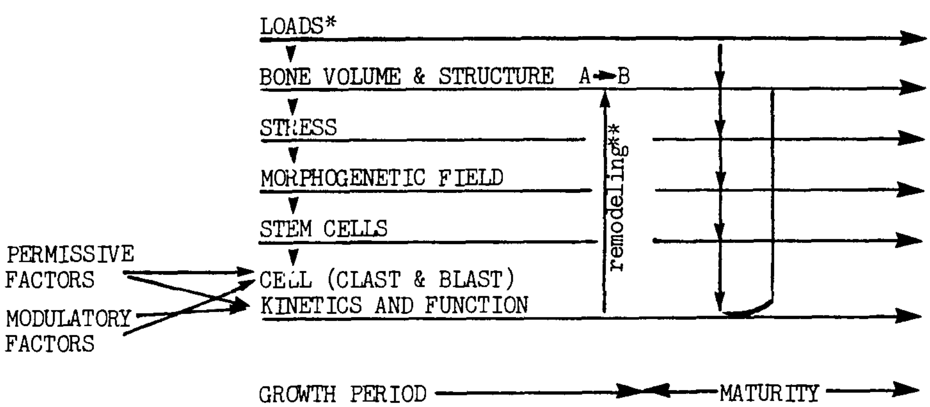

*MAIN INPUT

REMODELING AND MOVEMENT OF BONE TISSUE load and the sum of genetic, humoral and metabolic constraints – Jaworksi's 'permissive' and 'modulatory' factors. Second, the initial stimulus is an externally applied load, while the **operative stimulus is the magnitude of stress (strain) within the bone material. This latter fact permits two observations. If accumulated fatigue microfracture or localized bone necrosis disturbs the optimal stress/strain level at any point (control surface) within a bone, as suggested by Martin and Burr (1982), then remodeling should ensue to correct that disturbance. The same reasoning applies to the deformation of external bone surfaces as well. The second observation is that the models depict open feedback systems. As such the behavior of any given loop at a locale is predicated upon the product of the previous loop at that locale. Thus the models integrate the concept of functional adaptation.

Summary

Although diverse in scope, this chapter has attempted to make one point: that bone form can be explained in terms of functional adaptation. A bone reflects a specific life history (of forces which have acted upon it through growth and maturity) as well as phylogenetic history. Bone form is explained by Wolff's Law, which stipulates that bone tissue occurs in a quantity and quality wherein it functions most efficiently, where efficiency is averaged over time.

For external surfaces, bone is remodeled in accordance with the V–principle and the Flexure–drift tenet, the result of which is a change in bone size and shape with preservation of mass. Internally, Haversian remodeling proceeds in response to localized microscopic failure of the tissue resulting in an alteration of density and structure with preservation of external morphology.

The processes of internal and external remodeling are not independent. Recently, models have been proposed which integrate the two in terms of both ultimate stimulus, cellular mechanisms and cellular response. These models also stipulate that the potential for remodeling is not independent of the physiological state of the organism, and consequently views purporting that (specifically Haversian) remodeling is either mechanically or metabolically mediated, but not both, are no longer widely supported.

CHAPTER III

REMODELING IN BIOLOGICAL CONTEXT

Introduction

This chapter will put bone remodeling into biological context. The emphasis will be on variability in remodeling parameters associated with age, sex and side of body. This (and later) discussion will make reference to several biomechanical concepts which have yet to be adequately defined or described. A clear understanding of these concepts is required in order to develop the specific hypotheses to be tested in this thesis. Therefore, this chapter will begin with a simplified presentation of biomechanical principles and terms, followed by a short section dealing with the nature of the individual components of bone strength. The balance of this chapter will consider the biological variability which characterizes the geometric and physical property components of bone, specifically.

Biomechanical Referents and Norms

It would not be possible to enter into a discussion of bone biomechanics without a basic comprehension of certain precepts and terms used to describe the behavior of bones and bone tissue under various loading conditions. In part, the following discussion is restricted to the two-dimensional perspective applicable to cortical bone cross-sections. For more comprehensive treatment see Frost (1964, 1973), Evans (1973), Nordin and Frankel (1980) and Currey (1984e), from whose writings much of the following has been derived.

Forces

A force consists of any action "which changes the state of rest or motion of a body to which it is applied" (Frankel and Nordin 1980:293). There are three "pure forces" (Evans 1973:4) which can be applied to any surface. These are (1) **compression**, (2) **tension**, and (3) **shear**. In compression, tension and shear the intermolecular distances within the object are reduced, extended or obliquely displaced, respectively (Figure 5). Specific loading situations can combine these forces in various ways. For example, torsion generates a twisting shear and may include compression or tension. Bending, with implied compression and tension, may also incorporate torsion (see below).

Stress and Strain

When any external force is applied to any material the latter is deformed, regardless of our inability to measure it (Frost 1964). This response can be characterized in terms of stress and strain. **Stress** refers to the intermolecular resistance of a material to a deforming force. When considered with respect to area, stress constitutes a force in its own right which acts to restore the inertial (rest) state of the object (Evans 1973). **Strain** refers to the change in length (normal strain) or angle (shear strain) of an object in response to an externally applied force (Currey 1970; Nordin and Frankel 1980). Strain may be either **elastic**, in which case the material will recover its original dimensions when stress returns to zero; or it may be **plastic**, in which case a portion of the strain is permanent and non-recoverable. That is, stress energy reaches zero before strain energy reaches zero (Currey 1984e). In skeletal biomechanics, experimental results are reported in terms of both stress and strain, yet the latter is the only one which can be measured directly (though it is dimensionless, being the ratio of two lengths). Stress is a somewhat abstract construct of the human mind (Cowin 1984) which can be measured only as a ratio of force per unit area (Evans 1973).

Figure 5.
Forces and their resulting deformations.
The chords represent intermolecular relationships in tension, compression and shear.

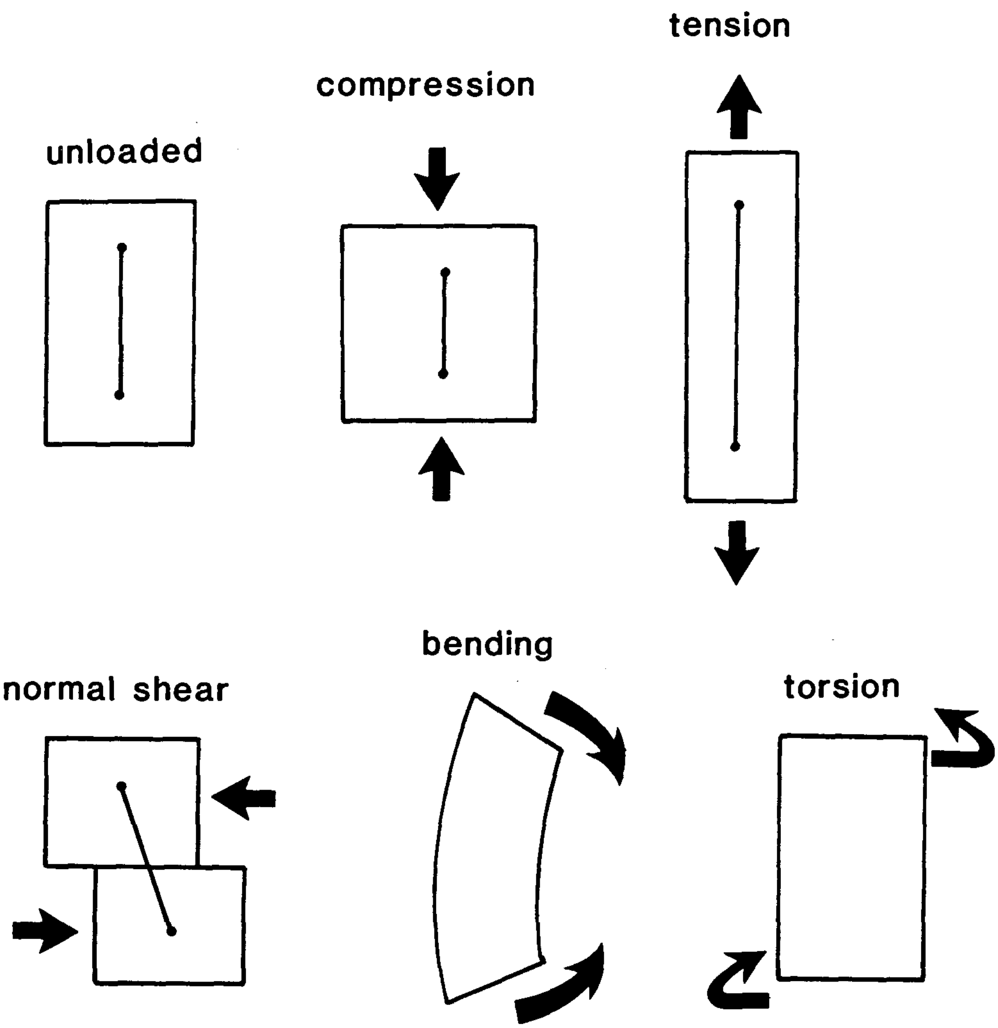
tension
compression
unloaded
bending
normal shear
torsion

It is the relationship between stress and strain which provides the two fundamental measures of the mechanical competence of bone tissue: strength and stiffness. The **stress-strain curve** (Figure 6) is a plot of applied load (ordinate) versus resulting deformation (abcissa). The amount of stress per unit strain is represented by the slope of the curve in the elastic region, and will be a function of **strain rate** (i.e., the velocity of load application) and material stiffness. The area under the curve equals the energy stored in the deformed material and, when calculated up to the point of failure, becomes a measure of the material's strength (Nordin and Frankel 1980)..

Currey (1984a,e) considers stiffness to be the most important property of bone tissue. The functional efficiency of contiguous elements is determined by their ability to act as levers, and 'soft' bones would be obviously less efficient than 'stiff' bones: they would simply bend hopelessly under load. Stiffness is determined by the degree of mineralization (Currey 1969a,b, 1984c,d; Minns et al. 1983). However, a point is reached beyond which further mineralization (though biochemically possible) results in a re-characterization of the tissue from 'stiff' to 'brittle'. This optimal mineral, or ash, content of limb bones has been determined to be about 68% by weight (Currey 1969a,b). The most significant consequence of increasing brittleness is that fracture 'toughness' decreases. That is, the ability of bone tissue to halt crack propagation diminishes. Glass, for example, is a very brittle material. It possesses little in the way of 'toughness', and undergoes virtually no plastic deformation prior to failure. Such brittle materials are structurally sensitive to slight surface defects, such as nicks and scratches (Currey 1984e). The change from stiff to brittle for a given material can be measured in terms of the **modulus of elasticity**, [E], or **Young's modulus**. This is the "ratio of stress to strain at any point in the elastic region of a load-deformation curve" (Frankel and Nordin 1980:295). In that this region of the curve is represented by a straight line (see below), the ratio of rise and run will be a constant for any two points on the line. Hence, E is an accurate representation of the elastic property of the material being tested.

Figure 6.
A generalized stress-strain curve.

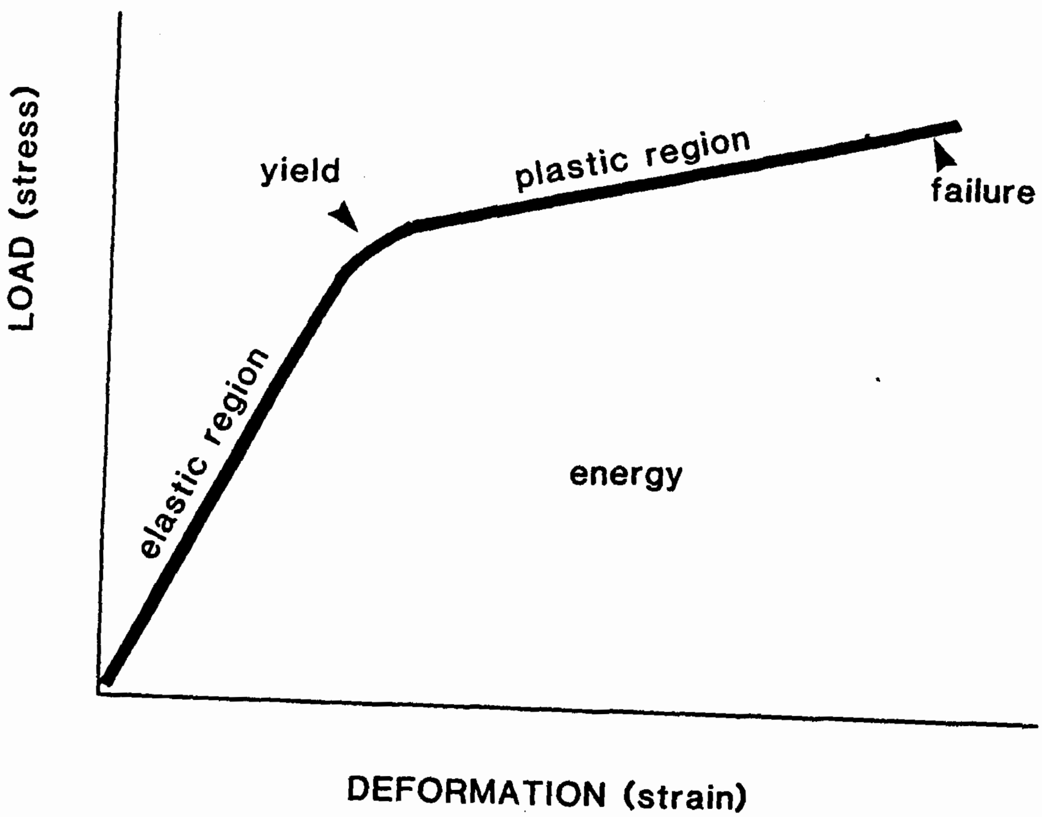
LOAD (stress)
yield
plastic region
failure
elastic region
energy
DEFORMATION (strain)

Before introducing further concepts, a short summary is desirable. Stiffness and strength are the fundamental measures of the material properties of bone and are interrelated by the relationship of stress and strain, as follows.

1. The area under a stress-strain curve is equal to the energy absorbed to failure;
2. energy absorbed is a measure of ultimate strength;
3. stiffness is a function of the mineral content of the tissue;
4. increasing stiffness reduces fracture toughness, and in turn the area under the plastic region (Currey 1969a). Hence, total area under the curve decreases depicting a measurable loss of strength;
5. in mechanical terms, increasing stiffness leads to an increased modulus of elasticity. At a given rate of strain, the material being stressed stretches more slowly. Graphically, the slope of the deformation curve becomes steeper, representing the fact that a greater stress (force per unit area) is required to produce a deformation equal to that which would have occurred under less stress at lower levels of mineralization;
6. finally, there is an optimum level of mineralization, approximating 68% ash content, for bones which bear mechanical loads (i.e., function as levers). This is a trade-off between reduced fracture toughness and reduced mechanical efficiency, which would result from 'soft' levers (see Currey 1984e:4).

The Elastic Constants, Isotropy and Anisotropy

Bone can be described as viscoelastic, plastic and transversely isotropic (Huiskes 1982). What does this mean? The stress-strain curve for bone is similar to that generalized in Figure 6. It possesses both an elastic and a plastic region. The point at which elastic deformation (fully recoverable) becomes plastic deformation (in part non-recoverable) is the **yield** point; and the area under each region equals the energy absorbed (1) to yield; and (2) to failure. It was noted in the preceding section that increasing the mineral content of the tissue reduces the energy absorbed to failure. Essentially, the amount of plastic deformation decreases before the bone breaks. It is equally possible to alter the energy absorbed to yield by manipulating the rate (velocity) of load application. The faster the strain rate, the greater the energy absorbed to yield. This can be measured in terms of the elastic modulus, E, and graphically as the slope of the elastic portion of the curve: both increase (Currey 1984e; Katz 1980). Since there is this time factor involved in the relationship of stress and strain in bone, it is more accurately characterized as **viscoelastic**, and in fact this property is possessed by all biological materials (Reilly and Burstein 1974; Gonza 1982).

The modulus of elasticity is but one of the proportionality constants which relate stress and strain in a material. The number of such constants varies inversely with the degree of symmetry of the material properties of the tissue (Reilly and Burstein 1974). If the properties differ in every direction in all planes, the material is referred to as **anisotropic**; while if one plane exists for which the properties are equal in all directions, the material is said to be **transversely isotropic**. Finally, if the material properties are equal in all directions for all planes, the material is **isotropic**. An isotropic material possesses two elastic constants: Young's modulus (E) and Poisson's ratio (v). Poisson's ratio is "the negative of the ratio of transverse strain to longitudinal strain in the direction of uniaxial loading" (Reilly and Burstein 1974:1003) and is "a measure of the materials ability to conserve volume when loaded in one direction" (ibid).

Bone is a transversely isotropic material, a model which accords well with its symmetrical histological picture in cross-section (Reilly and Burstein 1974), and which has been demonstrated experimentally (see Currey 1981b). Three elastic constants are commonly reported for a transversely isotropic material (though five exist): E, v, and G. The latter denotes the **shear modulus** and is measured as the ratio of induced shear to resulting shear strain (Reilly and Burstein 1974:1003). Table 1, reproduced from Currey (1984e:40), summarizes comparative values for these properties for both human and bovine bone.

Table 1. Technical Elastic Moduli for Compact Bone.

	Orientation	Reilly, Burstein & Frankel (1974)	Van Buskirk & Ashman (1981)	Reilly & Burstein (1975)	Reilly & Burstein (1975)
Species		Man	Man	Cow	Cow
Histology		Haversian	Haversian	Haversian	Fibrolamellar
Method		Mechanical	Ultrasound	Mechanical	Mechanical
Property:					
Young's Modulus	3	17.0	21.5	22.6	26.5
	2	11.5*	14.4	10.2*	11.0*
	1	11.5*	13.0	10.2*	11.0*
Shear Modulus	23	3.3*	6.6	3.6*	5.1*
	13	3.3*	5.8	3.6*	5.1*
	12		4.7		
Poisson's Ratio	31		.40	.36	.41
	32	.41*	.33	.36	.41
	21	.41*	.42	.51	

Sources cited in Currey (1984e), p. 40, Table 2.1.

Numbers in column 2 refer to sample orientation in a long bone: 1 = radial, 2 = tangential, 3 = longitudinal.

* indicates values equal on assumption of symmetry

Linear Elasticity

It was mentioned in Chapter Two that internal and external remodeling could be integrated in Cowin's (1984) analysis under the theory of elasticity, assuming that bone behaves as a linear elastic material. **Linear elasticity** describes any material which conforms to Hooke's Law (Popov 1978), which states that, up to a point, stress and strain are proportional, and is measured by 'E'. Hooke's Law applies to all materials to a greater or lesser degree (Popov 1978; Alexander 1983), though in some cases (e.g., concrete, cast iron) may be hardly noticeable. For linear elastic materials, the graph of stress/strain always exhibits a straight line in the elastic region of deformation. According to Cowin (1984:S100) "All data indicate that [Hooke's Law] represents a good approximation of the mechanical behavior of bone tissue in the normal physiological range of strain".

It is important that bones, which in life experience frequent intermittent loads (often of variable magnitude), behave elastically. If their elastic deformation was negligible, the plastic response would accumulate under repeated imposed loads, and would negate an effective cellular response to remodel the tissue according to every new or repetitive load.

Fatigue

The forces imposed on bones may be analyzed from either of two perspectives: (1) **statics**, in which the load is applied to bone in equilibrium (at rest) or (2) **dynamics**, in which the bone receiving the load is in motion. It is arguable to what degree data obtained from static testing of bone is meaningful in terms of functional adaptation (Lanyon and Rubin 1984; Currey 1979). Since the primary function of most bones tested (e.g., long bones) is locomotion, they should be adapted *in vivo* to dynamic loads. Over the past decade or so a growing body of literature has appeared which characterizes the dynamic response of bone *in vivo* (Chamay and Tschantz 1972; Lanyon et al. 1979; Lanyon and Rubin 1980, 1984; Hassler et al. 1980; Churches and Howlett 1981; Carter et al. 1981a,b; Amtmann and Doden

1981; Lanyon et al. 1982; O'Conner et al. 1982; Meade et al. 1984; Simon et al. 1984, 1985a–c; Burr et al. 1985). Specific results are discussed below.

In life, two types of dynamic loading situations exist for which bone in general, and certain bones in particular, must be adapted: (1) **impact** and (2) **fatigue** (Currey 1984a). The nature of impact loading is fairly self-evident, while that of fatigue is somewhat more obscure. The latter is of greater significance for functionally adaptive bone remodeling (Carter 1984) since it denotes a cyclic, repetitive process which, in the long term, would be more readily measured by natural selection than would infrequent, irregular impact events.

Fatigue "is the progressive failure of a material under cyclic or fluctuating loads. Under cyclic loading, materials fail at stress levels less than those required to cause static failure" (Carter and Hayes 1976:27). Clinically, it is probably true that the frequency of fatigue failure is underestimated "since most go on to heal with an unremarkable clinical course" (Carter and Hayes 1977:265; see also Baker et al. 1972). The effects of fatigue loading on bone stiffness and strength, and the relationship of fatigue failure to bone microstructure and density, are important considerations for understanding mechanically-based models of cortical remodeling (Martin and Burr 1982; Burr et al. 1985).

Two studies out of Carter's laboratory (Carter and Hayes 1976; Carter et al. 1976) have reported the effects of temperature, microstructure (primary and Haversian) and bone density on the fatigue life of bovine compact bone. Fatigue life refers to the number of 'cycles to failure' at a given strain rate. In fatigue studies, which often must be carried out over considerable periods of time, temperature effects can become significant (Currey 1984e). Carter and Hayes (1976) report a three-fold increase in fatigue life over a temperature decrease from 37° to 21° C, a result which should be considered since most testing laboratories are maintained at temperatures somewhat less than that of bone *in vivo.* They also found that fatigue life increased with bone density, and decreased with the extent of

Haversian remodeling. These results were confirmed by Carter et al. (1976). Interestingly, the latter were also able to show that in cases where primary and secondary (Haversian) bone were of more or less equal densities, the former still possessed a longer fatigue life. Two conclusions were drawn: (1) decreasing density leads to reduced fatigue life irrespective of histological character; and (2) Haversian bone is inherently weaker in fatigue than primary bone.

Carter and Hayes (1977) compared the fracture mechanism and appearance of bovine bone for monotonic bending (i.e., a static test involving a one-time load application) with flexural fatigue. In both cases fracture patterns were similar, with transverse fracture on the tension side and oblique fracture with bone chipping on the compression side. Subtle differences were apparent, however, in the fatigued specimens: (1) in that the oblique fracture surface was always larger; and (2) those specimens not fatigued to total failure "exhibited diffuse microscopic damage" (p. 269). This included osteon de-bonding and pull-out, where an actual physical separation between the concentric lamellae of Haversian systems and the surrounding interstitial or circumferential lamellae takes place, usually along the weak cement line junction (Moyle and Bowden 1984).

Recent studies have contributed further insights into the fatigue behavior of bone. Carter, Caler, Spengler and Frankel (1981) tested human cortical bone *in vitro* under tension and found that fatigue life was affected more by the strain range than by the mean strain. The smaller the strain range, the greater the number of cycles to failure. An *in vivo* study of dog radii by Carter, Harris, Vasu and Caler (1981) demonstrated the existence of a possible threshold for strain-mediated remodeling. Following unilateral ulnar ostectomy and tetracycline labelling, three of four experimental animals showed little or no new bone formation when compared to their contralateral control limbs. The fourth animal was much shorter and stouter, and showed considerable new bone deposition, accompanied by a reduced modulus of elasticity, in the experimental radius. The latter result was likely due to the lower ash content of the newly deposited bone matrix. The authors concluded that the hypertrophic formation response to increased cyclic strain levels (cf. Chamay and Tschantz 1972; Hert et al. 1972; studies by Lanyon and co-workers) was non-linear. It was suggested that normal bone can accomodate a wide range of strain, with little or no response, until a point is reached where accumulating fatigue microdamage causes the strain range to become excessive. This then threatens the bones structural integrity, which in turn activates a hypertrophic response. If true, it may well follow that for all bone tissue there is no 'optimum strain history' "toward which bone will spontaneously remodel" (Carter 1984:S19). That is, bone tissue at different sites within a single element will be sensitive to different strain histories, with a given strain range and frequency producing a remodeling response at 'point A' but not at 'point B', and so on. This is reasonable since, for any given externally applied load, the stress and strain experienced by bone tissue is determined, in part, by the existing configuration of material: stress with respect to area parameters and strain with respect to stiffness and strength (Lanyon 1981b). The concept of a strain threshold has been advanced in several recent papers by Frost (1985 and references therein). Frost argues for the existence of a Minimum Effective Strain (MES) below which no remodeling occurs. When the MES is exceeded, remodeling ensues to reduce it. More will be said along these lines in Chapter Four.

Bending

This introduction to fundamental biomechanics concludes with a short discussion of bending and related concepts. In articulation, most bones can be modeled either as cantilevers or beams (i.e., fixed at one or both ends). Consequently, the stresses generated by externally applied forces can rarely, if ever, be described as pure tension, compression or shear. In fact, the most frequent form of deformation experienced by (non-irregular) bones is bending (Wainwright et al. 1976) which incorporates all three stress modes distributed about the cross-section of the element (Evans 1973) (Figure 7).

Figure 7.
Stress distribution in three–point bending.
Restraint is assumed at either end, with the force directed upwards.
The size of the arrows indicates the relative magnitude of stress in the cross–section.
Tensile/compressive stress at the neutral axis is zero. The figure assumes a symmetrical cross–section.

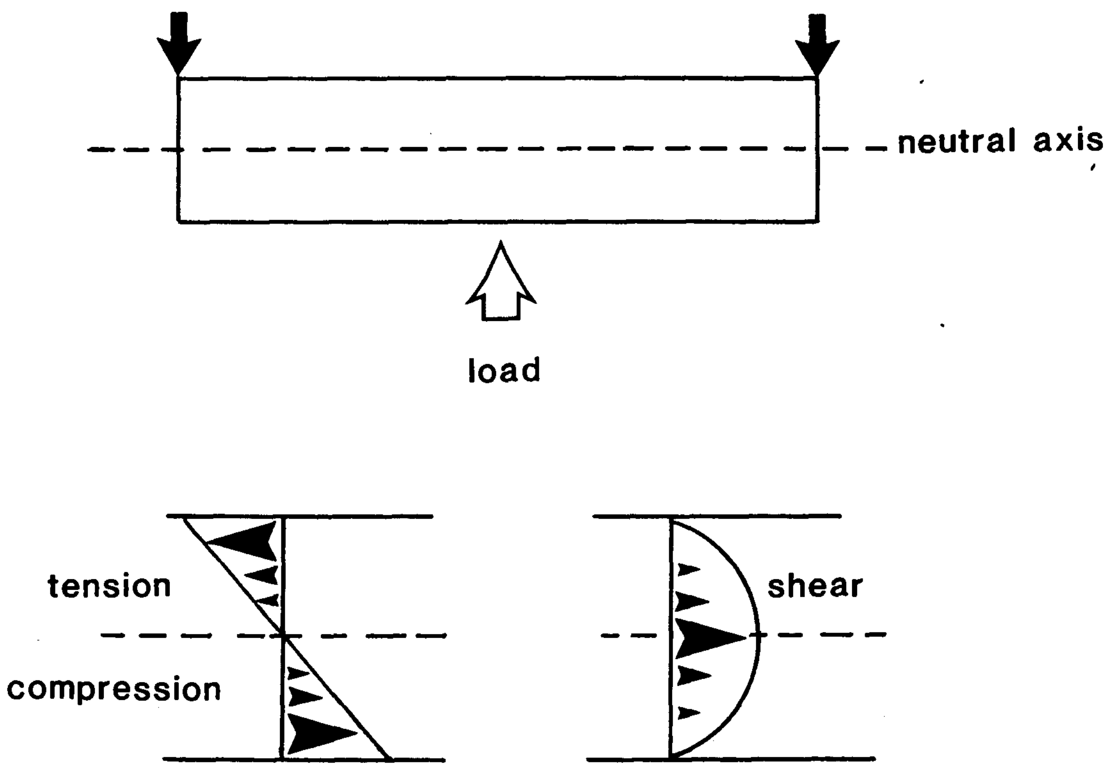
neutral axis
load
tension
compression
shear

Bending occurs about a **neutral axis**. Resulting tension and compression (shear is disregarded for the balance of this discussion) may be symmetrically or asymmetrically distributed on either side of this axis, as determined by the cross-sectional shape of the structure (Figure 7). This distribution reflects the fact that, in bending, the magnitude of stress is proportional to the distance of the outermost fibre of the material from the neutral axis in the plane of bending (Nordin and Frankel 1980). At the neutral axis, stress is zero.

In bending, the strength of an element is primarily a function of its cross-sectional geometry (Wainwright et al. 1976; Currey 1984a). This is because the bending moment (M) resulting from the application of any given force to a beam of fixed diameter is a constant. A **bending moment** is "A quantity at a point in a structure equal to the product of the applied force and the perpendicular distance from the point to the force line" (Frankel and Nordin 1980:291). The formula for calculating the normal stress in a beam subject to bending is

$$\sigma = \mathrm{M}y \;/\; I$$

where σ is the resulting stress; M is the bending moment; y is the distance away from the neutral axis; and I is a quantity known as the **moment of inertia** (a measure of the geometric resistance to deformation under load – see Chapter 5). Given the constancy of M, the only ways to reduce the resulting stress are (1) to decrease y, and/or (2) to increase I. The objective is to maximize the ratio I/y (Wainwright et al. 1976).

As detailed in Appendix I, the moment of inertia is calculated as the product of an area and the square of the distance from the neutral axis to that area. It is therefore expressed in units to the fourth power. The distance denoted by y, however, is strictly a linear dimension of unit value. The proportional effects of each upon bending strength are unequal. The positive contribution of y^2 in the calculation of I after any increase in y far outweighs the negative contribution of increasing y in order to distribute more material away from the neutral axis. Conversely, the gain in stress reduction obtained by decreasing y will generate a larger negative effect on bending stress through a proportionately greater reduction in the moment of inertia.

This relationship makes the moment of inertia extremely useful for interpreting the cross-sectional geometry of bones, given the premise that they remodel in response to external forces. One may optimize the strength per unit weight ratio of a structure which experiences bending in a single direction only by distributing as much material as possible in a line along the axis of bending. The result would be an I-beam. If two perpendicular bending forces predominate. a box-like structure would be most efficient. Finally, if bending is likely to occur equally in all planes, a circular cross-section is the best design to have which, in consideration of torsion, becomes a hollow cylinder (where the ratio of diameter to wall thickness is determined by the constraints of buckling) (Wainwright et al. 1976; Currey 1982a) (Figure 8).

It should be emphasized that the material presented in this section is an overly simplified account of a few of the fundamental concepts of bone biomechanics. The objective has been to familiarize the reader in order that concepts introduced in the text, in passing or in detail, will be minimally confusing.

Geometric, Physical and Material Properties

The strength of a bone derives from three sources: (1) its geometric properties, or how the material is distributed in space; (2) its physical properties, or the relationship between mass, density and porosity; and (3) its material properties, or how the bone is loaded in life.

Figure 8.
The relationship of cross-sectional shape to predominant bending force direction.
(a) One predominant plane of bending.
(b) Two orthogonal bending directions.
(c) Bending likley occurs in all planes with equal magnitude and frequency.

a

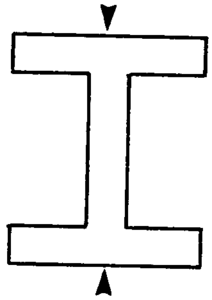

b

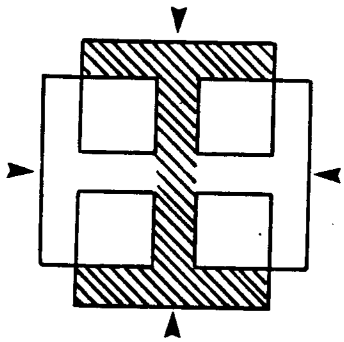

c

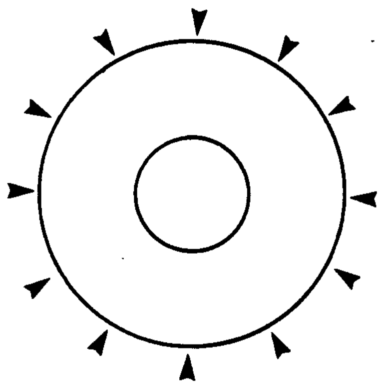

Geometric Properties

In the preceding section the point was made that, for a generalized beam, stress in the plane of bending can be reduced by maximizing the I/y ratio; and that the most economical distribution of material places it disproportionately in the predominant plane of bending, if one exists. The moment of inertia is but one of the descriptive parameters of the geometric properties of cross-sections. Others include the ratio I/y, hereafter referred to as the **section modulus**(Z) (Alexander 1983), and the **Polar Moment of Inertia** (J), which is a measure of the section's resistance to torsion about a centroidal axis. The section modulus comprises part of the general formula for flexural stress, and is a constant for any given direction in a cross-section (Popov 1978).

With regard to bone cross-sections, area parameters such as medullary area, cortical area and total area are significant geometric variables. According to Ruff and Hayes they are appropriate

> for evaluating internal resistance to pure axial loads, that is, loads applied perpendicular to the cross-section surface with the force resultant passing through the centroid, or center of area of the section [Ruff and Hayes 1983a:360].

However, in long bones such as the femur and tibia, area parameters are of less consequence than area moments of inertia (Ruff and Hayes 1983b; Ruff 1984) since axial loads are primarily compressive, and bone is more likely to fail under tension, torsion or bending.

As noted earlier, beams designed to withstand bending in any direction should be circular in shape, and the value for I will be equal for all axes. Non-circular sections, on the other hand, will have one axis for which I is a maximum and, perpendicular to it, one for which the moment of inertia is a minimum (Figure 9). These axes comprise the **Principle Moments of Inertia** of a section (Ruff and Hayes 1983a; Popov 1978). It should be apparent that the greater the deviation from circularity of a plane area, the greater the difference in

Figure 9.
The relationship between section shape and the maximum (Imax) and minimum (Imin) area moments of inertia.

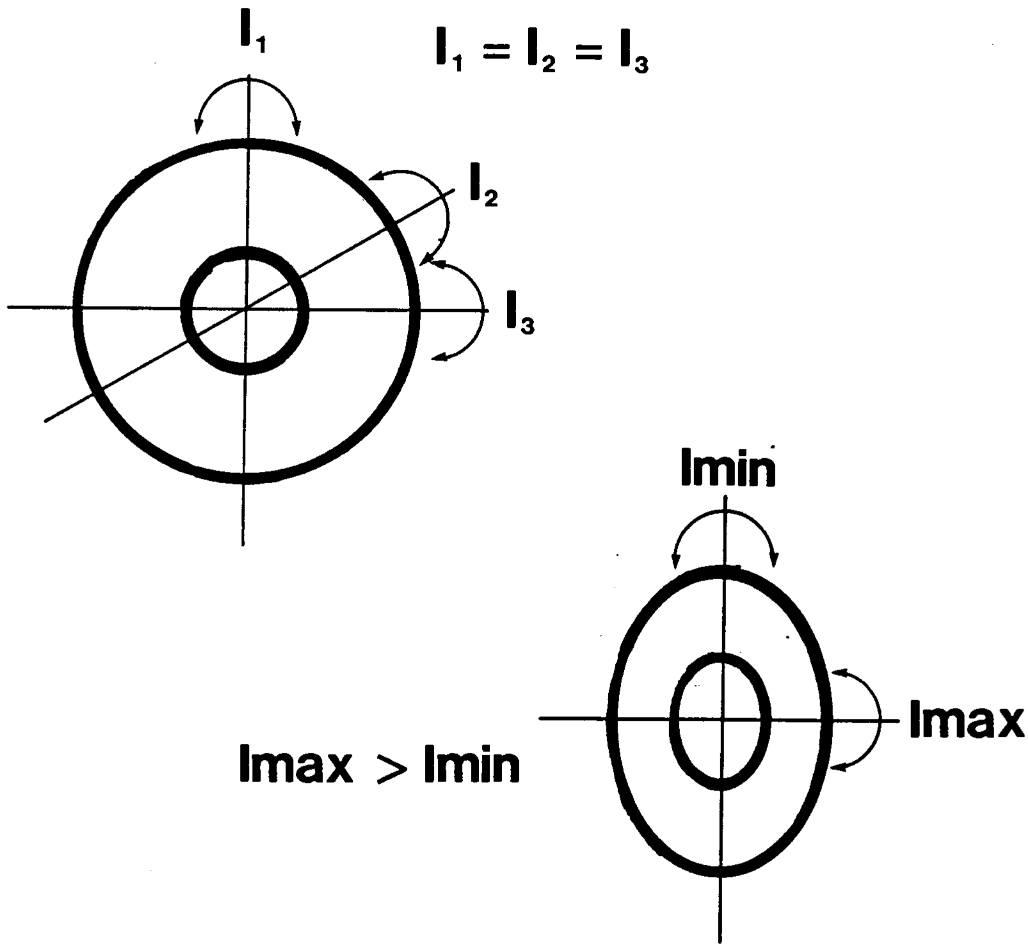
I_1
$I_1 = I_2 = I_3$
I_2
I_3
Imin
Imax
Imax > Imin

magnitude of the principle moments. Hence, the ratio of these values can be used as an index of shape (Ruff and Hayes 1983a).

Physical Properties

Two fundamental ratios underlie the physical properties of bone. The first is the proportion of inorganic to organic constituents (i.e., mineralization) and the second is the ratio of tissue mass to tissue volume. The former can be measured as dry density, which in bone approximates 68% by weight (Currey 1969a,b). In cross-section, the latter can be evaluated in terms of porosity.

The effect of mineralization on bone strength has been discussed previously. The effect of porosity is more complex, and is not well understood (Currey 1984e). Martin (1972) has modeled cancellous and cortical bone as a single bone type on a continuum of porosity. This would accord well with studies by Carter and co-workers (cited in Currey 1984e) who derived power functions for both compressive strength (proportional to D^2) and Young's modulus (to D^3) against apparent density (D) for human and bovine cancellous bone. Compact bone was found to fall on a continuum of these power-curves. The amount of cortical porosity in compact bone will be determined directly by the relative amounts of bone resorption which takes place as a consequence of the production of Haversian systems and, as will be seen in the following section, as a consequence of the net bone loss associated with aging.

Topographic variation in dry density in the human femoral diaphysis has been reported (Atkinson and Weatherell 1967; Amtmann 1971; Kimura and Amtmann 1984). Atkinson and Weatherell (1967) observed that a maximum mean density, determined radiographically, moves from the anterior quadrant of the proximal end to the posterior quadrant distally. Minimum mean density follows conversely, creating a 'spiral' effect. These results were interpreted in light of the structural alignment of the femur in standing, where the shaft is directed downwards, inwards and slightly forward. In this position the "denser parts of the cortex will be disposed along a vertical line" (Atkinson and Weatherell 1967:787). This explanation, however, considers axial loads only for a stationary body. Such loads are less likely determinants of femoral morphology than dynamic bending forces (Ruff and Hayes 1983a; Lanyon and Rubin 1984).

Material Properties

Material properties comprise the intrinsic strength and stiffness of bone. The elastic moduli (Table 1) and ultimate tensile, compressive and bending strength (Table 2) describe these properties.

As mentioned, the number of different elastic moduli increases with the degree of anisotropy of the material concerned. Bone, being transversely isotropic, is equally stiff in both the radial and tangential directions (Figure 10). However, it is anisotropic longitudinally, as both strength and stiffness are greater along this axis (Tables 1 and 2). This makes sense for a long bone since the most dangerous loads (bending and/or compression) applied *in vivo* act along its length (Wainwright et al. 1976). It is thus no accident that the composite nature of cortical bone sees the primary orientation of its constituents directed more or less longitudinally. This is true at both the ultrastructural (i.e., collagen fibre bundles) and microstructural (e.g., Haversian systems) levels (Katz 1980). Such an anisotropic composite permits one direction potentially to be very strong, though at the expense of increasing weakness in other directions (Wainwright et al. 1976; Currey 1984e). Frankel and Burstein (1970, cited in Nordin and Frankel 1980) depict gradually decreasing Young's modulus and energy absorbed to failure for human femoral specimens tested in tension in four directions: longitudinal, transverse (radial or tangential), and oriented at 30 and 60 degrees to the neutral axis of the bone. Both gradually decreased, from a high for the longitudinal axis to a low for the transverse axis.

Figure 10.
The three primary orientations in a long bone.

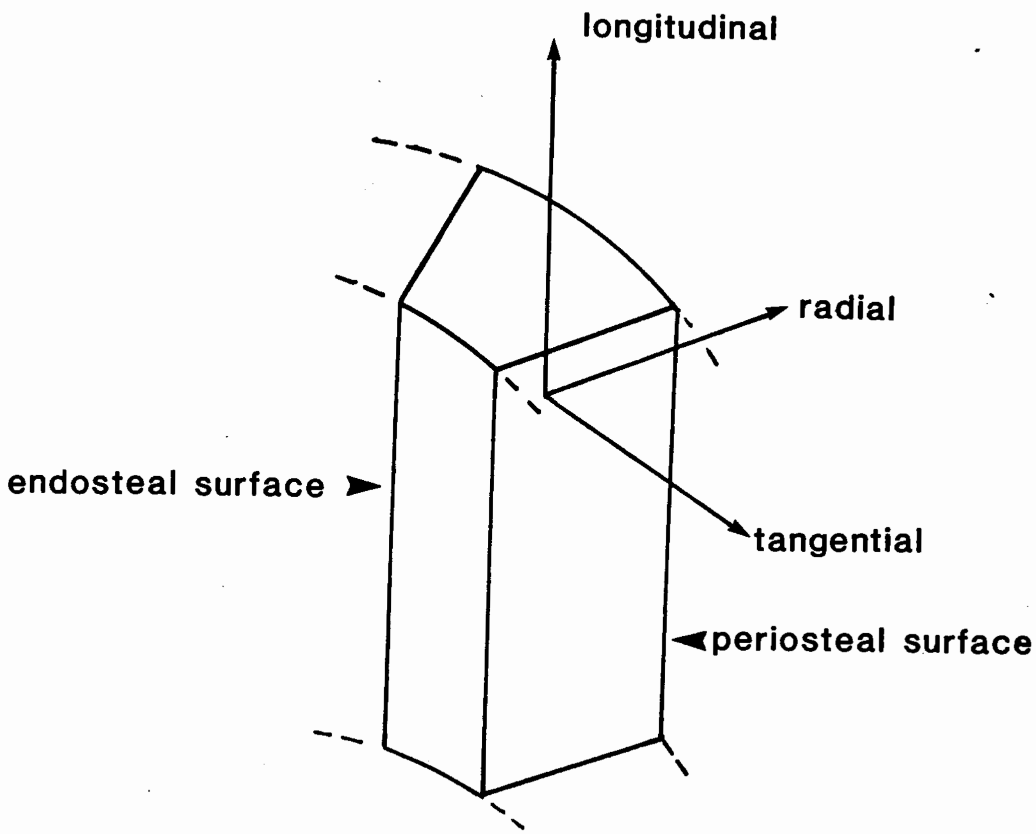
longitudinal
radial
endosteal surface
tangential
periosteal surface

Table 2. Orientation Differences in Human Bone Strength.

ORIENTATION	STRENGTH $x10^6$Pa			BONE	SOURCE*
	Compress	Tension	Bending		
Longitudinal		83.36		femur	Evans, 1964
		87.48		tibia	Evans, 1964
	199.95			femur	Sweeney et al., 1965
	203.91			femur & humerus	Dempster & Liddicoat 1952
			253.34	tibia	Dempster & Coleman, 1961
Radial		15.84		femur	Evans, 1964
		15.12		tibia	Evans, 1964
	150.30			femur	Sweeney et al., 1965
	132.40			femur & humerus	Dempster & Liddicoat 1952
Tangential		16.03		femur	Evans, 1964
		13.17		tibia	Evans, 1964
	128.61			femur & humerus	Dempster & Liddicoat 1952
			42.48	tibia	Dempster & Coleman, 1961

* = Evans (1973)

Age, Sex and Side Factors

Two changes occur in the geometric and physical properties of human long bones which can be characterized in terms of age and sex. These changes are directly associated with the processes of remodeling. They are (1) expansion of the medullary cavity, with increasing endosteal porosity (i.e., osteoporosis); and (2) continuous periosteal apposition. Each of these changes will be discussed below, in terms of age and sex variability. This section will conclude with consideration of the effect of age-related physical property alteration on the material properties of bone.

Osteoporosis

Osteoporosis can be defined as a net bone volume loss associated with aging and diagnosed, in clinical practice, most often by fracture (Lazenby 1985). By specifying a **net** bone loss, the point is made that both bone formation and resorption continue; however, the balance no longer favors formation. Generally, a negative bone balance exists in both men and women after middle adulthood. In women, the onset and rate of aging bone loss is earlier and greater than in men (Mazess 1982; Nordin 1983). Men lose about three per cent of total cortical bone volume per decade, and women nine per cent, after the age of 40 (Mazess 1982). In osteoporosis the chemical composition of bone is unchanged (unlike osteomalacia) - "there is simply less of it" (Nordin 1983:13). What is seen in cortical bone is expansion of the medullary canal and increased endosteal porosity. In spongey bone, particularly in vertebrae, osteoporosis proceeds with trabecular thinning and preferential loss of the horizontal struts (Nordin 1983). Detailed consideration of trabecular bone changes is beyond the focus of this thesis and will not be further discussed.

Osteoporosis may be distinguished as either primary or secondary; simple or accelerated. In simple primary osteoporosis bone loss proceeds at a rate characteristic for the age and sex of the individual, with no known presence of other diseases or disorders "known to produce an osteoporotic state" (Nordin 1983:37) [cf. Type I (post-menopausal) and Type II (senile) osteoporosis, defined by Cameron and Sutton (1985)]. Accelerated osteoporosis is defined when the tissue volume / element volume ratio of the individual falls below the mean level for the age and sex group to which he or she belongs. Such secondary osteoporosis exists when the subject experiences a disease or disorder known to produce bone loss. Examples include hyperthyroidism, hyperparathyroidism and disuse. Since most people tend to become less active with age, disuse can be a pervasive influence on a developing osteoporotic condition (Smith

1971).

One of the most (if not the most) diagnostic features associated with aging bone loss is fracture (Heaney 1983). Heaney lists four osseous factors contributing to osteoporotic fracture, admittedly not independent. These are (1) decreased skeletal mass; (2) inadequate skeletal repair; (3) altered architectural orientation; and (4) reduced skeletal strength. Only one extra-osseous factor seems to operate, and this is the affected individuals propensity to fall [although such related effects as reduced muscular coordination should be considered (Parfitt 1984a)]. Heaney (1983) argues that decreased skeletal mass is the most significant factor underlying osteoporotic fracture. Interestingly, he points out that although all incidences of osteoporotic fracture are associated with decreased skeletal mass, the converse does not hold true. In fact, "some persons with otherwise greatly reduced mass never suffer a fracture. Except for factors such as propensity to fall ... no good explanation for their being spared can be adduced" (Heaney 1983:127-8).

There is an extensive literature dealing with the clinical aspects of osteoporosis (see the edited volumes by Frame et al. (1973), Barzel (1979), Frost (1981) and Avioli (1983), as well as Gitman and Kamholtz (1965), Bartley et al. (1966), Garn (1970), Garn and Shaw (1976), Vose and Engel (1973), Plato and Purifoy (1982), Whedon (1984), Lohman et al. (1984), Harper et al. (1984) and Plato et al. (1984) for what must be considered a very small sampling of the available material). Similarly, a considerable volume of work has characterized the development of osteoporotic bone loss in several prehistoric and historic populations in both the Old and New Worlds (Dewey et al. 1969; Carlson et al. 1976; Van Gerven and Armelagos 1970; Van Gerven 1973; Perzigian 1973; Ericksen 1976, 1979; Ruff and Hayes 1983a,b; Martin et al. 1985). All of these studies confirm the general phenomenon of decreasing skeletal mass with increasing age and the fact that this loss is more pronounced in women than in men. Some of the available data depicting this relationship is summarized in Table 3. Note that comparison of the data given in Table 3 should be made within any given study, since some figures represent cortical areas, others cortical thicknesses. The table serves only to point out the consistently greater bone loss in the female skeleton relative to the male.

The actual remodeling mechanism thought to be involved in aging bone loss has yet to be precisely determined. At any given site a negative bone balance will accrue through increased resorption and/or decreased deposition. Either of these phenomena can be described as a product of two cellular-level attributes: (1) cell kinetics, or the number of active nuclei at a site; and (2) cell function, or the efficiency of each active nucleus in performance of its task (Jaworski 1981, 1984). According to Jaworski (1981) bone loss (through disuse) appears to be due to altered cell kinetics, and not altered efficiency. The accepted model of osteoclasis (Parfitt 1984a) sees continued recruitment of new multinucleate osteoclasts throughout the process of resorption. On the other hand, osteoblasis (deposition) proceeds as a result of a stable mononucleate cell population which does not benefit from cellular recruitment, and which is diminished as individual osteoblasts are incorporated into deposited matrix as osteocytes (Jaworski 1984). In normal, healthy individuals, rates of formation and deposition are roughly equal (e.g., about 50 microns per day in dog ribs (Jaworski 1984) where rate is calculated as efficiency per nucleus times the number of active nuclei). The calculated 20 to 40 times differential efficiency per nucleus favoring osteoclasts is roughly offset by a corresponding differential in osteoblast cell population at a given turnover site (Jaworski 1984). The existence of a negative bone balance in aging individuals thus is likely a reflection of diminished cellular kinetics rather than diminished cellular efficiency. That is, with aging fewer and fewer osteoblasts are directed to sites where bone formation is required. As a consequence, the rate of deposition is diminished for the site as a whole. Since resorption will tend to continue at a characteristic normal rate, the result is a net bone volume loss which will appear, intracortically, as progressively increasing porosity (Parfitt 1984a). Alternatively, Pinto et al. (1984) and Simonet and Kelley (1984) have suggested that a decrease in the pool of exchangable ionic calcium with age, demonstrated in dogs, coupled with an increase in stable, non-labile calcium may be at least partially responsible. This would result in parathyroid hormone (PTH) levels remaining elevated for longer periods of time, leading to increased resorption.

Table 3. Aging Bone Loss in Different Populations.

POPULATION	SEX	ELEMENT	% BONE LOSS	SOURCE
Arikara	males	femur	-7.33	Ericksen, 1976
	females		-22.88	
Pueblo	males		-7.43	
	females		-10.64	
Eskimo	males		-1.80	
	females		-21.82	
Nubian	males	femur	-12.94	Dewey et al. 1969
	females		-24.93	
Indian Knoll	males	radius	-7.0	Perzigan, 1973
	females		-13.0	
Hopewell	males		-20.0	
	females		-24.0	
Modern	males		-7.0	
	females		-15.0	
Mississip.	males	femur	-11.30	Van Gerven & Armelagos, 1970
	females		-29.90	
Utah Great Basin	males	femur	-16.7	Van Gerven, 1973
		tibia	-24.1	
		humerus	+14.2	
	females	femur	-34.1	
		tibia	-41.5	
		humerus	-25.9	
Pecos Pueblo	males	femur	-6.0	Ruff & Hayes, 1983b
	females		-18.0	

Increasing cortical porosity with aging is a consequence of altered Haversian remodeling dynamics. Several studies have described age changes in the histological picture of human cortical bone. Martin et al. (1980) provide a fairly comprehensive review of this topic, as well as original data for males. Generally, with age the total area of the Haversian system (as reported in the literature) either declines or remains unchanged. On the other hand, Haversian canal area either increases or remains unchanged. In no study did both system area and canal area remain constant with age, and in only one study (Jowsey 1966, using ribs) did both variables change with age: system area becoming smaller and canal area larger. Thompson (1980) reported data for Haversian canal area for males and females. The summed canal area in both sexes showed a general increase with age, though with different patterning. In subjects older than 50 years, the rate of increase was greater in males than in females, though the overall increase in porosity was greater in females when the entire age range (30 to 99 years) was considered. Therefore, the increase in canal area must have been much greater in females before 50 years of age. This finding is consistent with the general phenomenon of osteoporosis which sees earlier onset and a greater rate of loss in females when measured from early adulthood to old age. Interestingly, Thompson found no significant increase in the number of Haversian canals per unit area in women between the 5th and 8th decades, whereas such an increase was present in males. The apparent result of this increase in males was to equalize the total number of canals present in both sexes for the older age groups. Thus, not only was canal area greater in younger women, but also was the frequency of canals per unit area.

From the point of view of osteoporosis the size of Haversian systems may be of little consequence. It is increasing canal size which represents a net bone volume loss intracortically. However, the decreasing size of the Haversian system with age reported in some studies may be important since the rate of deposition decreases with age (Jowsey 1968). Smaller initial resorption cavities, which will determine Haversian system size, might compensate for an increased length of time required for infilling, thereby exposing the cortex to less dramatic losses of material over greater periods of time which would occur were resorption to continue to produce Haversian systems of a characteristic 'normal' size.

Continuous Periosteal Apposition

Continuous periosteal apposition refers to the deposition of circumferential lamellar bone on the periosteal surface which occurs throughout life (Epker and Frost 1966). The phenomenon was first extensively investigated in a cross-sectional study of human femora by Smith and Walker (1964) who considered the cause to be flexural stress with bending. However, it has since been observed in ribs (Epker and Frost 1966), skull (Israel 1968), second metacarpal and tibia (Garn 1970), humerus and tibia (Ruff and Jones 1981), and femur and tibia (Ruff and Hayes 1983b). Its occurrence in non-weight bearing bones (e.g., skull) would argue against Smith and Walker's hypothesis (Garn et al. 1972; Ruff and Hayes 1983b).

Epker and Frost's (1966) study of tetracycline-labelled ribs from 92 individuals aged two to 70 indicated that the incidence of periosteal apposition of new bone decreases with age, for any given age cohort. This is understandable since bone growth is expected in children and adolescents, but not expected in adults. Still, even for the 60 to 70 year age cohort, 33 per cent of the individuals exhibited some periosteal deposition. More interestingly, their study showed that at no age were all periosteal surfaces sites of active formation. From this they concluded that "periosteal bone formation is normally intermittent" (p. 576). This would accord well with current concepts such as flexure-drift, in which surfaces may be actively forming, actively resorbing, or at rest.

Garn and co-workers (1967, 1968, 1972) have presented extensive data on periosteal expansion of the second metacarpal in a number of different north and central American populations, including the Terry skeletal collection. In their 1967 study they were able to conclude that "bone growth continues through the eighth decade ... is not population-specific or sex-limited, and ... appears to be a general phenomenon in man" (p. 316). A significant finding was that second metacarpal expansion was both absolutely and relatively greater in females (Garn et al. 1968). Confirmation of this difference by Garn et al. (1972) using postero-anterior hand-wrist radiographs of 5660 North American adults of European ancestry "indicates that the sexes differ as systematically in adult periosteal gain as in adult endosteal loss, and hence the pattern of adult remodeling at both bone surfaces" (p. 377).

The existence of this sex-difference in age-related bone gain invites the interpretation, given our knowledge that geometry can contribute more to bone strength than density (Ruff and Hayes 1984a), that continuous periosteal expansion acts to compensate, mechanically, for endosteal bone loss. Women lose more bone endosteally, but gain more periosteally. This explanation has been cited on numerous occasions (e.g., Martin and Atkinson 1977; Garn et al. 1968, 1972; Ruff and Hayes 1983b; Martin and Burr 1984). That expansion would enhance bone strength cannot be questioned if we accept that increasing the cross-sectional moment of inertia increases the geometric resistance to bending and hence, increases strength. However, to infer that it does so in compensation for endosteal bone loss would seem to imply a more fundamental (i.e., genetic) relationship between the two, which has yet to be demonstrated. Parfitt (1984b) argues that since periosteal expansion (in adults) tends to precede accelerated bone loss and that it affects non-weight bearing bones, the mechanical compensation hypothesis is unlikely. He suggests that periosteal expansion represents the "minimal expression of a mechanism that, although dormant, must remain capable throughout life of responding to the need for fracture healing or to increased biomechanical demand" (p. S126). Martin and Atkinson (1977), in fact, were unable to demonstrate periosteal apposition in a series of 21 female femora of European origin. They concluded that the mechanical advantage of cortical expansion was only available to males and its absence in women may partially account for their problems with regard to osteoporosis. Ruff and Hayes (1983b), however, suggest that Martin and Atkinson's results may reflect sampling error, though they do admit the possibility of a true inter-population difference. In their own study of Pecos

Peublo femora and tibiae, periosteal expansion was present in both sexes, albeit variable with respect to location along the shaft (Ruff and Hayes 1982, 1983b). The magnitude of periosteal apposition, measured primarily at the mid-shaft, for various bones and populations is given in Table 4.

Side Differences

Although side differences in the gross morphology (e.g., size, weight) of the human skeleton have been investigated for over a century (see Ruff and Jones (1981) for a concise review), relatively little attention has been paid to bilateral asymmetry in any of the properties of cortical bone under present consideration. Mather (1967) examined several material properties of paired human femora, including Young's modulus. No significant differences were found with the exception of 'energy absorbed to failure', significant at the 0.05 level. Generally, Mather found that left femora had greater values but was confident in concluding that it was permissible to use paired elements as subject and control in an experimental situation.

Ruff and Jones (1981), in a archaeological sample from California, demonstrated considerable side asymmetry in cross-sectional breadth and area of the tibia and humerus, male and female. They found that

> Both bones showed significant bilateral asymmetry in size and shape, although the pattern of asymmetry varied by sex and age group. Males were more asymmetric in humeral dimensions (right side larger), females in tibial dimensions (left side larger). Bilateral asymmetry in both tibiae and humeri decreased with age [Ruff and Jones 1981:69].

Ruff and Jones hypothesize that the decline in asymmetry with age reflects either a biomechanical compensatory function or occurs through a decline in the real behavioral difference between the sexes which promoted the great asymmetry at earlier ages. In a second archaeological population from New Mexico, Ruff and Hayes (1983b) found area parameters of the femur and tibia to be generally larger on the left side, with the

Table 4. Per Cent Increase In Subperiosteal Parameters With Age[1]

AGE RANGE	SEX	SPECIMEN	AREA	DIAMETER	SOURCE
30 - 80	M	midshaft, second metacarpal; modern	2.94	1.46	Garn et al. 1968
"	F		8.55	4.18	"
25 - 85	M	"	2.80		Garn et al. 1972
	F	"	8.40		"
45 - 90	F	midshaft, femur; modern	11.49	10.91	Smith and Walker 1964
20 - 39 versus 40+	M	midshaft, femur;	6.7		Ruff and Hayes 1982
	F	archaeological	11.7		"
	M	midshaft, tibia;	12.4		"
		archaeological	12.9		"
21 - 30 versus 30+	M	proximal left tibia,	3.73		Ruff and Jones 1981
	F	archaeological	0.48		"
	M	proximal left humerus,	-2.44		"
	F	archaeological	2.35		"
24 - 56	M	cranium; modern		2.50	Israel 1968
	F	(ectocranial)		2.81	"

1. calculated ((older - younger) / younger) x 100 or taken directly from source

difference being greater in the female. As a final note, it is interesting that Garn et al. (1967:314) stipulate that measurements of radiographs of the second metacarpal are "free from systematic left-right asymmetry bias". It is possible that differences in the degree, or lack of, asymmetry between bones of the hand and those of the upper and lower limbs may reflect real functional and/or behavioral differences between various populations and between sexes, though such a hypothesis has never, to my knowledge, been explicitly tested.

Effects on Material Properties

Several studies have reported significant reductions in the material properties of bone as a consequence of aging. The relationship is not at all clear. For example, Smith and Smith (1976) examined ultimate tensile and compressive strength for four quadrants from each of 27 right femora obtained from individuals aged 19 to 87 years, both sexes. They found that ultimate tensile strength declined significantly with age. On the other hand, compressive strength did not significantly change. They were also able to measure mineral density, the magnitude of which accounted for 75 per cent of the variance in tensile strength and 85 per cent of the variance in compressive strength, in their data. They concluded that "mineral density was the major determinant of strength in [the] compact bone specimens studied" (p. 501). In contrast, Wall et al. (1979) examined ultimate tensile strength and density for the lateral quadrant in 26 femora (both sexes) from individuals aged 13 to 97 years. Their data indicate increasing strength and density up to the fourth decade, after which both decline. However, the rate of decrease in tensile strength was greater than in density, from which they concluded that bone density was not the sole determinant of strength. These two studies, though methodologically similar, are not strictly comparable which may account for their reaching essentially opposite conclusions regarding the relationship of mineral density to tensile strength. Smith and Smith (1976) tested all four quadrants of the femoral shaft and pooled their data in their final analysis; Wall et al. (1979) tested only the lateral quadrant. Interestingly, Smith and Smith found the lowest values for both strength and density in their lateral specimens. They may well have reached a similar conclusion to that of Wall et al. (1979) had they not pooled their data.

Burstein et al. (1976) evaluated tensile, compressive and torsional properties (e.g., ultimate stress and strain, Young's modulus, shear stress) in a diverse sample of femora and tibiae ranging in age from 21 to 86 years. Generally, all properties declined in magnitude with age, with the changes being more pronounced in the femur. Unfortunately, no direct measure of the physical properties of the bone samples tested was made, however, the authors report that, in tension, no significant differences were found in bones from normal versus osteoporotic individuals.

A more comprehensive study of the relationship of either apparent or dry density to material properties was reported by Currey (1979), who examined impact energy absorption in 39 femora, both sexes, aged three to 90 years. Physical properties measured included ash content, apparent and dry density, and porosity. Overall, a three-fold decrease in impact energy absorption was recorded. Currey attributes this increase to the greater mineralization seen in older bones. Porosity, which is high at either end of the age range, had a deleterious effect only in the older aged samples, likely in conjunction with the increased ash content. As Currey notes, the consequence of greater mineralization is decreased plastic deformation, hence a reduction in energy absorbed to failure.

In all of these studies bone specimens were tested, not whole bones. These specimens were machined to uniform dimensions, determined by each study. Hence, there are no data from these investigations from which it is possible to examine the effect of altered bone geometry on material properties. Studies reviewed above have shown that geometry does change with age, the result of which is that the magnitude of the cross-sectional moment of inertia (I) increases (Ruff and Hayes 1983b). Given that I is involved in calculating the magnitude of the normal stress in a beam subject to bending, it stands to reason that changes in bone geometry with aging will have an effect on the material properties of whole bones.

Summary

This chapter has been directed towards two goals. First was to provide a synopsis of concepts commonly referenced in the biomechanical literature; second was to provide a concise review of the biological variability which exists in various parameters of bone strength, as presently understood. Regarding this second goal, it is evident that a concensus has yet to be reached on many topics. Although some broad descriptive parameters for age and sex related variability are widely accepted (for example, endosteal bone loss and periosteal bone gain follow seemingly specific patterns along age and sex lines, as do certain products of Haversian remodeling) there is still considerable debate. What factor(s) are responsible at the cellular level, and how are they regulated? What is the degree of relationship between internal and external remodeling variability? What is the significance of the pattern and rate of remodeling variation at the endosteal and periosteal surfaces?

As pertains to bone strength two primary conclusions can be gleaned from the preceding discussion, upon which there is general acceptance. First, bone cross–sectional geometry can, theoretically, enhance bone strength through periosteal apposition in spite of endosteal bone loss. Second, increasing intracortical porosity can have but one effect upon bone strength, and that is to reduce it. The objective of this thesis derives from this contrary dichotomy: specifically, in what way does cross–sectional geometry relate to cortical porosity, and to implied or inferred predominant directions of bending? The balance of this thesis is directed towards investigating this question.

CHAPTER IV

THE INTERACTION OF GEOMETRY AND POROSITY: HYPOTHESES

Introduction

This chapter will present the hypotheses to be considered in this study. The aim is not to develop a quantitative model for the relationship of bone geometry and porosity. Rather, it is to characterize relationships which heretofore have not been investigated from the perspective of axis-specific bone strength conservation.

Age changes in the geometric and physical properties of bone have opposite effects on bone strength when each is considered alone. Whether alteration in either parameter proceeds independently of the other has yet to be demonstrated, although Martin and Burr (1984) and Martin et al. (1980) have given some indication that the two do not. Total independence would suggest that geometry and porosity are regulated by diverse and unrelated mechanisms, while interdependence would suggest a common controlling factor or factors. The models of the bone turnover system discussed in Chapter Two imply that some form of interdependent relationship between the products of remodeling, that is, geometry and porosity, should exist. These models argue that the same ultimate stimulus, cellular mechanisms and cellular response underlies remodeling processes at all bone surfaces. These processes effect a change in the total amount of bone present, and hence the apparent density (mass/volume) with every resorptive and depositional event.

At present this ultimate stimulus can best be identified as functional strain. Davidovitch et al. (1984) and Binderman et al. (1984) have reported measureable changes in various postulated biochemical transducers (e.g., prosteglandin E_2) with altered strain *in vivo.* These tranducers are the messengers; they transmit/translate the stimulus to the appropriate cell system.

Before any interactive relationship between the geometric and physical properties of bone can be hypothesized, the relationship of remodeling to functional strain must be clarified. This comprises the next section, which will be followed by an explicit statement of the hypotheses to be examined in this thesis.

Functional Strain and Remodeling

There is no question that bone remodeling is mediated by strain as opposed to stress (Carter et al. 1981, cited in Burr et al. 1985). The latter refers to an abstract notion of human creation which cannot be measured directly (Cowin 1984), whereas strain produces a real and measureable change in the bone's existing configuration.

Several studies have shown that bone will alter its structure when exposed to different strain environments (Lanyon et al. 1982; Carter et al. 1981b; Meade et al. 1984; Woo 1981). Lanyon et al. (1982) performed ulnar ostectomy on mature sheep and observed that new bone deposition on the radius acted to normalize the experimentally imposed compressive overstrain. In fact, they observed that the distribution of new bone was such that bending strains after ostectomy were reduced to below normal values. This suggested that the remodeling induced by their technique "may not be related to absolute strain levels but to the relative distribution of strain"(p. 141). In a study described earlier, Carter et al. (1981b) observed a hypertrophic response in only one of four experimental animals following ulnar resection. This result suggested that bone could accomodate a range of strain without responding, but once this range was exceeded response was considerable. Woo (1981) examined the effects of immobilization through plate-fixation on canine femora. Three groups were studied: (1) unfixed controls; (2) fixed with a graphite fibre plate; and (3) fixed with a Co-Cr alloy plate. The alloy plate possessed greater material stiffness than the fibre plate. The amount of bone atrophy was greatest in the alloy plate group; less in the fibre plate group and absent in the control group. The implication is that the alloy plate, being stiffest, transmitted less strain to the bone than the fibre plate. Consequently, the degree of bone loss was greater in this group due to a proportionately greater absence of strain.

It is apparent from these studies, among others, that bone does not remodel with the express purpose of **minimizing** strain. Such an interpretation is supported by analysis of the curvature and cross-sectional shape of certain long bones (e.g., metacarpals, radius, and tibia in dogs, sheep, turkeys and horses) (Rubin 1984). Frost (1973) first postulated that long bones were curved so as to offset the bending moments created during *in vivo* loading. The idea is that by naturally curving a bone in a direction opposite to the imposed bending, the magnitude of the resulting moment is reduced. That is, the load will be directed more in an axial direction, which will act to decrease resulting stress and strain. Similarly, the greatest resistance to bending in a cross-section is achieved by increasing the moment of inertia in the direction of bending (Currey 1984a). However, studies by Rubin (1984) and Lanyon (1981a) indicate that, in certain bones, curvature seems to be directed in parallel with the bending moment, thus increasing it. Furthermore, cross-sectional shape is not oriented to provide the maximum geometric resistance to bending. With regard to the latter, Rubin has concluded

> The main effect of the anatomical orientation of the elliptical cross-section is *not* to *resist* bending in the customary loading direction, but rather, at the risk of increasing the strain generated during normal loading, to restrict and co-ordinate the direction of loading that does occur [Rubin 1984:S13, emphasis in original].

It appears that the objective of bone remodeling is to maintain a given strain distribution (Lanyon 1981a, 1984), the benefits of which could be as diverse as increasing bone perfusion or maintaining an optimal electrical potential (Rubin 1984).

The role of strain as ultimate stimulus in osteonal remodeling is less clear. Martin and Burr (1982) have developed a model which perceives Haversian remodeling as a mechanism for repairing strain-induced microdamage (e.g., microcracks and de-bonded osteons) in bone, thereby extending the fatigue life of the element. Recently, Burr et al. (1985) demonstrated the relationship of Haversian remodeling to different frequencies and magnitudes of cyclic strain in the left forelimb of dogs, in support of the Martin and Burr model. They observed that (1) repetitive loading within physiologically normal limits could produce considerable microscopic damage in a short matter of time; and (2) that microcracks were associated with resorptive foci 44 times more frequently than expected by chance alone. These results suggested "a direct cause and effect relationship between microdamage production and intracortical remodeling"(p. 199). Strain remains the ultimate stimulus; fatigue microdamage the proximate cause.

However, full acceptance of the Martin and Burr model must be tempered by observations obtained in two other recent studies. Lanyon et al. (1982) observed that the newly deposited cortex on the caudal surface of sheep radii in response to increased load was extensively remodeled while that on other surfaces was not. They noted that "Since the degree of fatigue damage in the newly deposited bone is unlikely to be much greater than in the pre-existing cortex, it is possible that this Haversian remodelling was to achieve better material properties"(pp. 153-4). In other words, new bone should not be considered more likely to fail microscopically than old bone, and there should not be an inequitable distribution of osteonal remodeling of the magnitude observed. They continue to accept that the remodeling was under the control of the strain environment of the bone matrix, however. O'Conner et al. (1982) artifically loaded sheep radii intermittently within physiological ranges in the normal plane of bending and measured remodeling parameters. They observed that the ratio of the artifical strain range regime to the normal (control) strain range regime could account for 61 to 81 per cent of the variance in geometric changes, but for only 43 per cent of the Haversian remodeling variance between experimental and control limbs. As noted by Burr et al. (1985), this finding suggests that surface remodeling and Haversian remodeling may be responding to different stimuli. That is, the latter is less influenced overall by the strain environment of the cortex. However, the Martin and Burr model is not ruled out by the results of O'Conner et al. (1982), since the microdamage normally produced by *in vivo* strain may itself alter the local strain environment of the tissue - an influence which could not be controlled by O'Conner et al. in their study.

It seems reasonable to conclude that both internal and external remodeling phenomena are mediated by the strain environment of the element, the most significant aspect of which may be strain distribution rather than strain magnitude (though both play a role). The objective of both processes is, for the greater part, to maintain this distribution within the cortex. Given this understanding, it is now possible to identify a number of hypotheses relating bone geometry and intracortical porosity with the goal of conserving bone strength. The underlying mechanism will be the preservation of the strain distribution.

A Conservancy Model for Geometry/Porosity Interaction

The concept of 'conservancy', taken to be the wise use of natural resources, is implied within Wolff's Law and the concept of functional adaptation. For bone, these resources include the tissue constituents as well as the energy involved in growth, modeling and remodeling which produce a structure capable of meeting normal functional demands, both mechanical and physiological.

In formulating a model for geometry/porosity interaction the following points are accepted as given, based on work discussed in previous chapters. Regarding geometry, the following points are accepted as true.

1. Cross-sectional geometry is a product of surface remodeling. Two surfaces are involved, endosteal and periosteal.
2. With aging, cross-sectional geometry undergoes normal alteration due to two processes. First is endosteal expansion which produces an enlarged marrow cavity; second is

continuous periosteal apposition which produces a greater cortical diameter and total cross-sectional area. It is generally believed that the latter serves as a mechanical compensation for the former, though this has yet to be empirically determined.

3. For non-circular sections two orthogonal axes can be identified for which resistance to rotation (i.e., bending) has a maximum and minimum value. That is, there are directions for which the section is geometrically strongest and weakest. The existence of such axes implies that, in life, the structure was subject to bending more often in one plane than in any other, although it is not given that these axes identify this plane with precision.
4. Resistance to rotation is quantified as the cross-sectional moment of inertia which is determined as the product of bone area and the square of the distance from the axis of rotation to that area. Thus, more bone may be lost from the endosteal surface than is added to the periosteal surface without altering the value of the moment of inertia. This is because the latter is located at a greater distance from the axis of rotation.
5. Generally speaking, area parameters of bone cross-sections are appropriate measures for evaluating loads applied parallel to the long axis of the bone, while moments of inertia are appropriate for evaluating bending and torsional loads. Bending is likely the most significant and frequent mode of failure.

Regarding bone porosity, the following points are taken to be true.

1. Intracortical porosity is the product of Haversian remodeling processes, and is the primary determinant of the physical property component of bone strength. The other major determinant, dry density, is more or less constant throughout life.
2. In humans, increased bone porosity is a ubiquitous consequence of aging, the magnitude of which can be sexually differentiated. The negative bone balance associated with increased porosity is a consequence of reduced osteoblastic activity; osteoclastic activity remains more or less unchanged for any given remodeling event.

3. Increased porosity indicates reduced bone volume (m^3) which in cross-section translates to reduced area (m^2). Reduced bone area indicates reduced resistance to imposed loads whether axial, bending or torsional, and hence reduced bone strength.
4. For any two areas of bone, porosity will be either equal or unequal. Equal porosity implies an equal reduction in bone strength for that region of cortex; unequal porosity implies that strength reduction is greater in the one area than in the other.

In that geometry and porosity can have contrary effects on bone strength, and that these effects are variable in and of themselves, it is possible to contrive various theoretical combinations of geometry and porosity which optimize or minimalize strength. However, these combinations do not all conform to a model of conservancy.

Two scenarios are under consideration, given two axes of maximum and minimum geometric strength, labelled *Imax* and *Imin*. It is also assumed that porosity values along these axes are unequal. This is a reasonable assumption because, for non-circular sections, an equal porosity distribution throughout the cross-section would imply that there was no interaction between bone geometry and porosity. For the purpose of hypothesis formulation, unequal porosities are assumed. The two scenarios are labelled A and B. In scenario A, porosity is greater **along** the axis of least geometric resistance to bending; less **along** the axis of greatest geometric resistance to bending. In scenario B, the reverse situation exists. Porosity is greater **along** the axis of greatest geometric resistance; less **along** the axis of least geometric resistance. These two scenarios are illustrated in Figure 11. It is important to remember that the axis **about** which resistance to rotation is greatest indicates the direction **in** which resistance is least, and vice versa. This is true because the axes of maximum and minimum resistance are always orthogonal.

Scenario B combines the greater reduction in bone strength due to porosity with the greatest geometric strength; similarly, the lesser reduction in bone strength due to porosity is

Figure 11.
Scenarios for porosity/geometry interaction.
N = Direction of maximum bending strength.
X = Direction of minimum bending strength.

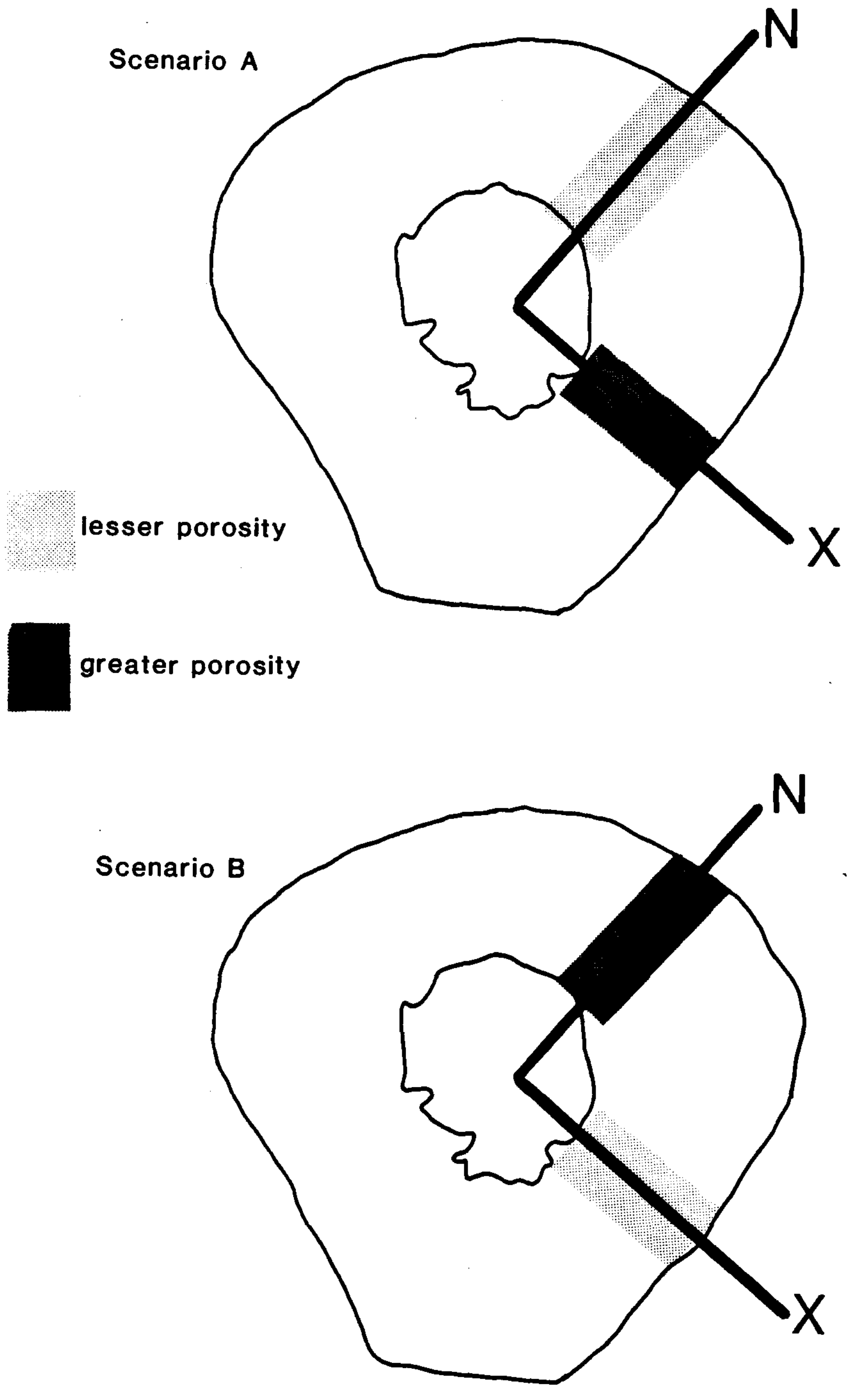
Scenario A
N
X
lesser porosity
greater porosity
Scenario B
N
X

associated with the least geometric strength. On the other hand, scenario A combines the weaker porosity situation with the weakest geometric situation, and the stronger porosity situation with the strongest geometric situation. Clearly, scenario B fulfills the requirements of a conservancy model, scenario A does not. In the latter, the 'natural resources' of the skeleton are not put to 'wise' use: the combination of two weak situations would seriously compromise the mechanical competence of the bone, while the combination of two strong situations is arguably inefficient and contradicts the 'maximum–minimum' corollary of Wolff's Law (Martin 1984).

If bone geometry and porosity vary independently, both scenarios are expected to occur, with potentially disastrous results in scenario A cases. A conservancy model for the interaction of bone geometry and porosity comprises the following major hypotheses, which will be subject to evaluation in the following chapters.

1. Greater porosity should occur **along** an axis of greatest geometric resistance to bending. This region of bone will be located perpendicular to the maximum moment axis **about** which resistance is greatest.
2. The magnitude of the difference in porosity for cortex perpendicular to the maximum and minimum moment axes should decrease as the difference between the moment of inertia values decreases. Greater similarity in the maximum and minimum moments of inertia indicates a more circular cross-sectional shape, and a greater likelihood of an absence of a dominant plane of bending in life. All components of bone strength should be equitably distributed in such a situation.

A corollary hypothesis concerning the relative movement of the periosteal and endosteal surfaces with aging can also be identified, based upon the (as yet unconfirmed) premise that continuous periosteal apposition **compensates** for expansion of the medullary cavity.

3. Changes in the distance from the section centroid (center of mass) to the endosteal and periosteal surfaces along an axis should be of the same sign, but not necessarily of the

same magnitude, in order to preserve an existing bending moment of inertia, *I*. An increase in the distance from the centroid to the periosteal surface, here termed the moment arm of the axis, can be considerably less than that from the centroid to the endosteal surface, since material further from the axis of bending contributes more to the moment of inertia. A minimum value does exist, however, below which the magnitude of *I* will be diminished, implying a loss of bending resistance along that axis (Lazenby 1986b). It is expected that changes in these distances (centroid to either surface) should be more sensitive to this minimum value along the maximum moment axis, which defines the direction of least bending resistance (see Chapter Five). As far as the mechanical competence of the element is concerned, deterioration of the minimum bending moment is potentially more disastrous than deterioration of the maximum bending moment. This is particularly true for cross-sections approximating a circle which implies a more-or-less equal likelihood of receiving large bending loads along all axes.

Support for these hypotheses would confirm a conservancy model for the interaction of the components of bone strength, and consequently for the interaction of the processes of internal and external remodeling. Lack of confirmation would lead to several questions immediately posed, not the least of which would be what factor(s) control the modeling and remodeling response and to what degree are they independent (Parfitt 1984a)?

CHAPTER V

MATERIALS AND METHODS

Sample Collection and Preparation

The sample for this investigation consists of 13 right femoral diaphyses (eight male and five female) obtained from medical school cadavers in the spring of 1981. All subjects had been embalmed in a phenol–formaldehyde solution. The mean age for males is 72.5 +/- 15.2 years, with a range of 50 to 96 years. For females, mean age is 78.2 +/- 5.6 years, with a range of 73 to 86 years. The sample taken as a whole has a mean age of 74.7 +/- 12.4 years, with 84.6 per cent falling in the range 72 to 82 years. Few of the specimens then, are from individuals less than 70 or greater than 82 years of age. At the time of collection, the main portion of the diaphysis was removed, wrapped in plastic bags and frozen. Although embalming is known to affect the material properties of bone (Reilly and Burstein 1974; Evans 1973; Burr 1980) no such effect has been recognized with regard to either geometric or physical properties. From each diaphysis, a single undecalcified transverse section was prepared for geometric and radiographic analysis.

In order to collect the different categories of data required, the sample was processed through various stages. These were:

1. location and removal of cross–sections from the diaphyses;
2. preparation of images of the cross–sections for geometric analysis; and
3. preparation of each cross–section for radiography and automated image analysis.

Each stage in turn involved a number of separate steps.

Preparation of Transverse Sections

The diaphyses were allowed to thaw at room temperature, after which the remaining soft tissue and periosteum were manually removed using forceps and the back (i.e., blunt) edge of a common kitchen knife. The bones were then towelled dry and the identification number marked directly on the bone surface with an indelible marker. As well, the sagittal plane was marked on the anterior surface of each bone. In that the proximal and distal ends were absent, standard methods for locating the sagittal plane of the femur (see Ruff and Hayes 1983a) could not be employed. Ruff and Hayes (1983a:362) argue that many geometric properties are highly sensitive to "bone positioning errors", and consequently that reference axes (e.g., sagittal and coronal) be defined "as precisely and consistently as possible". This stands to reason if specific inferences and conclusions are to be drawn, or if interindividual or interpopulational comparisons are to be made, with respect to these axes. In the present case, however, the reference axes serve only to locate the principal axes of interest (as detailed later in this chapter) and, since any two orthogonal axes will suffice for this purpose, the necessity for precise and consistent definition of the reference axes is relaxed. In this study then, a jig was improvised to provide a reference axis, consisting of a flat board into which a large nail was driven at either end. Between these nails a stout elastic band was stretched taut. Each diaphysis in turn was placed between the nails and under the elastic. With comparison to whole femora each diaphysis was positioned so that the elastic was stretched approximately along the sagittal plane, which was then marked using the elastic as a guide.

The diaphyses were then radiographed in an antero-posterior position. The bones were placed directly upon the film cassette, and supported such that the linea aspera faced the target in a plane perpendicular to the x-ray film. These radiographs were taken in order to determine the point at which the medullary canal has its minimum diameter. It was decided the cross-section should be taken at this site for two reasons. First, it would provide the largest cross-sectional area of cortex for evaluation (Smith and Smith 1976). Second, under the *a priori* acceptance of Wolff's Law, the point of greatest cortical thickness would be the point where the shaft is under its greatest osteogenic and/or remodeling stimulus, i.e., strain. It conforms, more or less, to the point depicted by Rybicki et al. (1972) as the site of maximum load, determined from a mathematical analysis of stress in the human femur considering both gravity and muscle load. Thus this region of the femur should have great potential for elucidating relationships between the various properties of bone considered in this study. The point of least medullary diameter was invariably located proximal to the estimated mid-point of the diaphysis.

After marking the location where the section was to be removed by superimposing the diaphysis on its radiographic image, a block was removed of suitable dimension for section cutting on a Beuhler Isomet slow speed saw (Figure 12). This block was removed on a bandsaw, and the marrow rinsed out under running water. Sections were cut at an average thickness of 0.48 mm on the Isomet saw. An initial cut per block was necessary in order to produce subsequent sections with parallel faces, suitable for grinding. The sections were clamped with Hoffman clamps between 50 x 75 mm glass slides and stored in tap water at room temperature to prevent dehydration.

Preparation of Images for Geometric Analysis

The onerous task of calculating the various geometric properties of the cross-sections (detailed below and in Appendix I) was made easier by employing enlarged image tracings of the sections, rather than the sections themselves. The approach used is similar to that of Martin and Atkinson (1977) in their analysis of the geometric variation in femoral cross-sections as a function of sex and age.

Images of the sections were obtained by placing them in contact with photographic paper, which was then exposed to light. They were subsequently developed and enlarged x4

Figure 12.
Section location and block technique for removal.
Block length was approximately 25 mm, and an approximately 7 mm 'handle' was cut at the distal end to facilitate loading the block into the chuck of the Isomet saw (Chris Justice, personal communication).

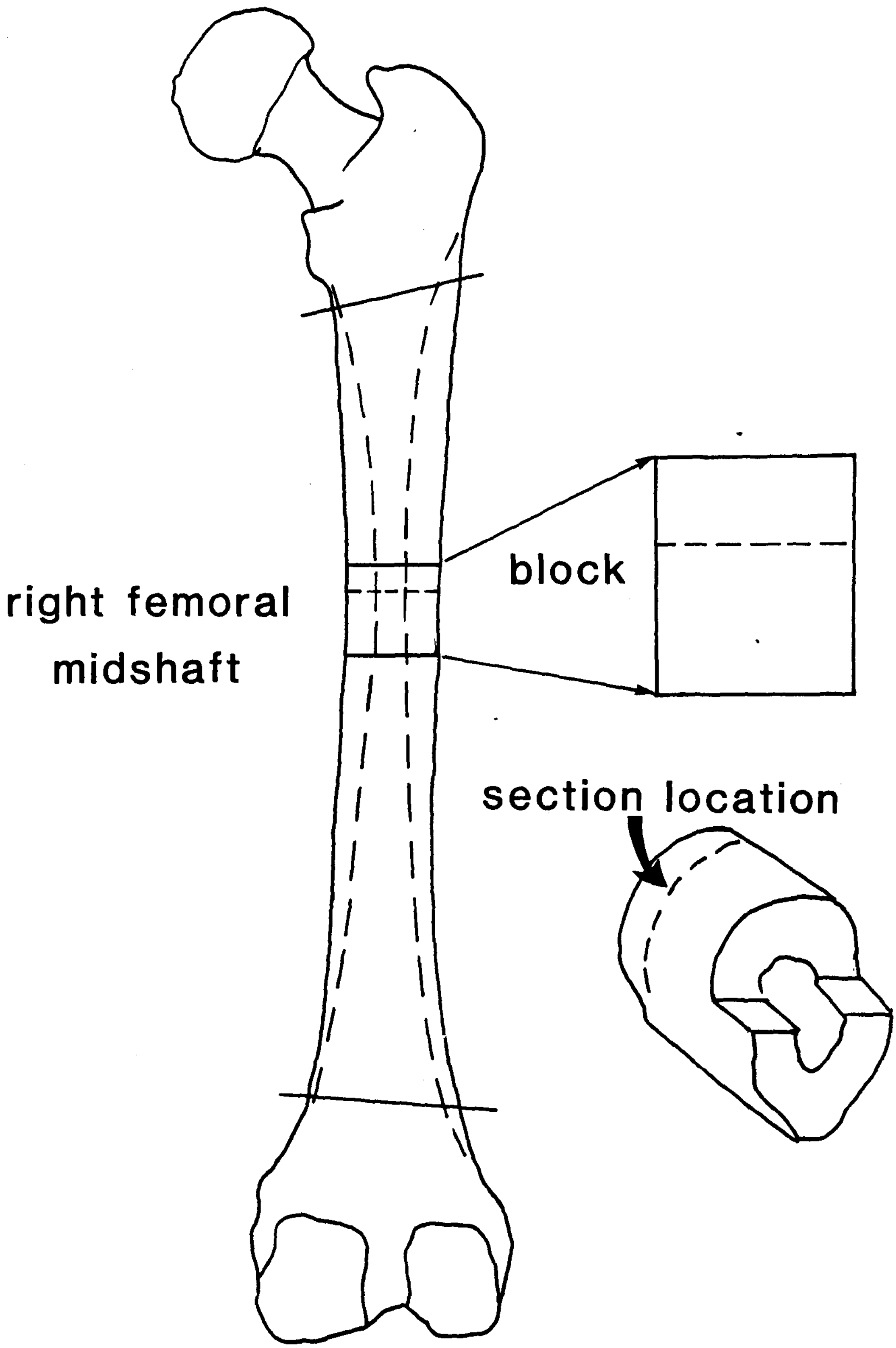
right femoral
midshaft
block
section location

on a Kargl Reflecting Projector and the inner and outer margins were manually traced. The position of the sagittal plane had been marked on the photograph with reference to the actual sections (by superposition), and was subsequently transferred to the enlarged tracing. The mean proportional error due to enlargement was determined by comparing antero–posterior and medio–lateral diameters of the enlarged image to those of the photograph, using needle–point dial calipers accurate to 0.05 mm. The error amounted to −2.2 +/− 0.51%. All geometric properties, with two exceptions (see below), were obtained from the enlarged image making the appropriate corrections for enlargement.

Preparation of Radiographs of the Cross- Sections

The preparation of sections for radiography involved hand–grinding (Frost 1958) to a final thickness of approximately 70 microns, after which they were ultrasonically cleaned in tap water and household detergent for at least thirty minutes. This removed the vast majority of grit which, using Frost's technique, tends to become trapped in the vascular spaces of the cortex. Sections were then placed between single sheets of filter paper, Hoffman clamped and allowed to air dry. Although some shrinkage would be expected in drying, on the order of two to three per cent in area (Frost 1976b), subsequent superposition of the radiographic image of the ground cross–section upon the 'un–ground' photographic image revealed this to be negligible or non–existent.

Radiographs were prepared by technicians at Forintek Incorporated, Vancouver, a forest research company which specializes in, among other things, fine–detail radiography of tree cores for dendrochronolgy. The radiographs were made using a Kevex K5020 power source with a tungsten target. The section was placed directly on the film cassette. The target to film distance was set at 11.5 cm and the film used was Kodak single–coated Industrex, type 'R'. The film was exposed at 5 kV/1.0 mA for 3 seconds. This technique resulted in x–rays of sufficiently long wavelength (i.e., 'softness') to produce an image of the variable density and porosity of the bone when viewed microscopically. It should be noted that the resulting image is not a microradiograph, in the strict sense (Jowsey 1973; Hobdell and Braden 1971; Boiven and Baud 1984). Microradiographs are produced using a significantly different apparatus and exposure (typically, longer exposure times and somewhat 'harder' x-rays). The radiographic images obtained in the present case are, however, comparable to true microradiographs in that they reveal the density variation as shades of grey. Higher density bone (i.e., a higher mineral/volume ratio) absorbs more x-rays, producing a lighter image. Lower density bone permits more x-rays to reach the film emulsion, which produces a darker image. Porous areas of the section offering no impedence to the the x-rays, such as vascular spaces, appear as totally exposed, black areas (Jowsey 1966). Occasionally, bits of extraneous grit would remain trapped within vascular spaces after ultrasonic cleaning. These bits are of a density and/or thickness exceeding that of the surrounding bone and would appear as bright, white inclusions radiographically. Their effect on the evaluation of the radiographs is discussed in a later section of this chapter.

Data Collection

Data for this study fall into two categories:

1. geometric properties; that is, those concerned with cross-section size and shape; and
2. physical properties; those dealing with mineral density variation and, particularly, cortical porosity which reflect internal remodeling dynamics.

Each category entailed a different methodological design for data acquisition and analysis.

Geometric Properties

Calculation of the geometric properties first required locating the section centroid. This was necessary in order to determine the position of the principal transverse orthogonal axes which in turn locate the microscopic fields to be investigated. The centroid can be considered equivalent to the center of gravity, assuming that all forces (i.e., weights) distributed throughout the area are equal. It is the point through which the longitudinal neutral axis passes, and at which (given an applied bending force) tensile and compressive stress and strain are zero. On either side of the neutral axis, depending on the direction in which the force is applied, tensile or compressive stress is created, the magnitude of which increases with increasing distance from the neutral axis (Nordin and Frankel 1980; see Figure 7).

Several techniques are available for locating the centroid of an irregular section, for example Mohr's method (Lovejoy et al. 1976), or suspension from two points (Martin 1975). In the present case, the centroid was determined using a point-count approach and the formula for finding the center of mass of a system of masses (Arya and Lardner 1979). A 20 x 20 cm grid with 1 cm spacing was superimposed over each enlarged section image and the rectangular co-ordinates of each grid intersection falling upon the represented cortical area was determined. Intersections which were crossed by the traced periosteal or endosteal borders were counted and ignored, alternately, following accepted stereological procedure (Villaneuva 1976). Points falling within the endosteal border (i.e., in the medullary space) were ignored. The formulae employed (Arya and Lardner 1979:346) were

$$\bar{x} = \frac{\sum_{k=1}^{n} m_k x_k}{\sum_{k=1}^{n} m_k} \qquad \bar{y} = \frac{\sum_{k=1}^{n} m_k y_k}{\sum_{k=1}^{n} m_k}$$

where $\bar{x}$ and $\bar{y}$ are the centroid co-ordinates; x and y are the rectangular co-ordinates for each intersection counted; and m is the mass of each intersection. In the present case, all masses were assumed to be equal and hence arbitrarily assigned a value of 1.0, which simplified the equations to

$$\bar{x} = \frac{\sum_{k=1}^{n} x_k}{n} \qquad \bar{y} = \frac{\sum_{k=1}^{n} y_k}{n}$$

The accuracy of such a point-count method will be a function of the spacing between points relative to the area over which the points are distributed in space (Villaneuva 1976). Thus, the greater the proportion of intersections lying within the area of interest, the lower the error involved in the estimate.

The reliability of this approach for locating the centroid was checked by applying the technique to regular geometric areas (circles, squares, triangles, rectangles) for which the precise centroid can be algebraically determined. As an illustration, a triangle is depicted in Figure 13. The true centroid is at one-third of its height, along a line from the apex to the base mid-point (Beer and Johnston 1981). The estimate of the centroid location was found to be $\bar{x}$ = 11.46, $\bar{y}$ = 12.83 The relative positions of centroids, known and estimated, are as shown, with the close agreement evident.

Having located the centroid for each enlarged section outline, the antero-posterior and medio-lateral reference axes (designated 'a' and 'l') were drawn in. The antero-posterior axis

Figure 13.
Locating the section centroid by point-count technique.

$\bar{x}$ co-ordinates:	$\bar{y}$ co-ordinates:
$8(3) = 24$	$10(7) = 70$
$9(5) = 45$	$11(8) = 88$
$10(8) = 80$	$12(8) = 96$
$11(9) = 99$	$13(7) = 91$
$12(7) = 84$	$14(5) = 70$
$13(6) = 78$	$15(5) = 75$
$14(4) = 56$	$16(3) = 48$
$15(3) = 45$	$17(2) = 34$
$16(1) = 16$	$18(1) = 18$
$\Sigma\ (46)\quad 527$	$\Sigma\ (46)\quad 590$

$$\bar{x} = \frac{527}{46} = 11.46$$

$$\bar{y} = \frac{590}{46} = 12.83$$

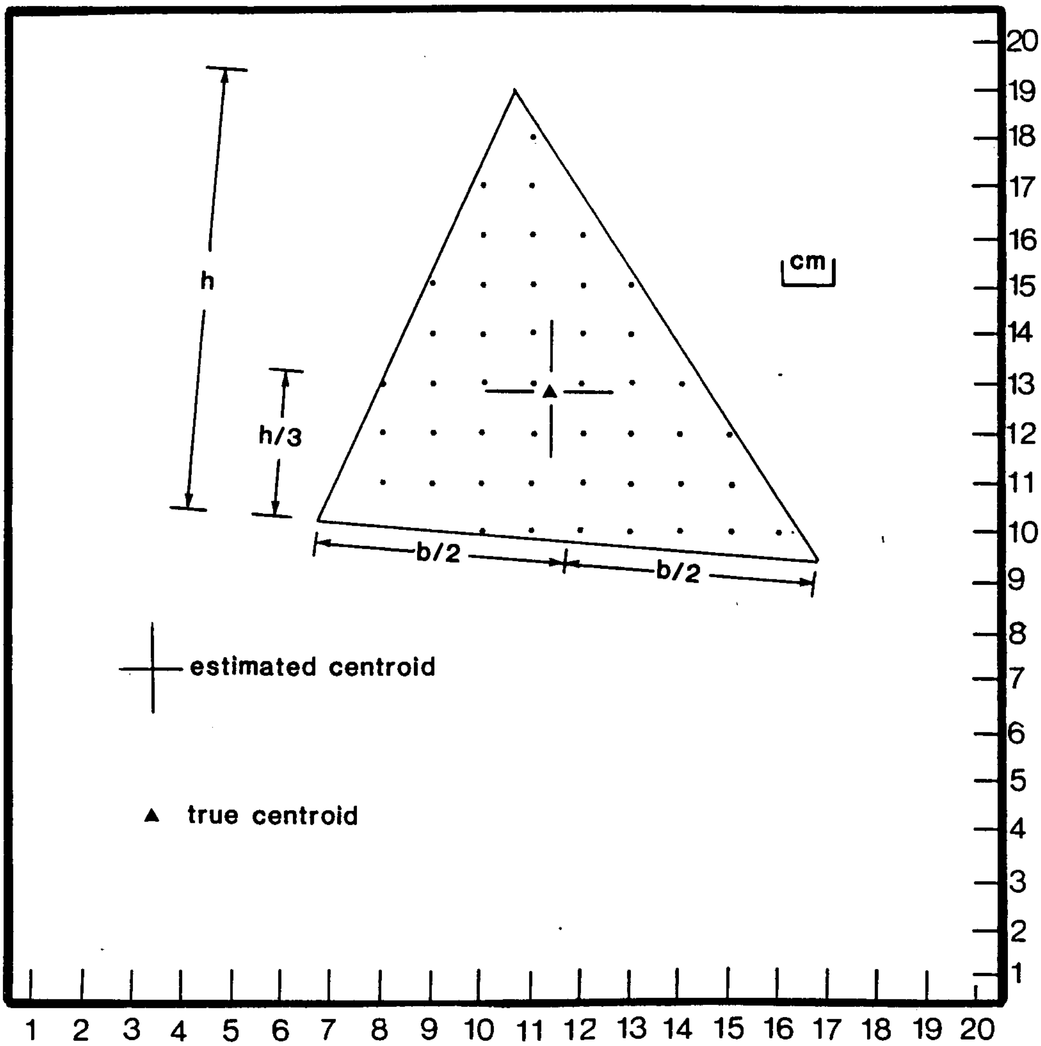

was defined by extending a straight line joining the centroid and the marked sagittal plane. The medio-lateral axis exists perpendicular to it, also passing through the centroid (Figure 14). With these two orthogonal centroidal axes in place, the following geometric properties were measured.

1. Total cross-sectional area [TAREA]: This is the total area circumscribed by the periosteal margin of the cross-section, including both bone and medullary cavity.
2. Medullary area [MAREA]: This is the marrow space area circumscribed by the endosteal margin.
3. Cortical area [CAREA]: This is the area of cortical bone contained between the endosteal and periosteal boundaries of the section.

Total Area and Medullary Area were measured using a point-count approach employing the same grid design as for centroid location. The areas were determined by the following formula (Villaneuva 1976):

$$\text{Unknown Area} = \bar{h}g / T400$$

where

h = the total number of 'hits', or intersections counted;

g = the known grid area, in this case 40,000 mm^2;

T = the total number of throws, which in this case was 4 per section; and

400 = the number of intersections in the entire grid.

Each 'throw' consists of counting the number of intersections within the area, after which the physical relationship between grid and area is altered randomly (e.g., by rotation) and a second count, or throw, is carried out. Increasing the number of 'throws' decreases the error of the area estimate (Villaneuva 1976).

4. Second Moment of Area about the centroidal axes [*Ia* and *Il*]: A 'moment' is defined as:

> A bending tendency that is calculated by multiplying the bending force times its lever or moment arm. Moment of inertia is a measure of the resistance of a given cross-section size and shape to bending and other kinds of deformation that occur when structures are loaded [Frost 1964:147].

The area moments about the centroidal axes refer to resistance offered by the distribution of bone on either side of these axes to rotation about these axes. The calculation of *Ia* and *Il* follows Lovejoy et al. (1976). It involves subdividing the area on either side of the reference axis into gridded squares of equal area, e.g., equal to x^2. Squares crossed by the endosteal or periosteal border will have variable areas, always less than x^2. The square of the distance from the reference axis to the **grid square centroid**, (i.e., not the cross-section centroid) for each grid square containing bone is multiplied by the area of bone within it. These products are then summed over the entire surface to determine the value of *I* for a given reference axis, which will be measured in units to the fourth power. The method is detailed in Appendix I.

5. The Principal Moments of Inertia [*Imax* and *Imin*]: For any given cross-sectional size and shape, two principal axes can be determined about which resistance to rotation has a maximum and minimum value. Because these axes are orthogonal, they also indicate direction in which resistance is greatest and least. The *Imax* axis is the axis **about which** resistance is maximum, and denotes the direction **in which** resistance is minimum. The converse holds for the *Imin* axis. Figure 14 clarifies this situation.

The values of *Imax* and *Imin* were calculated algebraically from the values of *Ia* and *Il*. Also required for this calculation was a value for the product moment of area *Ial*, the derivation of which is detailed in Appendix I. This value was not used in subsequent analyses. The formulae for calculating the Principal Moment Areas (Martin and Atkinson 1977) were:

$$Imax = \frac{Ia + Il}{2} + \sqrt{Ial^2 + 1/4\ (Ia - Il)^2}$$

$$Imin = \frac{Ia + Il}{2} - \sqrt{Ial^2 + 1/4\ (Ia - Il)^2}$$

Figure 14.
A typical cross-section depicting reference and principal moment axes.
A: Antero–posterior axis; L: Medio–lateral axis.
N: Minimum moment axis; X: Maximum moment axis.

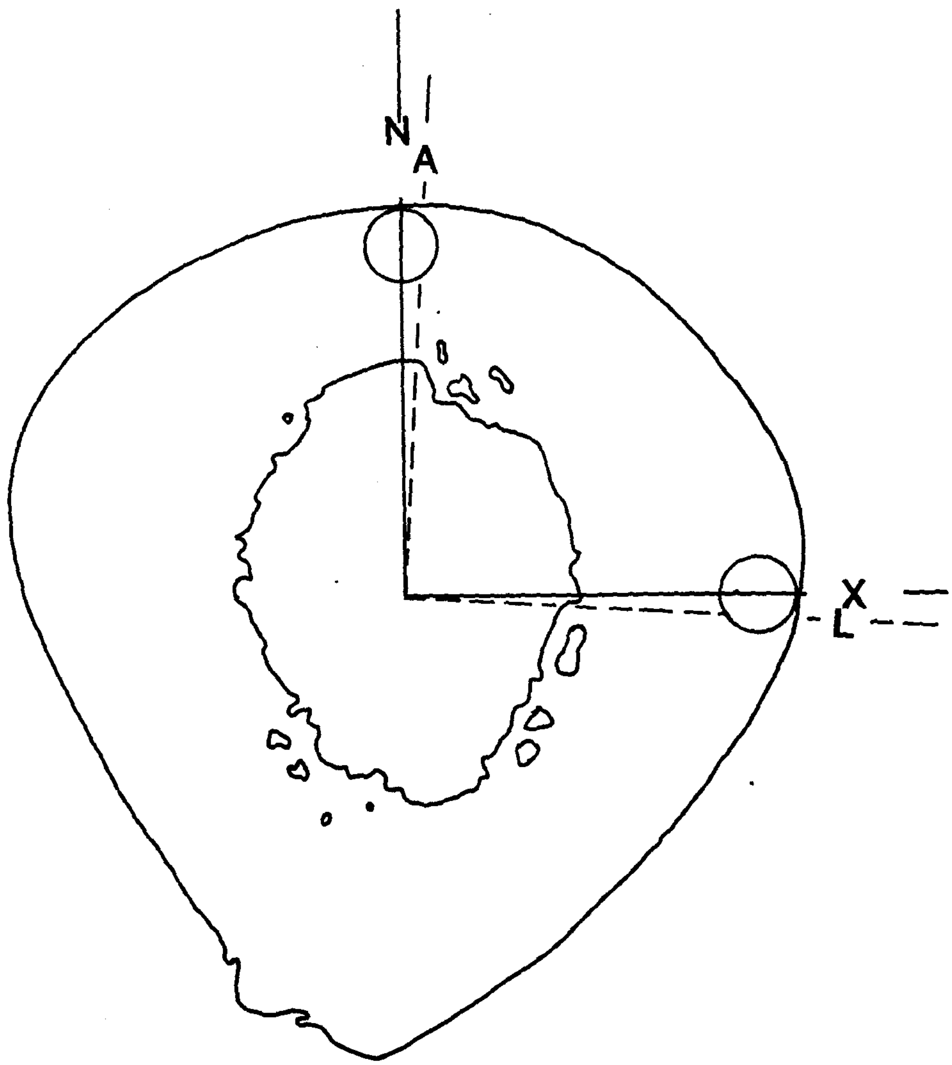
N
A
X
L

6. Angle Deviation to *Imax* [θ]: This variable is the degree of rotation of the *Imax* axis from the reference axis (e.g., *Ia*). The angle deviation was calculated algebraically from the following formula (Martin and Atkinson 1977):

$$\theta = \tfrac{1}{2} \tan^{-1} \left[\frac{2Ial}{Ia - Il} \right]$$

It is also possible to determine θ using a Mohr's Circle approach (Lovejoy et al. 1976). This method was used as a check, with excellent correspondance obtained in all cases. The direction of rotation of the principal axes is given by the sign of the product moment, *Ial*. If positive, axes are rotated clockwise; if negative, counter-clockwise (Lovejoy et al. 1976). The value of θ was not used in subsequent analyses. This value can only have biological meaning if the location of the reference axes (*Ia* and *Il*) is precisely determined for a sample, such as in Ruff and Hayes (1983a,b) and Ruff et al. (1984). In the present study θ serves only to locate the principal axes.

7. Polar Moment of Area [J]: The polar moment of area is "The effective resistance of a cross-section to rotation about its centroid, the axis of rotation being perpendicular to the plane of the section" [Frost 1964:148] (Figure 15). There is a positive relationship between the value of this variable and the strength and rigidity of the cross-section in torsion (Ruff and Hayes 1983a:361). Calculation of the polar moment is arithmetic, being the sum of any two orthogonal moments of area. Hence,

$$J = Ia + Il = Imax + Imin$$

8. The Principal Moment Ratio [MR]: In terms of bending moments, this ratio is an index of shape:

Figure 15.
The relationship of area and polar moment axes in three-dimensional space.
A_1: The longitudinal neutral axis in torsion. The polar moment of inertia is a measure of resistance about this axis.
A_2, A_3: Two possible neutral axes in bending. Resistance to rotation about either is measured by the area moment of inertia for each axis.

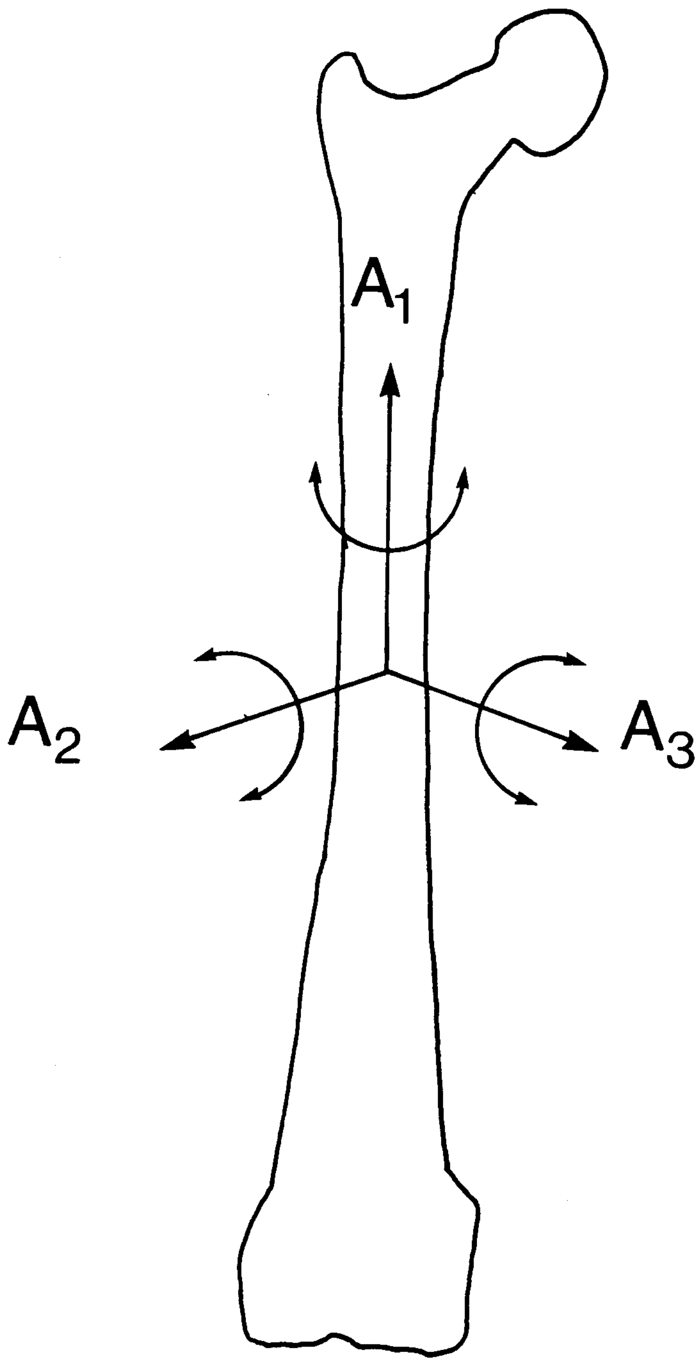
A1
A2
A3

> An Imax/Imin ratio close to 1.0 indicates near circularity of shape, while a ratio much greater than 1.0 indicates a significant departure from circularity and a strongly defined direction of greatest bending rigidity [Ruff and Hayes 1983a:369].

The parameter which most affects the value of any area moment is the distance from the centroid to the outermost fibre of the section, along the axis of interest (see Appendix I). A circular section has its centroid equally distant from any point around the circumference, hence the area moments for any two axes (orthogonal or not) will be equal and their ratio will be 1.0. For long bone cross-sections which approximate a cylinder, having an inner (endosteal) and outer (periosteal) circumference, the shape of the outer circumference will be more intimately associated with the ratio value, being further removed from the centroid. The ratio is therefore an index of the **external** shape of the section, an interpretation supported by the high degree of correlation obtained between this index and the ratio of antero-posterior and medio-lateral diameters in fossil prosimian and modern human femora and tibia (Jungers and Minns 1979).

9. Moment Arm [Y]: The moment arm constitutes part of the expression for normal stress in a beam (see Chapter Three). For the balance of this study, Y refers to the distance from the section centroid to the outermost fibre of the cross-section (i.e., the periosteal surface).

10. Section Modulus [Z]: In bending, the maximum tensile and compressive stresses will be found in the outermost fibres along an axis normal to the plane of bending. The value of Z is determined arithmetically, as I/Y where Y is the moment arm length, as defined above. Finding the maximum and minimum section moduli for a cross-section of irregular shape would require determining the ratio of all possible values of I and their corresponding distances, Y. Clearly, this would be an onerous task. Following Ruff and Hayes (1983a), two representative section moduli were determined in this study, associated with *Imax* and *Imin*. In that the section modulus is used in calculating the

maximum stress for any given bending force, the value of Z provides a relative measure of strength along an axis, all else being equal.

11. Cortical Thickness [CT]: The thickness of the cortex along the ***Imin*** and ***Imax*** axes was measured. Cortical thickness can be considered notionally equivalent to apparent density as determined by radiogrammetry (Johnston 1983), when considered relative to the width of the medullary canal. In the present case only the cortex along that portion of the respective moment axes directed anteriorly and laterally was measured. The reason for this restricted interest is given below. This variable is interpreted as apparent density when considered relative to the length of the moment axis, Y.
12. Cortical Thickness/Moment Arm Ratio [TMR]: Calculated for both principal axes, this ratio expresses the relationship between cortical thickness along an axis and the length of that axis. The ratio indicates the relative movement of the periosteal and endosteal surfaces perpendicular to a neutral axis of maximum [TMRN] and minimum [TMRX] resistance to bending. It was calculated arithmetically, as [CT / (Y−CT)], for each axis.

Table 5 lists the geometric variables used in this study; also depicted in Figure 16. Data for all variables but section modulus and cortical thickness were collected from the enlarged tracings of the actual bone sections, hence appropriate correction factors accounting for magnification were applied. The value of the correction factor equals the inverse of the magnification factor raised to the power of the variable dimension. For example, the appropriate correction for a moment of inertia is $1/4^4 = 1/256 = 0.00390625$. The section modulus was calculated using the corrected values for principal moments and Y measured directly from the cross-sections photographs, using needle-point dial calipers accurate to 0.05 mm. Similarly, cortical thickness was measured directly from the cross-section photographs used to prepare the enlarged image tracings.

Figure 16.
Geometric variables used in this study.
N and X denote the minimum and maximum area moment axes, respectively.
The shaded area represents an area of cortex, dA. Integration of all such areas with respect to distance squared equals the moment of inertia for that axis. The polar moment of inertia equals the sum of any two orthogonal area moments.

$$TMRN = \left[\frac{CTN}{YN - CTN}\right] \times 100$$

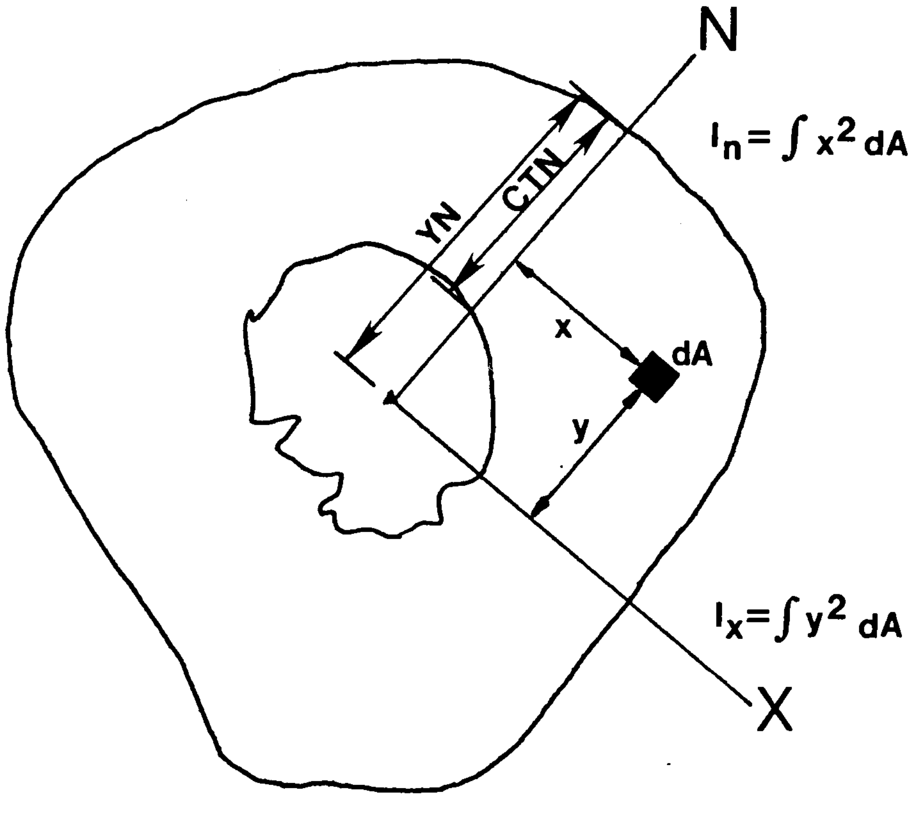

Table 5. **Geometric Variables Used in This Study.**

Variable	Symbol	Dimension	Correction
1. Total Area	TAREA	mm^2	0.0625
2. Medullary Area	MAREA	mm^2	0.0625
3. Cortical Area	CAREA	mm^2	0.0625
4. Principal Moments	I	mm^4	0.00390625
5. Polar Moment	J	mm^4	0.00390625
6. Moment Ratio	MR	none	none
7. Moment Arm	Y	mm^2	none
8. Section Modulus	Z	mm^3	none
9. Cortical Thickness	CT	mm	none
10. Thickness/Arm Ratio	TMR	none	none

Physical Properties

Two subperiosteal fields were located on the radiographs with reference to the principal moment axes (Figure 14). Each moment axis passes through the periosteal margin at two points. For *Imax* and *Imin* then, four possible fields would be available for evaluation. However, only one of each pair was selected. As reviewed in Chapter Three, bone is stronger under compression than under tension; therefore, it was deemed more profitable to seek out relationships between bone cross-sectional geometry and porosity properties in areas where their relative contributions to strength are more critically involved. Hence, fields directed anteriorly and laterally along the principal axes were selected, since the femur tends to be stressed in tension primarily in these regions. This decision is further supported by the fact that, according to Frost (1985), the level of strain above which remodeling is stimulated (i.e., the Minimum Effective Strain) is approximately 1000 microstrain less in tension than in compression. Thus, remodeling will be stimulated under lower strains in tension than in compression.

The two fields were viewed under a Nikon stereomicroscope at x40 magnification, and were evaluated for porosity using automated image analysis. In this technique, a videocamera transmits the microscope image to a black and white television monitor. The monitor image is composed of thousands of individual elements, called pixels, each of which has a particular value of greyness. The differences in greyness intensity provide the discrimination of features in the image. The intensity of each pixel is evaluated by the analyser, which then provides a measure of the pixel's optical density relative to all other pixels extracted for analysis. This process is referred to as 'grey level analysis' (Jarvis 1981). The total number of pixels having an equal intensity of grey comprise a grey level. The intensity which corresponds to a grey level does not necessarily have a single value, but may comprise a range of intensities. The width of this range can be selected by the operator in consideration of the goals of the analysis, image contrast and so on.

Two modes of analysis are available (Bradbury 1979). If the operator is using feature mode, then only those pixels forming a small part of the total image (i.e., the feature) are analysed. Alternatively, field mode may be used, in which all pixels on the monitor are evaluated. Whether in feature or field mode, the accuracy of image analysis will ultimately be determined by the size of the individual pixels; that is, by the resolution of the monitor, since a pixel is the smallest unit of area available for analysis (Smith and Jee 1983). For two monitors of equal area, progressively higher resolution is obtained by having progressively smaller pixel areas. The result is that more pixels are available for evaluation. Very high resolution image analysers, such as the Quantimet 720 (Cole and Bond 1972) have a pixel density on the order of 500,000 points (Jarvis 1981) and are thus eminently suited for fine-detail analyses such as of cellular ultrastructure (e.g., Sawicki et al. 1974; Nicolini et al. 1977).

Image analysis offers a number of advantages over traditional microscopical analysis, such as speed, decreased observer bias and decreased observer fatigue (Smith and Jee 1983). It also possesses particular problems, for example 'shading' (Cole and Bond 1972) or 'glare' (Jarvis 1981). These result when the transmission of light from the specimen to the videocamera is enhanced or degraded differentially by sources foreign to the specimen.

Typically, the analyser cannot discriminate among such artifacts, although more recent models may be coupled with components such as shading correctors (e.g., Nicolini et al. 1977). Thus, features having identical true optical densities may be evaluated as different (Cole and Bond 1972), or vice versa. In order to minimize these effects, it is best to standardize the operating conditions of the system. This would entail minimizing extraneous light sources and conducting periodic checks on the microscope optics to ensure consistent quality of illumination.

Two further sources of error arise with particular reference to image analysis of radiographs. First, the measured optical density of a radiographic image will be determined by the mineral **volume** of the bone specimen. In turn, mineral volume is determined by mineral density and by specimen thickness. Thus, in order to evaluate the two-dimensional variation in mineral density, it is necessary that the original sections be of uniform thickness. However, with regard to automated image analysis, Smith and Jee (1983:293) have noted "The systematic error introduced using 100 [micron] sections compared to infinitesimally thin sections has not been quantified experimentally". Therefore, although the presence of some systematic error in optical density measurement due to unequal bone volumes is expected, its magnitude cannot be assessed.

The second source of error has previously been mentioned. This concerns the inclusion within vascular spaces of high density debris as a result of the grinding process. Though most of this was removed by ultrasonic cleaning, some remained and appeared in the resulting radiographs as bright, white points or spots. Since these particles are trapped within vascular spaces, they account for a portion of the section's porosity. Therefore, the measure of porosity for those fields in which inclusions appear required consideration of the grey levels corresponding to both the bright white areas, as well as the totally-exposed, black areas.

The system used in this study was developed by Infrascan, Incorporated, of Richmond, British Columbia. It consisted of an RCA Vidicon videocamera and analyser interfaced with an Apple IIe microcomputer. The monitor has a pixel density of 49,152 which, while not offering high resolution, is comparable to systems employed elsewhere in image analysis of bone section radiographs (e.g., Phillips et al. 1978).

Output from this analysis is in the form of a relative frequency histogram, accompanied by a tabulated pixel count and relative pixel frequency for each interval. The number of intervals in the grey scale (i.e., black through greys to white) is set by the operator. Although written for general application, the HISTOGRAM program, as it is called, is particularly suited for the present purpose since information regarding optical density and porosity in bone radiographs is presented as a scale from black (zero density) to white (absolute density), the two extremes which are of direct interest in this study.

The area of bone evaluated by HISTOGRAM is that which appears on the monitor faceplate, and is equal to 2.08 mm by 1.49 mm, or 3.1 mm^2. The radiograph of each bone section was situated on the microscope stage such that the long axis of the monitor represented a periosteal to endosteal transit, with the periosteal margin aligned with one edge of the screen. In this way, more area along the principal axes could be evaluated, rather than adjacent areas which are more likely associated, mechanically, with somewhat different area moments.

In the present case only one parameter was derived from the automated image analysis: cortical porosity for the *Imax* and *Imin* fields. This could be assessed directly from the relative proportions of pixels scored in the 'black' interval scale (plus the 'white' interval scale, where debris inclusions had to be considered). An attempt was made to quantify the variation in mineral density based on a complete grey level analysis. While not required to test the specific hypotheses of this thesis, such data would have provided insight into the rate of new Haversian system formation based on the fact that newly deposited bone is less mineralized initially. However, the quality of the cortical bone radiographic image was deemed too variable for interfield comparison, likely due to non-uniform irradiation (Boivin and Baud 1984). Although considerable variation in mineral density was apparent within any given *Imax* or *Imin* field, it was not possible to standardize interval scales between fields for any single section, which would have been necessary for a valid comparison of the two fields. In future, such an analysis will no doubt provide useful information on the relationship of modeling and remodeling processes.

Data were analyzed using the SPSS-X programs available through the MTS system at Simon Fraser University. The absolute pixel counts for porosity were converted to relative percentages since the total pixel density for the monitor was known and the area evaluated for each field was constant for all sections.

Bivariate and multivariate analyses were performed. A Pearson product-moment correlation matrix and a principal components analysis were used to explore the data set for general porosity-geometry relationships. Various parametric (t-test) and nonparametric (sign test) statistical tests were used to identify specific relationships in magnitude and direction for porosity, apparent density and geometry. Chapter Six presents these results along with discussion of their significance in terms of the hypotheses presented earlier.

CHAPTER VI

RESULTS AND DISCUSSION

Results

The results from this study will be presented in several parts. The first part will deal with general patterns of variation and relationships in the data set. The second will examine specific relationships between geometry, apparent density and porosity which refer directly to the hypotheses formulated in Chapter Four. The second half of this chapter presents a discussion of specific results in terms of conservation of bone strength and preservation of the strain environment.

General

The data set for all 13 individuals is presented in Table 6. The Table includes a ratio variable not previously defined, namely, PORRAT. This variable is the ratio of porosity values for the *Imin* and *Imax* fields, here designated PMIN and PMAX. It indicates the difference in magnitude of porosity and, as the ratio approaches a value of 1.0, it signifies an increasingly similar degree of porosity for the two fields. This variable was calculated specifically to test Hypothesis Two (Chapter Four). Two analyses were performed to examine the general degree and pattern of linear association in the data. A Pearson product-moment correlation matrix was calculated based on all variables, and a principal components analysis was performed excluding the ratio variables.

Examination of the correlation matrix (Table 7) shows a definite lack of correlation between porosity variables (PMIN, PMAX, PORRAT) and any of the geometric variables. As would be expected, significant correlations occur with respect to closely related variables (IMAX or IMIN with CAREA) and certain ratios and their constituents (TMRX, TMRN with

Table 6. The Data Set Used In This Study

SUBJECT	AGE	SEX	TAREA[1]	MAREA[1]	CAREA[1]	IMAX[2]	IMIN[2]	ZMAX[3]	ZMIN[3]	J[2]	MR	PMAX[4]	PMIN[4]	PORRAT
11	52	M	719.5	126.6	592.9	14258	11660	950	728	25918	1.22	9.16	13.91	0.66
13	72	M	643.8	85.9	557.9	12765	8776	926	536	21542	1.45	1.53	3.85	0.40
14	73	F	479.7	79.7	400.0	6970	5340	614	427	12311	1.31	6.32	7.05	0.90
16	80	M	667.2	139.1	528.1	13149	9161	960	556	22310	1.44	9.05	5.99	1.51
17	76	F	414.8	62.5	352.3	4880	4631	488	408	9512	1.05	3.14	4.36	0.91
18	86	F	585.9	183.6	402.3	9955	6381	716	428	16366	1.56	20.64	48.54	0.43
20	50	M	660.9	182.0	478.9	10588	10110	756	706	20698	1.05	3.13	5.24	0.60
24	74	F	909.4	232.8	676.6	22880	15451	1397	874	38331	1.48	8.68	13.31	0.65
26	79	M	593.0	178.9	414.1	9879	7658	725	526	17538	1.29	2.88	6.45	0.45
31	82	F	568.8	174.2	394.6	8340	6877	606	492	15218	1.21	2.86	4.39	0.65
32	72	M	775.8	84.4	691.4	17534	13563	1223	806	31097	1.29	2.36	4.06	0.58
34	79	M	825.8	179.7	646.1	16884	15315	1036	939	32199	1.10	4.01	5.43	0.74
39	96	M	728.9	213.3	515.6	12764	11569	819	908	24327	1.10	9.74	14.09	0.69

1. mm^2 2. mm^4 3. mm^3 4. %

TAREA = Total Area; MAREA = Medullary Area; CAREA = Cortical Area; IMAX = Maximum Moment of Inertia; IMIN = Minimum Moment of Inertia; ZMAX = Section Modulus, Imax Axis; ZMIN = Section Modulus, Imin Axis; J = Polar Moment of Inertia; MR = Principal Moment Ratio; PMAX = Porosity; Imax Field; PMIN = Porosity, Imin Field; PORRAT = Porosity Ratio

Table 6. The Data Set Used In This Study cont'd...

SUBJECT	AGE	SEX	CTX[5]	YX[5]	CTN[5]	YN[5]	TMRX	TMRN
11	52	M	9.1	15.0	8.1	16.0	1.54	1.03
13	72	M	8.4	13.8	8.2	16.4	1.56	1.00
14	73	F	7.0	11.3	5.6	12.5	1.63	0.81
16	80	M	6.2	13.7	9.3	16.5	0.83	1.29
17	76	F	6.6	10.0	7.2	11.3	1.94	1.76
18	86	F	6.5	13.9	5.1	14.9	0.88	0.52
20	50	M	6.5	14.0	5.7	14.3	0.87	0.66
24	74	F	8.4	16.4	6.5	17.7	1.05	0.58
26	79	M	7.1	13.6	5.6	14.5	1.09	0.63
31	82	F	6.6	13.8	4.8	14.0	0.92	0.52
32	72	M	10.0	14.3	8.7	16.8	2.33	1.07
34	79	M	9.2	16.3	6.4	16.3	1.30	0.65
39	96	M	5.6	15.6	7.3	12.7	0.56	1.35

5. mm

CTX = Cortical Thickness, Imax Axis; YX = Moment Arm Length, Imax Axis;
CTN = Cortical Thickness, Imin Axis; YN = Moment Arm Length, Imin Axis;
TMRX = Thickness/Moment Arm Ratio, Imax Axis; TMRN = Thickness/Moment Arm Ratio, Imin Axis

Table 7. Pearson Product-Moment Correlation Coefficients

	TAREA	MAREA	CAREA	IMAX	IMIN	ZMAX	ZMIN	MR	J	PMAX	PMIN	PORRAT
TAREA	1.0000											
MAREA	.5756	1.0000										
CAREA	.9195	.2079	1.0000									
IMAX	.9747	.4650	.9425	1.0000								
IMIN	.9741	.4657	.9413	.9437	1.0000							
ZMAX	.9281	.3218	.9555	.9833	.9003	1.0000						
ZMIN	.8974	.5041	.8311	.8187	.9491	.7488	1.0000					
MR	.1422	.0913	.1262	.2677	-.0390	.3273	-.2638	1.0000				
J	.9822	.4721	.9552	.9897	.9813	.9612	.8866	.1391	1.0000			
PMAX	.0433	.4438	-.1615	.0251	-.0911	-.0199	-.0849	.4953	-.0230	1.0000		
PMIN	-.0102	.3962	-.2027	-.0251	-.1406	-.0739	-.1539	.5429	-.0746	.9334	1.0000	
PORRAT	-.1071	-.1611	-.0507	-.0853	-.0810	-.0360	-.0795	-.2089	-.0850	-.0160	-.3409	1.0000
AGE	.0244	.5977	-.2581	-.1551	-.0301	-.2743	.1936	-.2613	-.1028	.5266	.4506	-.0136
TMRX	-.1771	-.8033	.1767	-.0494	-.0315	.0729	-.1126	-.1186	-.0426	-.5317	-.4017	-.1158
TMRN	-.3010	-.5163	-.1119	-.2788	-.1941	-.2104	-.0625	-.4125	-.2464	-.2081	-.3438	.4633
CTX	.5538	-.1937	.7556	.6273	.6322	.6760	.4622	.1024	.6382	-.4302	-.2874	-.3392
YX	.9252	.7686	.7374	.8359	.8622	.7422	.8311	.1274	.8592	.1715	.1514	-.2374
CTN	.2830	-.3797	.5210	.3399	.3252	.4479	.2797	.0193	.3380	-.2439	-.3912	.4332
YN	.7878	.2811	.8073	.8448	.7074	.8721	.4687	.5482	.7973	.0130	.0156	-.0744

Table 7. Pearson Product-Moment Correlation Coefficients cont'd...

	AGE	TMRX	TMRN	CTX	YX	CTN	YN
AGE	1.0000						
TMRX	-.7527	1.0000					
TMRN	.0652	.3001	1.0000				
CTX	-.6653	.6382	-.2556	1.0000			
YX	.2967	-.4536	-.4646	.3488	1.0000		
CTN	-.2102	.3068	.6635	.2511	.0522	1.0000	
YN	-.3441	-.0139	-.4227	.6484	.6872	.3570	1.0000

CTX and CTN, respectively).

More informative are the variable combinations revealing low correlations. Medullary area (MAREA) is not associated with cortical area (CAREA) and only weakly associated with total area (TAREA) (p=.054, two-tailed) of which it forms a part. Interestingly, MAREA has significant negative correlations with TMRX and TMRN, though somewhat weaker with the latter. This is reasonable since TMRX and TMRN provide measures of the amount of cortical bone relative to medullary space along a moment arm perpendicular to a neutral axis. More insight is gained into this relationship by breaking down TMRN and TMRX into constituent variables. MAREA is positively correlated with YX (r=.7234, p=.005) but not with YN (r=.2359, p=.438). At the same time, MAREA is negatively associated with CTN and CTX, though not significantly. The relationship of MAREA to these variables suggests attempted maintenance of cortical thickness along the *Imax* axis - the axis along which resistance to bending is least. Increases in MAREA are countered by increases in YX. Cortical thickness is apparently not maintained along the *Imin* axis. More will be said about this relationship later.

In order to further elucidate relationships in the data set a principal components analysis was employed. Principal components analysis is a data reduction technique which seeks out variable combinations (components) that account for a majority of the variance in the data. Unlike factor analysis, principle components analysis requires no assumptions regarding the sources of variance in the data (Rummel 1970) and thus provides an elegant tool for exploring relationships among variables. The first component extracted in the analysis accounts for the greatest proportion of the total variance; further components account for increasingly smaller portions of the remaining variance. Since the variance accounted for at each step is unique, each component is considered independent (i.e., orthogonal) from every other one. As successive components (also called factors) are determined, progressively less variance is explained, until only a trivial amount is associated with each new component.

The output of principal components analysis consists of a matrix of factor scores which have both magnitude and direction. The size of a factor score, ranging between zero and 1.0, reflects the strength of association of a variable to a factor, while the sign signifies the behavior of a variable relative to another on the same component. A variable with a negative factor score varies inversely with one having a positive score. The interpretation of individual components is achieved through examination of the variable combinations which load (score) significantly on that particular factor. This interpretation must consider both score magnitude and sign, and in fact consideration of both often eases the task of interpretation.

In principal components analysis the number of possible components equals the number of variables (Rummel 1970; Kim 1975). However, many factors will account for very little of the total variance in the data. In practice, the number of components of interest to the analyst is often determined by the sum of the square of the factor scores for each variable. This sum is the eigenvalue, and it is commonly the case that only components having eigenvalues greater than 1.0 are considered in subsequent analysis. This is the first step in data reduction.

The first component is selected to account for the maximum amount of variance, a procedure which *"often locates the first factor between independent clusters of interrelated variables"* (Rummel 1970:373, emphasis in original). Thus, although variance is explained, clusters of interrelated variables are not necessarily defined. Such clusters may be located by rotating the orthogonal axes in multidimensional space, where the number of dimensions equals the number of factors. Rotation is the next step in data reduction. Several methods of rotation are available depending upon whether the analyst wishes to simplify the variables (rows) or factors (columns) in a matrix. In the former instance, Quartimax rotation attempts to rotate axes such that a variable will have a high score on one factor and very low scores on all others (Kim 1975). On the other hand, Varimax rotation is concerned with simplifying component complexity (Rummel 1970; Kim 1975) and has as a strong feature an "ability to discern the same cluster of variables regardless of the number or combinations of other variables in the analysis" (Rummel 1970:392). Such factorial invariance reinforces the analyst's conviction in the interpretation of results: the variable clusters are most always meaningful. This feature has made Varimax the method of choice in most analyses (Rummel 1970). Other rotational techniques, such as Equimax (Kim 1975) or Target (Rummel 1970) will not be dealt with here.

In the present study, both Quartimax and Varimax rotation was applied and though both provided similar results, the relationships among the variables in the data set were more distinct using the Quartimax solution. No ratios were subjected to this analysis, leaving a data set of 13 variables. It was felt that using ratio variables with their constituent variables would introduce redundant variance into the data set. It should be noted that the number of variables in this analysis equals the number of cases. Since the number of factors potentially extractable is equal to or less than the rank of the data matrix (which in turn equals the smaller side of the matrix), it is considered appropriate to have a greater number of cases than variables. As pointed out by Rummel, though,

> When the interest is only in *describing* data variablility, then a factor analysis will yield such a description regardless of variables exceeding cases in number. Analysing 30 variables for 5 cases will still allow up to 5 independent factors to appear. And these 5 or less factors will still divide the 30 variables into major patterns of relationship for the 5 cases [Rummel 1970:220, emphasis in original].

Only when the objective of the analysis is to draw statistical inferences is it necessary that the number of cases exceed the number of variables by a healthy margin. The objective of the present analysis is descriptive.

Three components were extracted, accounting for 85.9 per cent of the total variance in the sample. The rotated factor matrix is given in Table 8, while plots of the rotated factor axes are depicted in Figure 17.

Table 8. Quartimax Rotated Factor Matrix.

VARIABLE	FACTOR 1	FACTOR 2	FACTOR 3
J	.99161	−.02588	.00391
TAREA	.98977	.00858	.11812
IMAX	.98044	.04598	−.02971
IMIN	.96840	−.12295	.04839
CAREA	.95036	−.08531	−.26567
YX	.89476	.11094	.35012
YN	.84791	.11947	−.23520
CTX	.64698	−.18000	−.53523
PMAX	.02218	.96365	.18692
PMIN	−.02639	.94377	.21093
MAREA	.44748	.19903	.84415
CTN	.35352	−.03743	−.70000
AGE	−.12629	.29652	.44241

Component 1: This component accounts for 54.3 per cent of the data variance. Variables such as total area, cortical area, polar and principal moments of inertia, maximum and minimum moment arm lengths and cortical thickness along the *Imax* axis are positively and highly loaded on this factor. Medullary area is only weakly loaded with a score of 0.44748. Component 1 is interpreted as a geometric component concerned with the cortex and the **external** geometry of the section. Moments of inertia, total area and cortical area all have factor scores greater than 0.9.

Component 2: This factor accounts for 21.9 per cent of the residual variance. Only two variables, PMIN and PMAX, load highly on this factor. In spite of this, however, the factor is meaningful. It is easily interpretable as a physical property (porosity) component. The next highest factor score is for the variable AGE, which would be expected in the present sample where the majority of individuals are over 70 years old and in light of the recognized increase in porosity with age. Nevertheless, the age association on this component is quite weak.

Component 3: Just over nine per cent (9.2) of the remaining variance is explained by this factor. This is the only component where high bipolar associations occur (i.e., high positive and negative scores). Medullary area and age are positively associated, while cortical thickness along both axes (CTX, CTN) is negatively scored. This is to be expected since expansion of the medullary canal must occur at the expense of cortical thickness. The direction of this relationship indicates that endosteal resorption outpaces periosteal apposition. Again, interpretation is rather straightforward. The component is seen to be a geometric factor concerned with the **internal** geometry of the cross-section.

Figure 17 depicts plots of all possible component pairs. The point co-ordinates correspond to the factor scores for each variable. The separation of the porosity factor from either geometric factor is readily apparent. Less clear, but still distinct, is the separation of the internal and external geometric components.

In summary, the principal components analysis confirms suspicions raised by the product-moment correlation matrix: there appears to be little linear relationship between the magnitude of cortical porosity along the *Imin* and *Imax* axes and the geometry of the cross-section. Age is only associated with internal geometric variation, though very weakly with porosity as well. Disregarding the possibility of significant curvilinear relationships, this exploratory analysis of the data intimates that porosity magnitude may be more or less independent of geometry. If so, any relationship between bone geometry and porosity is hypothesized, as per Chapter Four, to be a directional one.

Porosity and Geometry

Hypothesis 1: *Greater porosity should occur along the axis of greatest geometric resistance to bending. This region of bone will be located perpendicular to the maximum moment axis about which resistance is greatest.*

Figure 17.
Quartimax rotated factor axes.
Separation of porosity and geometry is distinct. Less clear but evident is separation of internal and external geometric components.
1. TAREA, 2. MAREA, 3. CAREA, 4. IMAX, 5. IMIN, 6. J, 7. PMAX, 8. PMIN, 9. AGE, 10. CTX, 11. YX, 12. CTN, 13. YN.

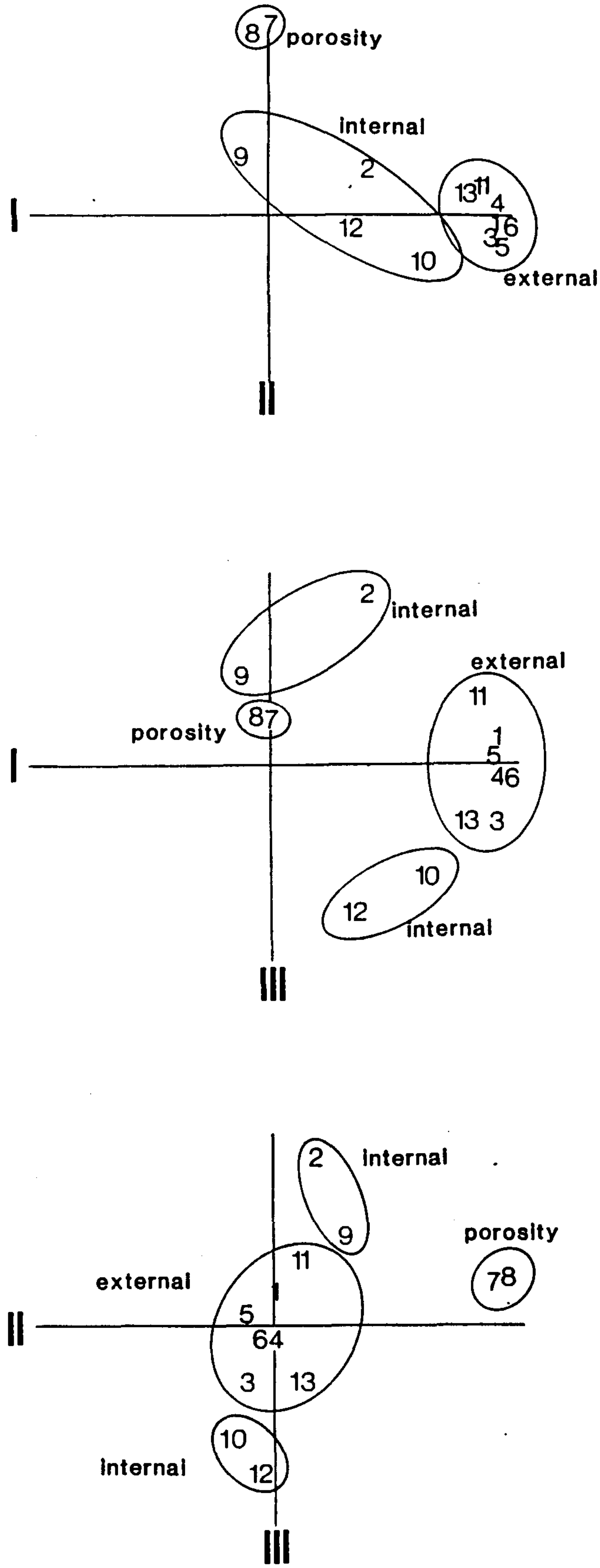
8 7 porosity
internal
9
2
13 11 4
I
1 6
12
3 5
10
external
II
2 internal
external
9
11
8 7
porosity
1
5
I
4 6
13 3
10
12 internal
III
2 internal
9
porosity
11
7 8
external
1
5
II
6 4
3 13
10
internal
12
III

This hypothesis was tested by subjecting PMIN and PMAX to a one-tailed t-test for paired samples and a sign test. The former tests for significant differences in relative porosity magnitude along the two axes, while the latter tests for directional differences. In a sign test the number of positive and negative differences are counted (zero differences are ignored) and evaluated under the hypothesis that the *n* positive and negative signs are sampled from a population in which they occur equally. Such a population implies that no true differences between paired samples exist for the variable in question (Sokal and Rohlf 1969).

The hypothesis that PMIN is greater than PMAX was evaluated by the t-test, and accepted (t=-1.94, one-tailed p=.038). At the same time, the sign test recorded 12 instances where PMAX was less than PMIN, and only one where the converse was true (Subject 16). A binomial one-tailed p=.0017 was calculated. These results support Hypothesis 1. There appears to be a preferential loss of bone along the axis which can most afford to lose bone without precipitously compromising strength. Alternatively, there may be preferential bone preservation along the axis which most requires it. To this stage, the analysis has only described the relationship, not explained it.

Hypothesis 2: The magnitude of the difference in porosity for cortex perpendicular to the maximum and minimum moment axes should decrease as the difference between the moment of inertia values decreases.

For the purpose of testing this hypothesis, Subject 16 was omitted. This individual was anomalous with respect to the directional behavior of PMIN and PMAX, as confirmed in the previous analysis. The magnitude of the difference between field porosities is measured by the variable PORRAT. The difference disappears as PORRAT approaches 1.0. Similarly, an IMIN/IMAX ratio approaching 1.0 signifies an increasingly circular section. A scattergram of these two ratios (Figure 18) confirms Hypothesis 2, though a certain amount of variation about any visualized regression line is evident; for this plot, r=.56.

Figure 18.
A scatterplot of porosity and moment ratios.

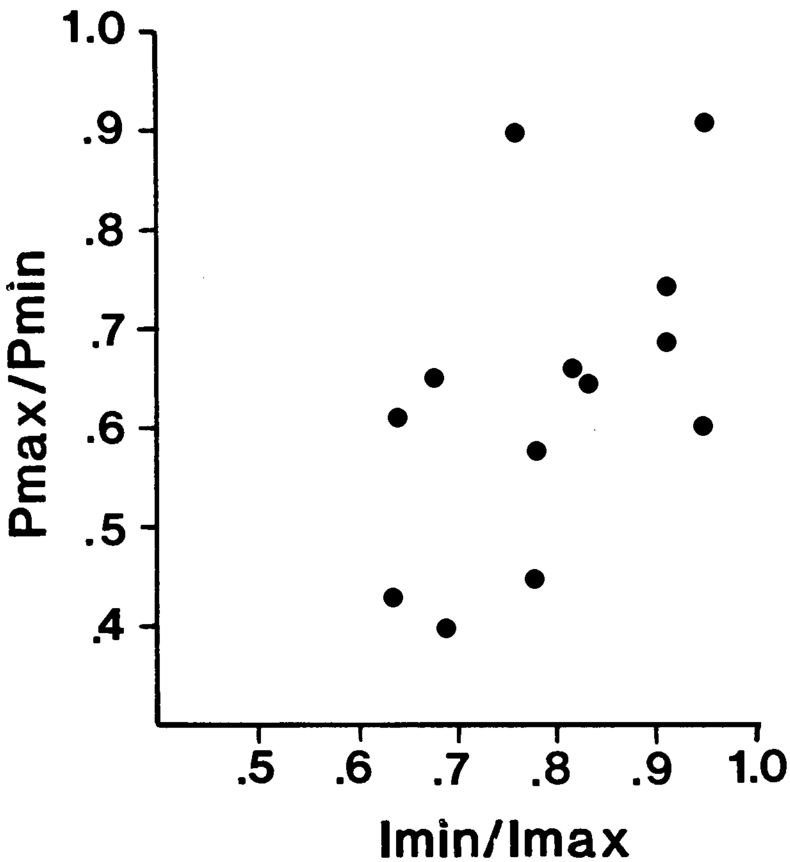
1.0
.9
.8
.7
.6
.5
.4
Pmax/Pmin
.5
.6
.7
.8
.9
1.0
Imin/Imax

These two hypotheses, confirmed in the data analysis, indicate that a directional relationship between cross-sectional geometry and porosity exists. Greater porosity occurs along the axis of greatest geometric resistance to bending; as well, the difference in porosity between fields declines as section circularity increases.

Apparent Density and Geometry

In examination of the product-moment correlation matrix it was evident that cortical thickness, or apparent density, was maintained along the *Imax* axis. This was seen in the relationship between medullary area and the ratio TMRX, and more clearly still when this variable was reduced to its constituents, CTX and YX. The specific hypothesis which relates apparent density and geometry, reiterated from Chapter Four, is as follows.

Hypothesis 3: Changes in the distance from the section centroid to the endosteal and periosteal surfaces along an axis should be of the same sign, but not necessarily of the same magnitude, in order to preserve an existing bending moment of inertia, I. *Increases in the centroid to periosteal surface distance can be less than an increase in the centroid to endosteal surface distance, though must be above a certain proportion of the latter in order to prevent a reduction in* I. *Surface movements should be more responsive along the* Imax *axis.*

Implicit within this hypothesis is the idea, long held, that periosteal apposition occurs as compensation for endosteal bone loss (Garn 1970; Martin and Atkinson 1977; Martin and Burr 1984). Although both processes have been shown to occur throughout life, no definitive empirical study has yet demonstrated such a relationship. Recently, Parfitt (1984b) has argued that since periosteal apposition precedes endosteal bone loss (Garn 1970), it therefore cannot serve as mechanical compensation, since such would imply a response of the former to the latter. Data reported here may help towards resolving this controversy.

Table 9 restates the data for the 'apparent density' variables, taken from Table 6. Visual examination of the ratio variables TMRN and TMRX shows the latter to be greater in 11 of 13 cases. This is confirmed by a sign test for paired samples (one-tailed p=.0113). Each being a ratio of two variables, this consistent difference could result in a number of ways. For example, CTX could be greater than CTN when YX equals YN. As well, YN could be greater than YX when CTX equals CTN. Finally, CTX could be greater than CTN and YN greater than YX. This third alternative is supported by the data in Table 9, again confirmed by a sign test. CTX is greater than CTN 10 of 13 times, p=.0462; and YN is greater than YX 11 of 12 times (one tie), p=.0032.

Table 9. Cortical Thickness and Moment Arm (mm); Ratios - Age-Ranked.

SUBJECT	AGE	CTN	CTX	YN	YX	TMRN	TMRX
20	50	5.7	6.5	14.3	14.0	0.66	0.87
11	52	8.1	9.1	16.0	15.0	1.03	1.54
13	72	8.2	8.4	16.4	14.3	1.00	1.56
32	72	8.7	10.0	16.8	14.3	1.07	2.33
14	73	5.6	7.0	12.5	11.3	0.81	1.63
24	74	6.5	8.4	17.7	16.4	0.58	1.05
17	76	7.2	6.6	11.3	10.0	1.76	1.94
26	79	5.6	7.1	14.5	13.6	0.63	1.09
34	79	6.4	9.2	16.3	16.3	0.65	1.30
16	80	9.3	6.2	16.5	13.7	1.29	0.83
31	82	4.8	6.6	14.0	13.8	0.52	0.92
18	86	5.1	6.5	14.9	13.9	0.52	0.88
39	96	7.3	5.6	12.7	15.6	1.35	0.56

Interpretation of these results is as follows. Cortical thickness is a product of periosteal apposition and endosteal resorption, while moment arm length is solely a product of periosteal apposition. The relationships CTX > CTN and YN > YX establishes that cortical thickness is an important parameter along the axis of least bending strength. The fact that moment arm length is greater along the *Imin* axis is not totally unexpected. This axis is oriented perpendicular to the axis about which bending resistance is at a maximum. Given the distance and area relationship which defines an area moment of inertia quantitatively, this maximum is achieved by distributing more material at a greater distance (i.e., moment arm length) from the neutral axis. This does not, however, resolve the question of 'compensation', since these relationships do not by themselves indicate that a specific response has taken place periosteally in light of endosteal surface movement. It is necessary to examine apparent density in terms of age in order to shed further light on this particular question.

Although the variable AGE was not strongly defined on any of the components extracted in the previous analysis, it was most highly scored on Component Three, which dealt with cortical thickness and internal geometry. In that 11 of 13 individuals in this sample are over 70 years of age, it was considered reasonable to re-analyse the relationship of cortical thickness to age considering only these 11 subjects. Both specimens under 70 derived from males, and it is recognized that men do not normally lose significant amounts of bone endosteally prior to age 65 (Mazess 1982).

Scattergrams of CTX, CTN, YX, YN, TMRN and TMRX were prepared (Figure 19). Table 10 provides the associated statistics.

Table 10. Correlation and Significance For Apparent Density Versus Age.

VARIABLE	r	p
CTX	−.66527	.01274
CTN	−.21017	.26754
YX	.29675	.18778
YN	−.34409	.15007
TMRN	.06525	.42442
TMRX	−.75274	.00375

Several of these relationships are obviously curvilinear. The two most significant, CTX and TMRX are also presented as log transformations in Figure 20, and have $r = -.71$ and $r = -.85$, respectively.

Figure 19.
Scattergrams of the apparent density variables versus age.

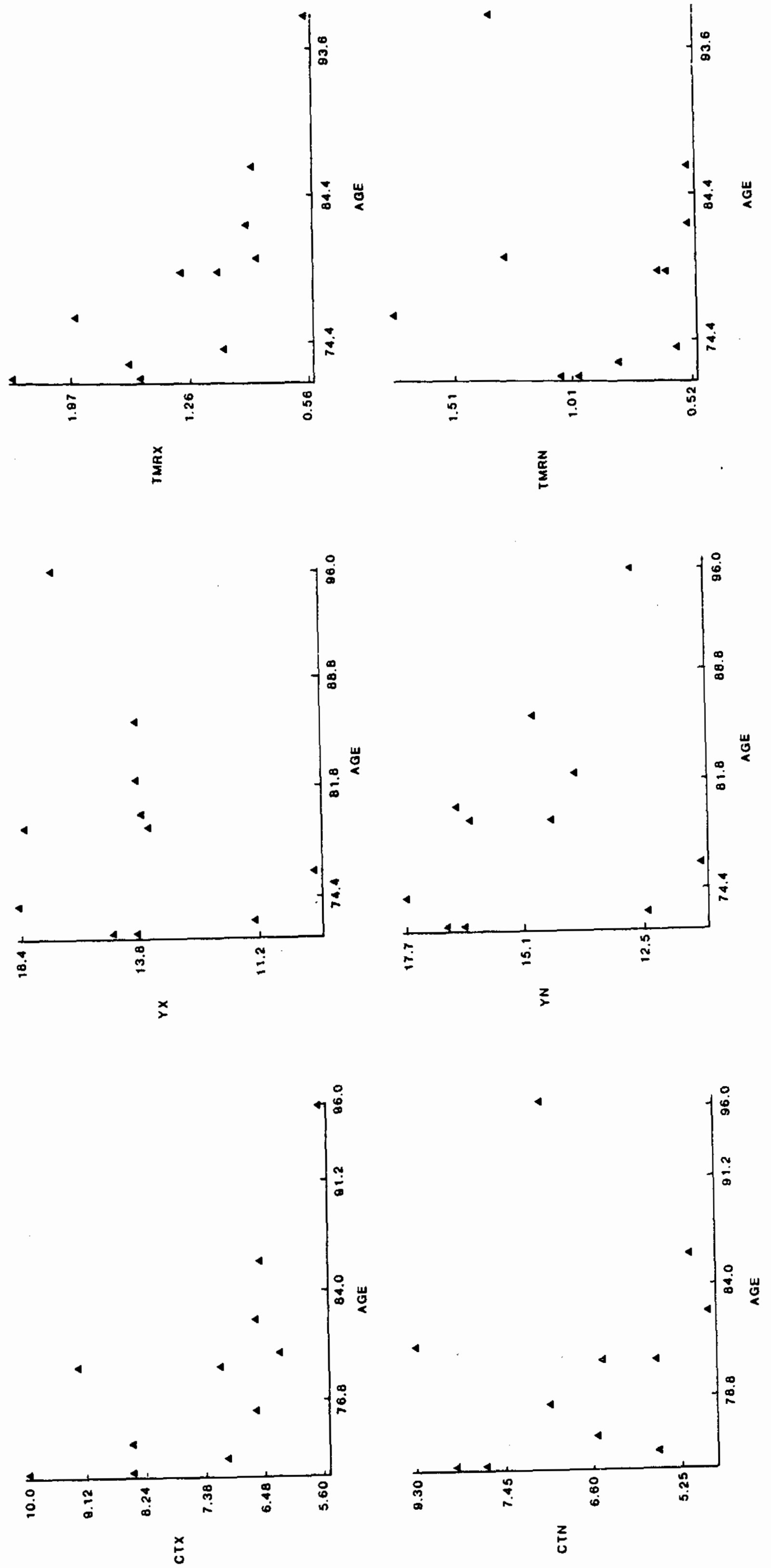
TMRX
1.97
1.26
0.56
74.4
84.4
93.6
AGE
TMRN
1.51
1.01
0.52
74.4
84.4
93.6
AGE
YX
18.4
13.8
11.2
74.4
81.8
88.8
96.0
AGE
YN
17.7
15.1
12.5
74.4
81.8
88.8
96.0
AGE
CTX
10.0
9.12
8.24
7.38
6.48
5.60
76.8
84.0
91.2
96.0
AGE
CTN
9.30
7.45
6.60
5.25
76.8
84.0
91.2
96.0
AGE

It is evident that, with age, significant declines in cortical thickness and the thickness/moment arm ratio occurs in this older sub–sample along the *Imax* axis. The decrease in TMRX results from the decrease in CTX. Since YX actually increases with age, as a product solely of periosteal apposition, the decrease in CTX must occur as a result of endosteal resorption. This relationship provides a stronger indication that periosteal apposition may occur in response to expansion of the medullary cavity with age. More significantly, this response occurs along the *Imax* axis as per Hypothesis Three (Chapter Four). It is, however, only indirect evidence. Longitudinal studies using methods such as tetracycline labelling (Frost 1969) would provide direct evidence that such compensation is in fact occurring. Although the intimation is clear, that the increase in YX is a specific response to a decrease in CTX must await the development of a more robust model for the interaction of endosteal and periosteal surface movements in the preservation of bending moments (Cowin 1983; Cowin et al. 1985; Frost 1985; Lazenby 1986b).

Along the *Imin* axis, moment arm length (YN) **decreases**, as does cortical thickness (CTN). However, TMRN remains essentially unchanged over the three decades spanned by this sub–sample, though values less than 1.0 predominate indicating that cortical thickness accounts for less than one–half moment arm length. The decrease in cortical thickness and moment arm length is likely due to resorption at the periosteal surface. This is the most parsimonious explanation for the proportional reduction in YN and CTN necessary to produce no directional trend in their ratio, TMRN. This conclusion bears closer examination at a future date, with a larger sample having a greater age range.

This age–specific variability is interesting in light of previously defined relationships for apparent density between fields. Although CTX undergoes a more significant decline with age than CTN, it remains greater than the latter in the majority of cases. Similarly, YN declines somewhat (though not significantly) with age, and YX tends to increase. In spite of this, YN remains larger than YX. The maintenance of these relationships with age indicates that the directional differences between fields in cortical thickness and moment arm length are lifetime normal conditions. CTX was greater than CTN and YN was greater than YX prior to the advent of endosteal bone loss.

Summary

The results of this study can be summarized as follows, and are illustrated in Figure 21.

1. As suggested by principal components analysis, it is possible that the magnitude of cortical porosity is independent of cross-sectional geometry; however, the axial direction of developing porosity is not.
2. Porosity is greater along the axis of greatest geometric resistance to bending.
3. The difference in porosity between the maximum and minimum moment axes decreases as their associated moments of inertia approach equivalence.
4. Apparent density is greater along the maximum moment axis, while the moment arm is greater along the minimum moment axis. This relationship is constant throughout life.
5. With age, both the endosteal and periosteal surfaces along the *Imax* axis move away from the section centroid.
6. Along the *Imin* axis, only the periosteal surface moves relative to the centroid. This movement is towards the centroid indicating periosteal resorption, hence a reduction in moment arm length.

Discussion

It is clear that a conservancy model can be defined for the interaction of cortical porosity, apparent density and geometry. The hypotheses specified in Chapter Four have all found support in the present analysis. The ramifications of such a model have particular regard for the preservation of bone strength and conservation of the strain environment

Figure 20.
TMRX and CTX plotted against AGE on logarithmic co-ordinates.

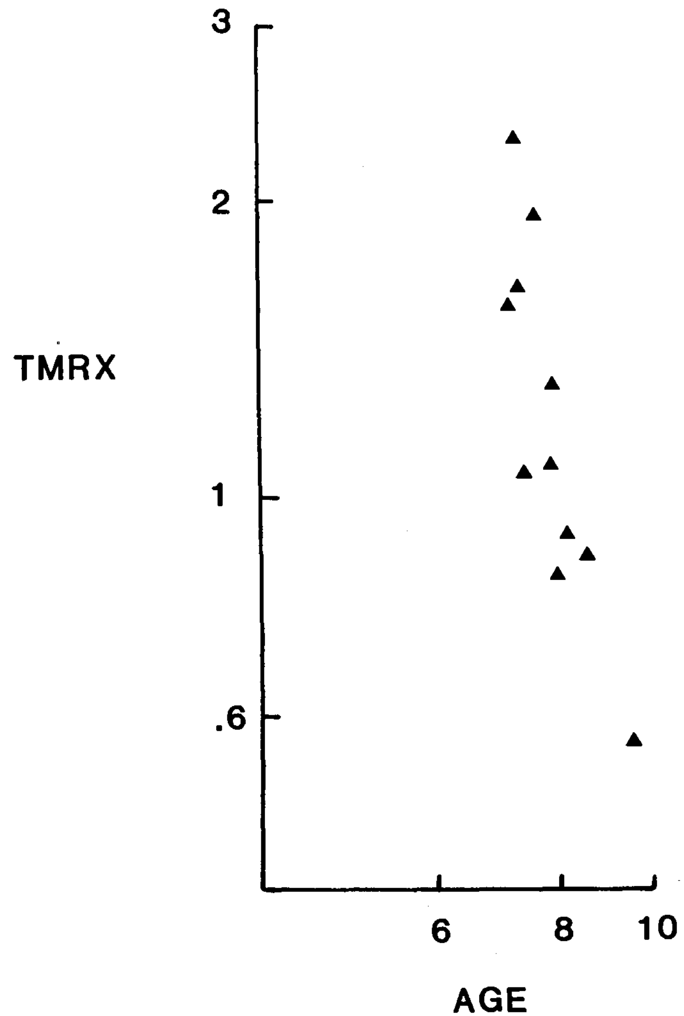
TMRX
3
2
1
.6
6
8
10
AGE

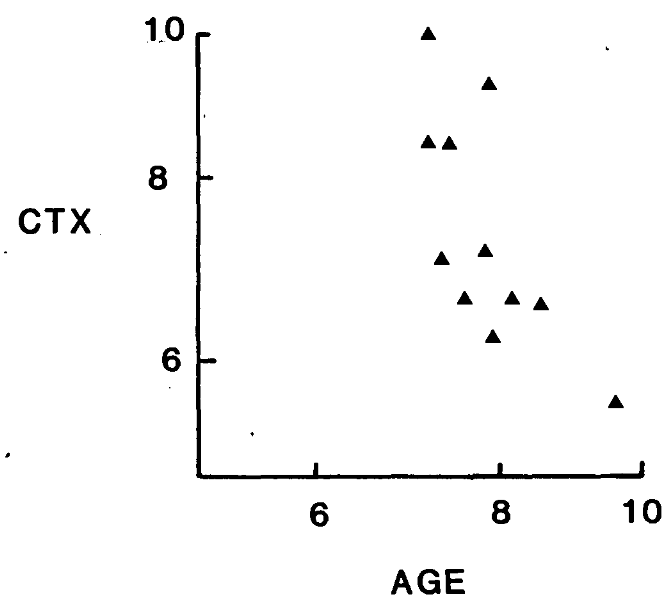
CTX
10
8
6
6
8
10
AGE

within bone cortex. The former is implicitly the objective of functional adaptation; the latter the implicit objective of remodeling processes.

The results obtained in this study are consistent with the idea that internal and external remodeling interacts to preserve, as far as possible, the mechanical competence of bone in spite of the net bone loss that occurs with aging. This interaction results in a differential distribution of porosity when predominant bending planes can be inferred, and an absence of such a distribution when no predominant direction of bending exists. Following traditional arguments, this interaction also produces a response at the periosteal surface associated with endosteal bone loss along the axis of minimum bending strength, but not along its orthogonal counterpart. These arguments may require significant revision, as discussed below.

Few studies have examined the relationship between porosity and geometry. Martin and Burr (1984) investigated porosity distribution in the mid-shaft of several limb bones, but not relative to any specific axis nor in terms of moments of inertia. They reported "consistent relationships between porosity distribution and the most common neutral axis". Greater porosity was found in the anterior and posterior femoral cortex "which contain the neutral axis when the femur is bent by hip forces during walking". Using various mathematical relations, Martin and Burr calculated that the observed porosity topography "enhanced bending stiffness up to 18% relative to that which would exist if porosity were uniformly distributed in the bone". In the present study, the axis of greatest bending strength was commonly directed antero-posteriorly and the axis of least strength medio-laterally (Appendix II). A similar study to that of Martin and Burr (1984) was published by Martin et al. (1980), in which comparable results were reported and which, in fact, formed a part of Martin and Burr's (1984) paper. Martin (1984), modeling porosity and specific surface relationships (where the latter is the surface available for remodeling) refers to the results of the previously cited studies and notes that porosity tends to develop in less-stressed regions of cortex. He also notes that porosity tends to be greater towards the endosteal surface for the same reason, as torsional stresses become smaller away from the periosteal surface. This endosteal-periosteal relationship was not considered in the present study, though its existence was readily apparent in a casual observation of the cross-section radiographs.

Neither of the above studies examined porosity distribution in terms of cross-section circularity. The decrease in porosity differences between fields which occurs as the section becomes more circular likely reflects an equalization of the quantity or quality of stimulus responsible for remodeling. In the femur, circularity can be produced by combined antero-posterior (A-P) and medio-lateral (M-L) loading of more-or-less equal magnitude (Ruff and Hayes 1983a). Several studies (reviewed by Ruff and Hayes 1983a; Kummer 1972) indicate that the femur experiences significant loads in both the A-P and M-L planes along the mid-diaphysis, either in normal gait or through the stance phase (Paul 1971; Rybicki et al. 1972). This region also produces sections primarily circular in shape. In the proximal femur, however, M-L bending tends to predominate (Ruff and Hayes 1983a), primarily due to the action of the hip abductor muscles (Rybicki et al. 1972). In this region large tensile (lateral) and compressive (medial) bending stresses can be generated, though Rybicki et al. (1972) have shown that various amounts of tension in the tensor faciae latae can reduce these stresses three-fold and the resulting strain energy 10-fold.

Cross-sections used in the present study were taken from the proximal mid-diaphysis, and thus likely reflect a large measure of predominant M-L bending. However, examination of the cross-section outlines (Appendix II) reveals that the medio-lateral plane contains the axis of least resistance to bending. This situation is the reverse of that depicted by Ruff and Hayes (1983a) for Pecos Pueblo femora, but mirrors that indicated in Martin and Atkinson's (1977) study using modern specimens. This discrepancy was noted by Ruff and Hayes (1983a:377) and ascribed to "the smaller and more heterogeneous" sample used by Martin and Atkinson. The problem, however, traces to either a conceptual or semantic error on the

Figure 21.
The primary results of this study.
The upper figure depicts directional differences in porosity magnitude, while the lower figure indicates the reduction in the porosity difference between axes with increasing section circularity. Arrows indicate relative endosteal and periosteal surface movements with age.

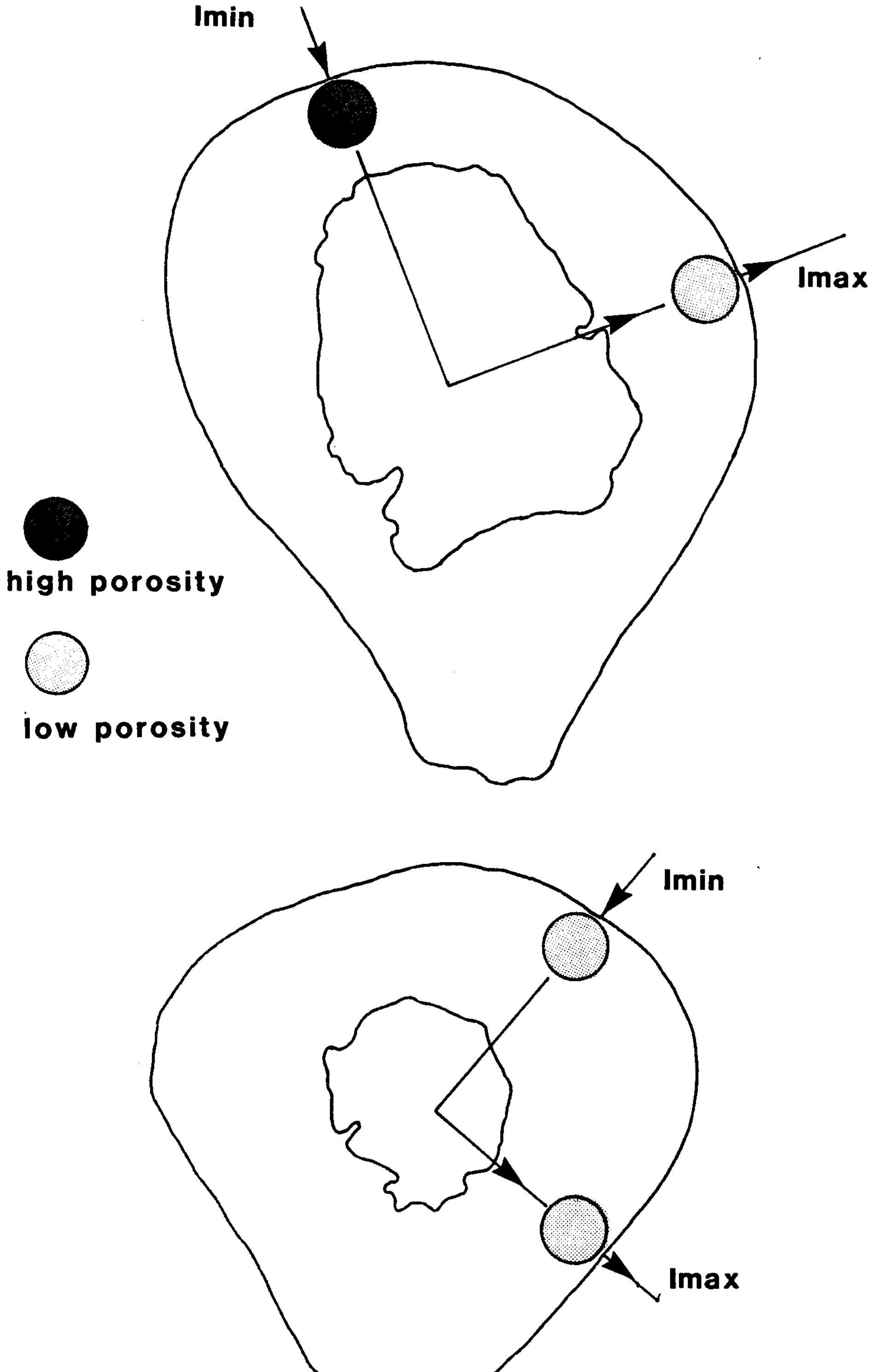
Imin
Imax
high porosity
low porosity
Imin
Imax

part of Ruff and Hayes. They note

> The maximum and minimum second moments of area ... are particularly important because they indicate the relative magnitude of greatest and least bending rigidity of a section respectively. The principal axes of a section define the directions of greatest and least bending rigidity (major axis - greatest, minor axis - least) [Ruff and Hayes 1983a:360].

This is incorrect, as noted in Chapter Three. By definition (Popov 1978:127), the maximun moment axis is the axis **about** which bending rigidity is greatest, the direction of which is indicated by the orthogonal minimum moment axis. Either Ruff and Hayes have misidentified their principal axes, or they have failed to distinguish rotation about an axis as oppossed to rotation along an axis. As will be argued below, however, the present orientations have real functional significance. They confirm the contention put forward by Rubin (1984) and Lanyon (1981a), based on *in vivo* strain gauge studies performed on a number of different animals, that the orientation of an elliptical cross-section "is directed to provide the least resistance in the direction in which bending normally occurs" (Rubin 1984:S13). Thus, the ***Imin*** axis not only denotes the direction of greatest **geometric** resistance to bending, but also the direction of **least** bending. The converse holds for the ***Imax*** axis: the direction of least geometric bending strength is indicated, as well as the direction of greatest bending. [As an aside, it should be pointed out that if cross-sectional shape does not indicate the direction of the maximum and minimum bending moments, its use to infer past behavior in human populations (Ruff and Hayes 1983b; Ruff et al. 1984; Martin et al. 1985) is called into question (Lazenby 1986a)]. As noted in Chapter Four

> The main effect of the anatomical orientation of the elliptical cross-section is *not* to *resist* bending in the customary loading direction, but rather, at the risk of increasing the strain generated during normal loading, to restrict and co-ordinate the direction of the loading that does occur [Rubin 1984:S13, emphasis in original].

This relationship helps to explain the apparent paradox regarding the dichotomy of bone loss seen in the present study. Cortical porosity is greater in the anterior cortex, along the ***Imin*** axis, while endosteal bone loss is greater in the lateral cortex, along the ***Imax*** axis.

The clinically accepted principle that mechanical stress inhibits the development of osteoporosis (Martin et al. 1980; Heaney 1983) does not alone account for this dichotomy, though it does have explanatory power. Following Rubin's (1984) argument, data from the present study can be explained as follows.

1. Along the *Imax* axis bending stresses are at a maximum. This axis is oriented medio–laterally. The strain here is expected to be high since this axis denotes the direction of least bending strength and largest bending moments. Conservation of the strain environment **within** the cortex is likely an important consideration for this region since high strain is expected to expose the element to a greater risk of failure than low strain. It would therefore be optimal to minimize any increase in cortical porosity. Endosteal bone loss along this axis occurs in conjunction with periosteal apposition. Whether the moment of inertia about the relevant neutral axis is diminished, maintained or increased cannot be determined (Lazenby 1986b). This response must be seen as an attempt to conserve the existing strain environment for this region of cortex.
2. Along the *Imin* axis, oriented antero–posteriorly, bending stresses will be at a minimum. Strain should be low (possibly highly variable), and the constraint for conserving the strain distribution of the cortex will be relaxed. Porosity would be expected to increase, given the clinical principle cited above. The movement of the periosteal surface with age, relative to the section centroid, reflects an absence of a sufficient modeling stimulus for the maintenance of bone along this axis, in keeping with the concept of functional adaptation.

Given the directional dichotomy in the type of bone loss seen in the femoral cortex, it can be suggested that internal and external remodeling, though integrated in terms of ultimate stimulus, biochemical/electrical transducer(s) and cellular response, have qualitatively and/or quantitatively different control systems (Burr et al. 1985). As per Carter (1984), the remodeling response to strain is probably site–specific. Osteoporotic bone loss is inhibited under high bending-induced strain regimes, while at the same time the inner and outer bone surfaces respond to the implied flexural stress (Frost 1980, 1982). Low strain regimes permit the development of intracortical porosity and intimate the absence of flexural stress to which the endosteal and periosteal surfaces would respond.

The above argument implies that the rate of initiation of cortical remodeling events may be reduced in the lateral, less porous, cortex. This is supported by O'Conner et al. (1982) who noted that altering the strain environment of sheep radii within physiological limits could account for the greater part of modeling variance, but much less of the remodeling variance, in the normal plane of bending. The argument does not deny that a general increase in cortical porosity occurs with age (Martin et al. 1980; Carter and Spengler 1978). However, it specifies that cortex under a high degree of strain will be less porous than cortex elsewhere. Alternatively, the rate of initiation of cortical remodeling may be higher in the lateral cortex; however, the time required to produce a new Haversian system may be sufficiently short that the cortex is not exposed to extended periods of higher porosity. This time would be equal to that of similar events seen in young adults; that is, in the lateral cortex there will have been no age-degradation of remodeling efficiency.

CHAPTER VII

SUMMARY AND CONCLUSION

This thesis has investigated interdependence between bone porosity and cross-sectional geometry, under the premise that these two aspects of bone structure account for the lifetime variability of a skeletal element's mechanical competence. The objective was not to demonstrate that porosity is non-randomly distributed throughout the cortex, since such was previously known (Evans and Lebow 1951; Atkinson 1969; Martin et al. 1980; Martin 1984). Rather, the point was to determine if specific relationships exist between porosity and geometry which could be interpreted from the broader point of view of bone strength preservation.

It is acceptable to presume, for a number of reasons, that such relationships might exist. First, both porosity and geometry vary as a result of the same cellular processes – resorption and deposition (Frost 1980, 1982, 1985). Second, each is known to vary as a general consequence of aging (Mazess 1982; Garn 1970). Third, age-related increases in porosity (osteoporosis) are known to reduce bone strength. Fracture is the most common clinical manifestation of osteoporosis (Heaney 1983), usually resulting from minimal trauma (Sutton and Cameron 1985). On the other hand, cross-section geometry **can** be so arranged to maximize strength (taken here to be primarily resistance to bending). Finally, specific relationships should obtain given acceptance of the general tenets of functional adaptation and Wolff's Law, to whit: bone material will occur in a quantity and quality so as to serve a demonstrable need, and will be removed in the absence of that need (Cowin 1983).

This study undertook to examine whether or not the distribution of greater and lesser porosity was determined relative to several geometric parameters in femoral cross-sections; specifically, with regard to the axes of maximum and minimum geometric resistance to bending. A descriptive model was outlined proposing that strength-reducing porosity should occur to a greater degree along the axis of maximum bending strength, i.e., where it can be most afforded. Furthermore, interaction between porosity and geometry should see a more equitable porosity distribution when cross-sections become more circular in shape; less equitable with increasing non-circularity. In biomechanics, circularity implies optimum resistance to "all strain-inducing modes" (Lovejoy et al. 1976:505), and it thus stood to reason that all variable components of bone strength should be distributed equitably in such cases. The model was deemed a conservancy model, reflecting the underlying principles of functional adaptation.

Results pertinent to these questions support the proposed model. Although the overall magnitude of porosity was found not to be determined with regard to geometry (nor with age), the distribution of porosity was so found. Greater porosity occurred in the direction of maximum geometric bending strength, less in the direction of minimum bending strength. This distribution has the effect of combining a weak porosity scenario with a strong geometric scenario. To consider the opposite, i.e., weak with weak and strong with strong, would be to entertain a potentially disastrous situation.

The study also undertook to examine the contention that continuous periosteal apposition mechanically compensates for endosteal resorption (Martin and Burr 1985), the latter also a ubiquitous consequence of aging (Garn 1970). This idea is generally accepted, though empirically unproven, and has been recently criticized (Parfitt 1984b). Results indicate, interestingly, that if such geometric compensation does occur, it is restricted to the direction of minimum bending strength (but see below). It was found that along this axis both the endosteal and periosteal surfaces moved away from the section centroid with age.

What seemed to be an interesting paradox in aging bone loss became apparent in consideration of cortical porosity on the one hand, and endosteal expansion of the medullary cavity on the other. The former was much greater along the axis of maximum bending strength; the latter greater along the axis of minimum bending strength. This could not be explained given the generally accepted engineering principle that the direction of greatest resistance to bending should indicate the direction of predominant bending. Such a one-to-one relationship would require both greater porosity and greater endosteal bone loss to occur along the axis of maximum bending resistance, since the first two result in a loss of strength. Reconciliation of this directional dichotomy in aging bone loss was explained, however, by acceptance of recent suggestions that elliptical cross-sections do not orient to maximally reduce bending moments, but to maintain a given strain distribution and in effect co-ordinate the bending that does occur (Lanyon 1981a; Rubin 1984). Thus, the axis along which bending resistance is a maximum is also the axis of least bending, and vice versa. Given this, greater porosity will occur along this axis in the absence of significant mechanical loads. Along the axis of least bending strength, cortical porosity is inhibited, and periosteal apposition develops in response to larger loads, as noted in several *in vivo* experiments (e.g., O'Conner et al. 1982). It is suggested that endosteal bone loss along this axis occurs **in response** to periosteal apposition, with the objective of maintaining a given strain environment within the cortex.

In conclusion, this study has determined or clarified a number of significant points not previously recognized. First, bone geometry and cortical porosity do interact to preserve bone strength. This implies direct feedback between internal and external remodeling stimuli. That this is the case is supported by the fact that the distribution of porosity is equalized with respect to orthogonal axes as the cross-section becomes geometrically uniform in terms of bending strength. Second, apparent density along the maximum and minimum axes varies with age so as to conserve a given strain environment in the cortex. The idea that periosteal apposition occurs as compensation in response to endosteal bone loss would seem to be reversed: endosteal bone loss compensates for periosteal bone gain. These findings further confirm the role of strain as the ultimate remodeling stimulus.

APPENDIX I

This appendix describes how the area moments of inertia were calculated for the reference antero-posterior (A-P) and medio-lateral (M-L) axes; and how the product moment of inertia for these axes was derived. All three were required to determine the maximum and minimum moments of inertia (see Chapter Five for the mathematical formulae employed).

The method used was taken from Lovejoy et al. (1976). The enlarged image tracing of the cross-section was placed on a light table. A transparent metric grid with 1 mm ruling was laid over the tracing. The section image had previously been divided into four quadrants by drawing the A-P and M-L axes through the section centroid. (Refer to Chapter Five for the method of locating the centroid.) Each cm^2 of grid was treated as an individual unit of area. For each quadrant, the amount of each unit of area occupied by bone was determined, to an accuracy of one mm^2. For each unit, area values could range from one to 100. This value was then multiplied by the squared distance from the center of the unit to the reference axis. This gave a product having a dimension of mm^4. All such products within a quadrant were summed; subsequently these quadrant sub-totals were summed to give the value for the area moment of inertia. Appropriate magnification correction was then applied. Note that, using this method the axis from which the distance value is derived is the axis about which resistance to rotation is being measured.

The product moment of inertia is determined in a similar fashion. However, rather than multiplying the unit area value by distance squared to an axis, it is multiplied by the product of its distance to either axis. Thus, it equals [area (mm^2)] times [the product of the distance to the A-P axis (mm) and the distance to the M-L axis (mm)], again giving a result having a dimension of mm^4.

APPENDIX II

This appendix provides representations of the femoral cross-sections used in this study. Each is approximately 1.6 times actual size. Indicated are the anterior reference axis (A), and the maximum (X) and minimum (N) moment axes used to locate the microscopic fields (circles) analyzed. The triangle in the medullary space locates the section centroid. The subject numbers correspond to the following age/sex distribution.

11 - 52 year old male

13 - 72 year old male

14 - 73 year old female

16 - 80 year old male

17 - 76 year old female

18 - 86 year old female

20 - 50 year old male

24 - 74 year old female

26 - 79 year old male

31 - 82 year old female

32 - 72 year old male

34 - 79 year old male

39 - 96 year old male

17

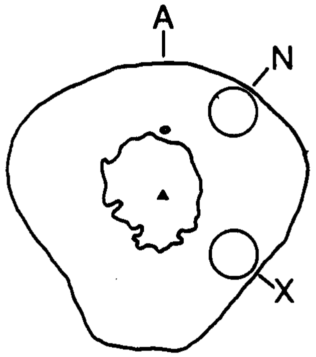

16

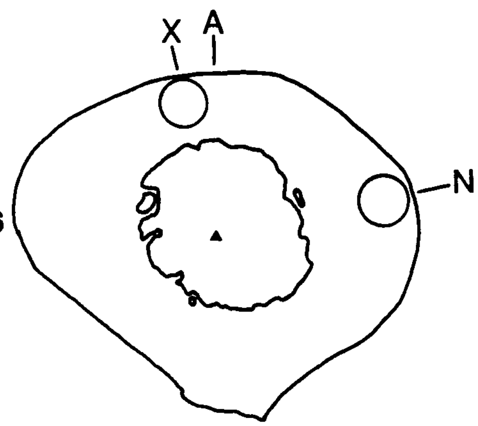

14

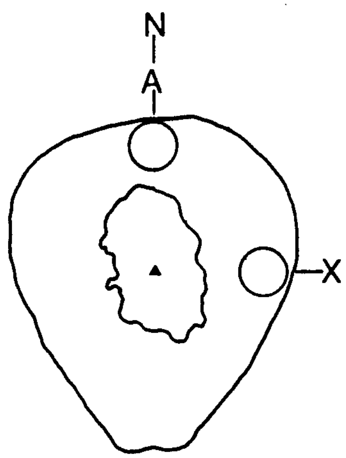

13

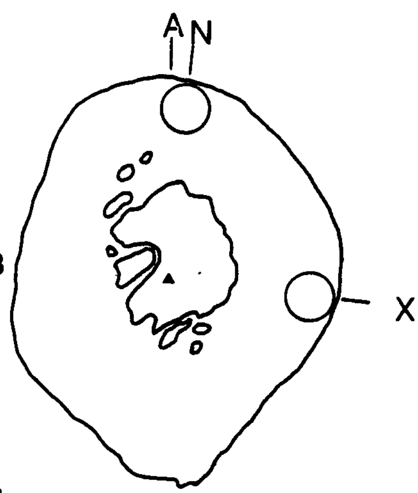

11

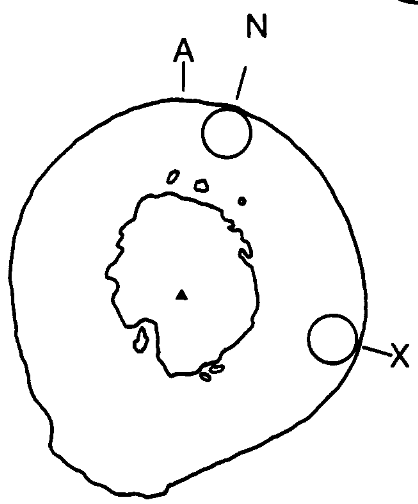

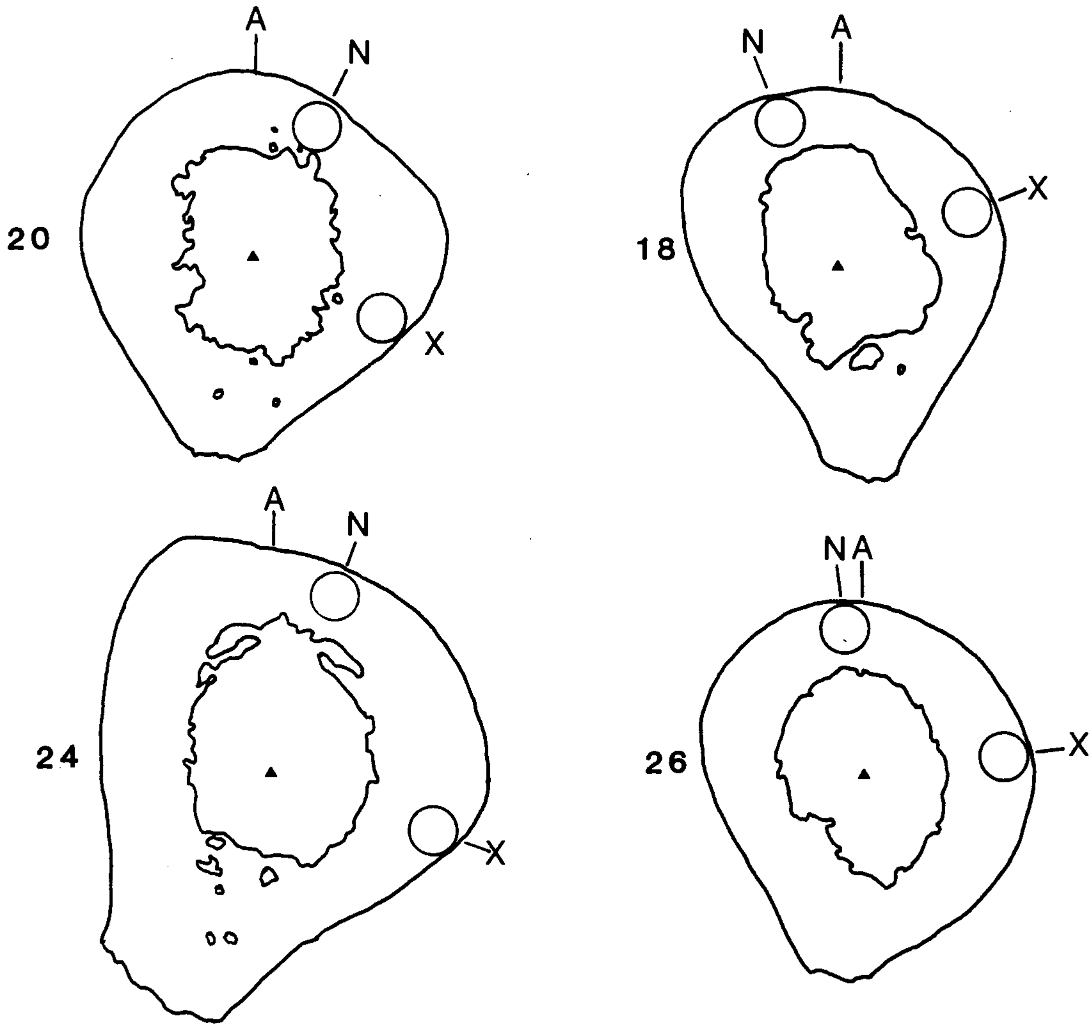
A
N
20
X
N
A
X
18
A
N
24
X
NA
X
26

39

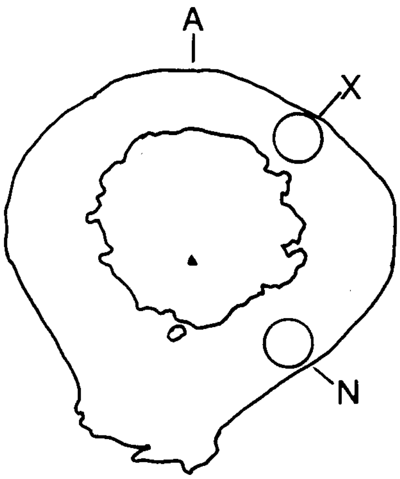

34

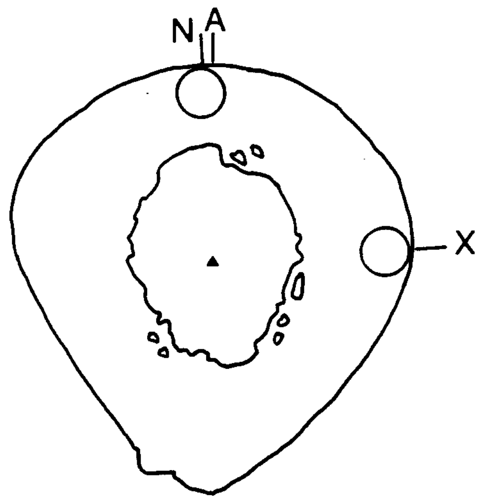

32

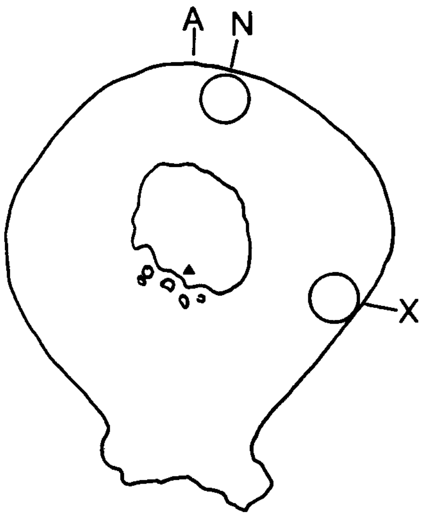

31

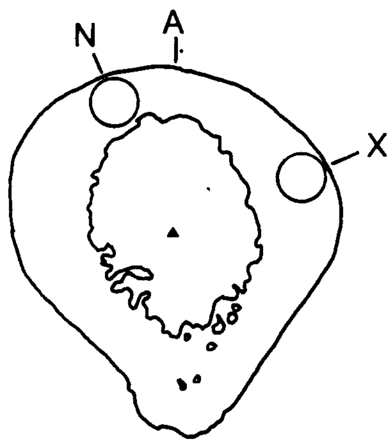

REFERENCES CITED

Ahlqvist, J. and D. Damsten
1969 A Modification of Kerley's Method for the Microscopic Determination of Age in Human Bone. *J. Forensic Sci.* 14:205–212.

Alexander, R. McN.
1983 *Animal Mechanics.* Blackwell, Oxford.

Amprino, R.
1948 A Contribution to the Functional Meaning of the Substitution of Primary by Secondary Bone Tissue. *Acta Anat.* 5:291–300.

__________ 1967 Bone Histophysiology. *Guy's Hosp. Rept.* 116:51–69.

Amtmann, E.
1971 Mechanical Stress, Functional Adaptation and the Variation Structure of the Human Femur Diaphysis. *Advances in Anat., Embryol. and Cell Biol.* 44:7–87.

Amtmann, E. and E. Doden
1981 Anpassung der Knochenstruktur an mechanische Beanspruchung. *Zeits. fur Morphol. Anthropol.* 72:1–21.

Arya, J.C. and R. Lardner
1979 *Mathematics for the Biological Sciences.* Prentice–Hall, Englewood Cliffs.

Ascenzi, A.
1980 Contribution of Biomechanics to Bone Research. *Calcif. Tiss. Int.* 31:1–3.

Atkinson, P.J.
1969 Structural Aspects of Aging Bone. *Gerontologia* 15:171–173.

Atkinson, P.J. and J.A. Weatherell
1967 Variation in the Density of the Femoral Diaphysis with Age. *J. Bone Jt. Surg.* 49(B):781–788.

Avioli, L. (editor)
1983 *The Osteoporotic Syndrome.* Grune and Stratton, New York.

Baker, J., V.H. Frankel, and A. Burstein
1972 Fatigue Fractures: Biomechanical Considerations. (abstract) *J. Bone Jt. Surg.* 54(A):1345–1346.

Bartley, M.H., J.S. Arnold, R.K. Halsam, and W.S.S. Jee
1966 The Relationship of Bone Strength and Bone Quantity in Health, Disease and Aging. *J. Gerontology.* 21:517–521.

Barzel, U.S. (editor)
1979 *Osteoporosis II.* Grune and Stratton, New York.

Beer, F.P., and E.R. Jonhston, Jr.
1981 *Mechanics of Materials.* McGraw-Hill, New York.

Bevan, B.
1826 On the Strength of Bone. *Philosophical Magazine.* 68:181-182.

Biewener, A.A.
1982 Bone Strength in Small Mammals and Bipedal Birds: Do Safety Factors Change with Body Size? *J. Exp. Biol.* 98:289-301.

Binderman, I., Z. Shimshoni, and D. Somjen
1984 Biochemical Pathways Involved in the Translation of Physical Stimulus into Biological Message. *Calcif. Tiss. Int.* 36(Supp. 1):S82-S85.

Boivin, G. and C.-A. Baud
1984 Microradiographic Methods for Calcified Tissues, In *Methods of Calcified Tissue Preparation,* edited by G.R. Dickson, pp. 391-412. Elsevier, New York.

Bradbury, S.
1979 Microscopical Image Analysis: Problems and Approaches. *J. Microscopy.* 115:137-150.

Brock, S.L.
1985 Biomechanical Adaptations of Human Lower Limb Bones in the Prehistoric American Southwest. (abstract) *Am. J. Phys. Anthropol.* 66:150.

Bronner, F.
1982 Calcium Homeostasis. In *Disorders of Mineral Metabolism. Vol. II: Calcium Physiology,* edited by F. Bronner and J.W. Coburn, pp. 43-102. Academic Press, New York.

Burr, D.B.
1980 The Relationship Among Physical, Geometrical and Mechanical Properties of Bone, With a Note on the Properties of Non-Human Primate Bone. *Yearbook Phys. Anthropol.* 23:109-146.

Burr, D.B., R.B. Martin, M.B. Schaffler, and E.L. Radin
1985 Bone Remodelling in Response to *In Vivo* Fatigue Damage. *J. Biomechanics.* 18:189-200.

Burstein, A.H., D.T. Reilly, and M. Martens
1976 Aging of Bone Tissue: Mechanical Properties. *J. Bone Jt. Surg.* 58(A):82-86.

Carlson, D.S., G.J. Armelagos, and D.P. Van Gerven
1976 Patterns of Age-Related Cortical Bone Loss (Osteoporosis) Within the Femoral Diaphysis. *Hum. Biol.* 48:295-314.

Carter, D.R.
1984 Mechanical Loading Histories and Cortical Bone Remodeling. *Calcif. Tiss. Int.* 36(Supp. 1):S19-S24.

Carter, D.R., W.E. Caler, D.M. Spengler, and V.H. Frankel
1981 Uniaxial Fatigue of Human Cortical Bone. The Influence of Tissue Physical Charcteristics. *J. Biomechanics.* 14:461–470.

Carter, D.R., W.H. Harris, R. Vasu, and W.E. Caler
1981 The Mechanical and Biological Response of Cortical Bone to *In Vivo* Strain Histories. In *Mechanical Properties of Bone.* AMD–Vol. 45, edited by S.C. Cowin, pp. 81–92. American Society of Mechanical Engineers, New York.

Carter, D.R., and W.C. Hayes
1976 Fatigue Life of Compact Bone. I. Effects of Stress Amplitude, Temperature and Density. *J. Biomechanics.* 9:27–34.

____
1977 Compact Bone Fatigue Damage – A Microscopic Examination. *Clin. Orthopaed.* 127:265–274.

Carter, D.R., W.C. Hayes, and D.J. Schurman
1976 Fatigue Life of Compact Bone. II. Effects of Microstructure and Density. *J. Biomechanics.* 9:211–218.

Carter, D.R. and D.M. Spengler
1978 Mechanical Properties and Composition of Cortical Bone. *Clin. Orthopaed.* 135:192–217.

Chamay, A. and P. Tschantz
1972 Mechanical Influences in Bone Remodeling. Experimental Research on Wolff's Law. *J. Biomechanics.* 5:173–180.

Chestnut, III, C.H., W.B. Nelp, J.D. Denney, and D.J. Sherrard
1973 Measurement of Total Body Calcium (Bone Mass) by Neutron Activation Analysis: Applicability to Bone Wasting Disease. In *Clinical Aspects of Metabolic Bone Disease*, edited by B. Frame, A.M. Parfitt, and H. Duncan, pp. 50–54. Excerpta Medica. Amsterdam.

Churches, A.E. and C.R. Howlett
1981 The Response of Mature Cortical Bone to Controlled Time–Varying Loading. In *Mechanical Properties of Bone.* AMD–Vol. 45, edited by S.C. Cowin, pp. 69–80. American Society of Mechanical Engineers, New York.

Cole, M. and C.P. Bond
1972 Recent Advances in Automatic Image Analysis Using a Television System. *J. Microscopy.* 96:89–96.

Cowin. S.C.
1981 Continuum Models of the Adaptation of Bone to Stress. In *Mechanical Properties of Bone.* AMD–Vol. 45, edited by S.C. Cowin, pp. 193–210. American Society of Mechanical Engineers, New York.

____
1983 The Mechanical and Stress Adaptive Properties of Bone. *Annals Biomed. Engnr.* 11:263–295.

______ 1984 Mechanical Modeling of the Stress Adaptation Process in Bone. *Calcif. Tiss. Int.* 36(Supp. 1):S98–S103.

Crawford, G.N.C.
1940 The Evolution of the Haversian Pattern in Bone. *J. Anat.* 74:284–299.

Currey, J.D.
1959 Differences in the Tensile Strength of Bone of Different Histological Types. *J. Anat.* 93:87–95.

______ 1962 Stress Concentrations in Bone. *Quart. J. Microscopial Sci.* 103:111–133.

______ 1964 Metabolic Starvation as a Factor in Bone Reconstruction. *Acta Anat.* 59:77–83.

______ 1968 The Adaptation of Bone to Stress. *J. Theoret. Biol.* 20:91–106.

______ 1969a The Mechanical Consequences of Variation in the Mineral Content of Bone. *J. Biomechanics.* 2:1–11.

______ 1969b The Relationship Between the Stiffness and the Mineral Content of Bone. *J. Biomechanics.* 2:477–480.

______ 1970 The Mechanical Properties of Bone. *Clin. Orthopaed.* 73:210–231.

______ 1975 The Effects of Strain Rate, Reconstruction and Mineral Content on Some Mechanical Properties of Bovine Bone. *J. Biomechanics.* 8:81–86.

______ 1979 Changes in the Impact Energy Absorption of Bone with Age. *J. Biomechanics.* 12:459–469.

______ 1981a What is Bone For? Property–Function Relationships in Bone. In *Mechanical Properties of Bone,* AMD–Vol. 45, edited by S.C. Sowin, pp. 13–26. American Society of Mechanical Engineers, New York.

______ 1981b Properties of Bone, Cartilage, and Synovial Fluid. A. Bone. In *An Introduction to the Biomechanics of Joints and Joint Replacement,* edited by D. Dowson and V. Wright, pp. 103–107. Mechanical Engineering Publications, London.

______ 1982a 'Osteons' in Biomechanical Literature. *J. Biomechanics.* 15:717.

———— 1982b Bone as a Mechanical Structure. In *Biomechanics: Principles and Applications,* edited by R. Huiskes, D. VanCampen, and J. DeWin, pp. 75–85. Martinus Nijhoff, The Hague.

———— 1984a What Should Bones Be Designed to Do? *Calcif. Tiss. Int.* 36(Supp. 1):S7–S10.

———— 1984b Can Strains Give Adequate Information for Adaptive Bone Remodeling? *Calcif. Tiss. Int.* 36(Supp. 1):S118–S122.

———— 1984c Comparative Mechanical Properties and Histology of Bone. *Amer. Zool.* 24:5–12.

———— 1984d Effects of Differences in Mineralization on the Mechanical Properties of Bone. *Phil. Trans. R. Soc. Lond. (Biol.)* 304:509–518.

———— 1984e *The Mechanical Adaptations of Bones.* Princeton University Press, Princeton.

Dabek, J.T., B.H.B. Robinson, B.J. Thomas, K. Al-Hiti, P.W. Dykes, J.H. Fremlin, and D.A. Heath
1977 Partial Body Phosphorous by Neutron Activation Analysis and Its Clinical Applications, In *Phosphate Metabolism,* edited by S.G. Massry and E. Ritz, pp. 405–413. Plenum Press, New York.

Davidovitch, Z., J.L. Shanfield, P.C. Montgomery, E. Lally, L. Laster, L. Furst, and E. Korostoff
1984 Biochemical Mediators of the Effects of Mechanical Forces and Electric Currents on Mineralized Tissues. *Calcif. Tiss. Int.* 36(Supp. 1):S86–S97.

Dewey, J.R., G.J. Armelagos, and M.H.Bartley
1969 Femoral Cortical Involution in Three Nubian Archaeological Populations. *Hum. Biol.* 41:13–28.

Enlow, D.H.
1962a A Study of the Post-Natal Growth and Remodeling of Bone. *Am. J. Anat.* 110:79–101.

———— 1962b Functions of the Haversian System. *Am. J. Anat.* 110:269–305.

———— 1966 An Evaluation of the Use of Bone Histology in Forensic Medicine and Anthropology. In *Studies on the Anatomy and Function of Bone and Joints,* edited by F.G. Evans, pp. 93–112. Springer-Verlag, New York.

———— 1976 The Remodeling of Bone. *Yearbk. Phys. Anthropol.* 20:19–34.

Enlow, D.H. and S.O. Brown
1956 A Comparative Histological Study of Fossil and Recent Bone Tissues. Part I. *Texas J. Sci.* 8:405–443.

____
1957 A Comparative Histological Study of Fossil and Recent Bone Tissues. Part II. *Texas J. Sci.* 9:186–214.

____
1958 A Comparative Histological Study of Fossil and Recent Bone Tissues. Part III. *Texas J. Sci.* 10:187–230.

Epker, B. and H.M. Frost
1966 Periosteal Appositional Bone Growth from Age Two to Age Seventy in Man. *Anat. Rec.* 154:573–578.

Epker, B., M. Kelin, and H.M. Frost
1965 Magnitude and Location of Cortical Bone Loss in Human Ribs with Aging. *Clin. Orthopaed.* 4:198–203.

Ericksen, M.F.
1976 Cortical Bone Loss with Age in Three Native American Populations. *Am. J. Phys. Anthropol.* 45:443–452.

____
1979 Aging Changes in the Medullary Cavity of the Proximal Femur in American Blacks and Whites. *Am. J. Phys. Anthropol.* 51:563–570.

Evans, F.G.
1973 *Mechanical Properties of Bone.* Charles Thomas, Springfield.

____
1976 Age Changes in Mechanical Properties and Histology of Human Compact Bone. *Yearbk. Phys. Anthropol.* 20:57–70.

____
1980 Bone and Bones. *J. Biomech. Engr.* 104:1–5.

Evans, G.D. and S. Bang
1967 Differences and Relationships Between the Physical Properties and the Microscopic Structure of Human Femoral, Tibial and Fibular Cortical Bone. *Am. J. Anat.* 120:79–88.

Evans, F.G. and M. Lebow
1951 Regional Differences in Some of the Physical Properties of the Human Femur. *J. Appl. Physiol.* 3:563–572.

Evans, F.G. and R. Vincentelli
1969 Relation of Collagen Fibre Orientation to Some Mechanical Properties of Human Cortical Bone. *J. Biomechanics* 2:63–71.

Fleisch, H.
1980 Homeostasis of Inorganic Phosphate. In *Fundamental and Clinical Bone Physiology*, edited by M.R. Urist, pp.268–282. J.B. Lippencott, Philadelphia.

Foote, J.S.
1916 A Contribution to the Comparative Histology of the Femur. *Smithsonian Contributions to Knowledge*. 35:ix + 242 pp, 35 plates.

Frame, B., A.M. Parfitt, and H. Duncan
1973 *Clinical Aspects of Metabolic Bone Disease*. Excerpta Medica, Amsterdam.

Frankel, V.H. and M. Nordin
1980 *Basic Biomechanics of the Skeletal System*. Lea and Febiger, Philadelphia.

Frost, H.M.
1958 Preparation of Thin, Undecalcified Bone Sections by a Rapid Manual Method. *Stain Technol*. 33:272–276.

____
1960 Presence of Microscopic Cracks *In Vivo* in Bone. *Henry Ford Hosp. Bull.* 8:25–35.

____
1964 *The Laws of Bone Structure*. Charles Thomas, Springfield.

____
1969 Tetracycline-based Histological Analysis of Bone Remodeling. *Calcif. Tiss. Res.* 3:211–237.

____
1973 *Bone Modeling and Skeletal Modeling Errors*. Charles Thomas, Springfield.

____
1976a Some Concepts Crucial to the Effective Study of Bone Turnover and Bone Balance in Human Skeletal Disease and in Experimental Models of Skeletal Physiology and Pathophysiology. In *Bone Morphometry*, edited by Z.G.F. Jaworski, pp. 219–223. Univ. of Ottawa Press, Ottawa.

____
1976b The Numerical and Statistical Approach. In *Bone Morphometry*, edited by Z.F.G. Jaworski, pp. 24–34. Univ. of Ottawa Press, Ottawa.

____
1980 Skeletal Physiology and Bone Remodeling. In *Fundamental and Clinical Bone Physiology*, edited by M.R. Urist, pp. 208–241. J.P. Lippencott, Philadelphia.

____
1982 Mechanical Determinants of Bone Modeling. *Metab. Bone Dis. and Rel. Res.* 4:217–229.

———
1985 The "New Bone": Some Anthropological Potentials. *Yearbk. Phys. Anthropol.* 28:211–226.

Frost, H.M. (editor)
1981 Syposium on the Osteoporoses. *Orthopaed. Clin. N. Am.* 13:473–737.

Garn, S.M.
1970 *The Earlier Gain and Later Loss of Cortical Bone.* Charles Thomas, Springfield.

Garn, S.M., A.R. Frisancho, S.T. Sandusky and M.B. McCann
1972 Confirmation of the Sex Difference in Continuing Subperiosteal Apposition. *Am. J. Phys. Anthropol.* 36:377–380.

Garn, S.M., C.G. Rohmann, B. Wagner, and W. Ascoli
1967 Continuing Bone Growth Throughout Life: A General Phenomena. *Am. J. Phys. Anthropol.* 26:313–318.

Garn, S.M. and H.A. Shaw
1976 Extending the Trotter Model of Bone Gain and Bone Loss. *Yearbk. Phys. Anthropol.* 20:45–56.

Garn, S.M., B. Wagner, C.G. Rohman, and W. Ascoli
1968 Futher Evidence for Continuing Bone Expansion. *Am. J. Phys. Anthropol.* 28:219–222.

Gitman, L. and T. Kamholtz
1965 Incidence of Radiographic Osteoporosis in a Large Series of Aged Individuals. *J. Gerontol.* 20:32–33.

Glassman, D.M.
1985 Age Effects on Intracortical Microstructure and Cortical Thickness in Adult Saddle–Back Tamarins. *Primates.* 26:315–324.

Gonza, E.R.
1982 Biomechanics of Long Bone Injuries, In *Biomechanics of Musculoskeletal Injury,* edited by E.R. Gonza and I.J. Harrington, pp. 1–24. Williams and Wilkins, Baltimore.

Gould, S.J.
1985 The Flamingo's Smile. *Nat. Hist.* 94:6–19.

Harper, A.B., W.S. Laughlin, and R.B. Mazess
1984 Bone Mineral Content in St. Lawrence Island Eskimos. *Hum. Biol.* 56:63–77.

Hassler, C.R., E.F. Rybicki, K.D. Cummings, and L.C. Clark
1980 Quantification of Bone Stresses During Remodeling. *J. Biomechanics.*

Hayes, W.C. and B. Snyder
1981 Toward a Quantitative Formulation of Wolff's Law in Trabecular Bone. In *Mechanical Properties of Bone,* AMD–Vol. 45, edited by S.C. Cowin, pp. 43–68. American Society of Mechanical Engineers, New York.

Heaney, R.P.
1983 Prevention of Age-Related Osteoporosis in Women, In *The Osteoporotic Syndrome*, edited by L.V. Avioli, pp. 123-144. Grune and Stratton, New York.

Hert, J., P. Kucera, M. Vavra, and V. Volenik
1965 Comparison of the Mechanical Properties of Both the Primary and Haversian Bone Tissue. *Acta Anat.* 61:412-423.

Hert, J., E. Pribylova, and M. Liskova
1972 Reaction of Bone to Mechanical Stimuli. Part 3. Microstructure of Compact Bone of Rabbit Tibia After Intermittent Loading. *Acta Anat.* 82:218-230.

Hobdell, M.H. and M. Braden
1971 An Investigation into Some Diffraction Effects Observed in Microradiographic Images of Bone Sections. *Calcif. Tiss. Res.* 7:1-11.

Hoyer, H.-E., K. Flentche, and H, Lippert
1983 Osteonzahl und Bruchfestigkeit menschlicher Metakarpalia und Grundphalangen. *Z. Orthop.* 121:653-656.

Huiskes, R.
1982 On the Modelling of Long Bones in Structural Analyses. *J. Biomechanics.* 15:65-69.

Israel, H.
1968 Continuing Growth in the Human Cranial Skeleton. *Archs. Oral Biol.* 13:133-137.

Jarvis, L.R.
1981 Microdensitometry with Image Analyser Video Scanners. *J. Microscopy* 121:337-346.

Jaworski, Z.F.G.
1981 Physiology and Pathology of Bone Remodeling. *Orthop. Clin. North Am.* 12:485-512.

____
1984 Lamellar Bone Turnover System and Its Effector Organ. *Calcif. Tiss. Int.* 36(Supp. 1):S46-S55.

Johnston, Jr., C.C.
1983 Noninvasive Methods for Quantitating Appendicular Bone Mass, In *The Osteoporotic Syndrome*, edited by L.V. Avioli, pp. 73-84. Grune and Stratton, New York.

Jowsey, J.
1966 Studies of Haversian Systems in Man and Some Animals. *J.Anat.* 100:857-864.

____
1968 Age and Species Differences in Bone. *Cornell Veternarian* 58:74-94.

———
1973 Microradiography: A Morphological Approach to Quantitating Bone Turnover, In *Clinical Aspects of Metabolic Bone Disease*, edited by B. Frame, A.M. Parfitt, and H. Duncan, pp. 114–123. Excerpta Medica, Amsterdam.

Jungers, W.L. and R.J. Minns
1979 Computed Tomography and Biomechanical Analysis of Fossil Long Bones. *Am. J. Phys. Anthropol.* 50:285–290.

Katz, J.L.
1980 The Structure and Biomechanics of Bone, In *The Mechanical Properties of Biological Materials*, edited by J.F.V. Vincent and J.D. Currey, pp. 137–168. Cambridge Univ. Press, Cambridge.

———
1981 Composite Material Models for Cortical Bone, In *Mechanical Properties of Bone*, AMD–Vol. 45, edited by S.C. Cowin, pp. 171–184. American Society of Mechanical Engineers, New York.

Katz, J.L., H.S. Yoon, S. Lipson, R. Maharidge, A. Meunier, and P. Christel
1984 The Effects of Remodeling on the Elastic Properties of Bone. *Calcif. Tiss. Int.* 36(Supp. 1):S31–S36.

Kerley, E.R.
1965 The Microscopic Determination of Age in Human Bone. *Am. J. Phys. Anthropol.* 23:149–163.

Kim, J.-O.
1975 Factor Analysis, In *SPSS: Statistical Package for the Social Sciences, 2nd Ed.*, edited by N.H. Nie, C.H. Hull, J.G. Jenkins, K. Steinbrenner, and D.H. Bent, pp. 468–514. McGraw-Hill, New York.

Kimura, T. and E. Amtmann
1984 Distribution of Mechanical Robustness in the Human Femoral Shaft. *J. Biomechanics* 17:41–46.

Kimura, T. and H. Takahashi
1982 Mechanical Properties of Cross-Section of Lower Limb Bones in Jomon Man. *J. Anthrop. Soc. Nippon* 90(Supp):105–118.

Kummer, B.K.F.
1972 Biomechanics of Bone: Mechanical Properties, Functional Structure, Functional Adaptation, In *Biomechanics: Its Foundations and Objectives*, edited by Y.C. Fung, N. Perrone, and M. Anliker, pp. 237–271. Prentice-Hall, New York.

Lanyon, L.E.
1981a Adaptive Mechanics – The Skeleton's Response to Mechanical Stress, In *Mechanical Factors and the Skeleton*, edited by I.A.F. Stokes, pp. 72–82. J. Libbey, London.

———
1981b The Measurement and Biological Significance of Bone Strain *In Vivo*, In *Mechanical Properties of Bone*, AMD-Vol. 45, edited by S.C. Cowin, pp. 93–105. American Society of Mechanical Engineers, New York.

———
1984 Functional Strain as a Determinant for Bone Remodeling. *Calcif. Tiss. Int.* 36(Supp 1):S56–S61.

Lanyon, L.E., A.E. Goodship, C.J. Pye, and J.H. MacFie
1982 Mechanically Adaptive Bone Remodeling. *J. Biomechanics* 15:141–154.

Lanyon, L.E., P.T. Magee, and D.G. Baggot
1979 The Relationship of Functional Stress and Strain to the Processes of Bone Remodeling. An Experimental Study on the Sheep Radius. *J. Biomechanics* 12:593–600.

Lanyon, L.E. and C.T. Rubin
1980 Loading of Mammalian Long Bones During Locomotion. *J. Physiology* 303:72P.

———
1984 Static Vs. Dynamic Loads as an Influence on Bone Remodelling. *J. Biomechanics* 17:897–905.

Lazenby, R.A.
1985 The Interaction of Geometry and Porosity Towards Conservation of Bone Strength. Paper presented at the 13th Annual Meetings, Canadian Association for Physical Anthropology, Thunder Bay, Ontario, Dec. 4–8.

———
1986a Can Behavioral/Adaptational Inferences Be Drawn from Bone Cross-Sectional Geometry? Ms. on file with author.

———
1986b Surface Movements in Bone With Aging: What Constitutes Mechanical Compensation? Ms. in preparation, on file with author.

Lipson, S.F. and J.L. Katz
1984 The Relationship Between Elastic Properties and Microstructure of Bovine Cortical Bone. *J. Biomechanics* 17:231–240.

Lohman, T.G., M.H. Slaughter, R.A. Boileau, J. Bunt and L. Lussier
1984 Bone Mineral Measurements and Their Relation to Body Density in Children, Youth and Adults. *Hum. Biol.* 56:667–679.

Lovejoy, C.O., A.H. Burstein, and K.G. Heiple
1976 The Biomechanical Analysis of Bone Strength: A Method and Its Application to Platycnemia. *Am. J. Phys. Anthropol.* 44:489–506.

Martin, R.B.
1972 The Effects of Geometric Feedback in the Development of Osteoporosis. *J. Biomechanics* 5:447–455.

____
1975 Measuring the Moment of Inertia of Irregular Cross-Sections. *Rev. Sci. Instrum.* 46:838-839.

____
1984 Porosity and Specific Surface of Bone. *CRC Crit. Rev. Biomed. Engr.* 10:179-222.

Martin, R.B. and P.J. Atkinson
1977 Age and Sex-Related Changes in the Structure and Strength of the Human Femoral Shaft. *J. Biomechanics* 10:223-231.

Martin, R.B. and D.B. Burr
1982 A Hypothetical Mechanism for the Stimulation of Osteonal Remodelling by Fatigue Damage. *J. Biomechanics* 15:137-139.

____
1984 Mechanical Implications of Porosity Distribution in Bones of the Appendicular Skeleton. (Abstract). Paper presented at the 30th Annual ORS Meetings, Atlanta, Georgia, Feb. 7-9. *Othopaed. Trans.* 8:342-343.

Martin, R.B., D.B. Burr, and M.B. Schaffler
1985 Effects of Age and Sex on the Amount and Distribution of Mineral in Eskimo Tibiae. *Am. J. Phys. Anthropol.* 67:371-380.

Martin, R.B., J.C. Pickett, and S. Zinaich
1980 Studies of Skeletal Remodeling in Aging Men. *Clin. Orthopaed.* 149:268-282.

Mather, B.S.
1967 The Symmetry of the Mechanical Properties of the Human Femur. *J. Surg. Res.* 7:222-225.

Mazess, R.B.
1982 On Aging Bone Loss. *Clin. Orthopaed.* 165:239-252.

Meade, J.B., S.C. Cowin, J.J. Klawitter, W.C. Van Buskirk, and H.B. Skinner
1984 Bone Remodeling Due to Continuously Applied Loads. *Calcif. Tiss. Int.* 36 (Supp 1): S25-S30.

Minns, R.J., A. Atkinson, and F.S. Steven
1983 The Role of Calcium in the Mechanical Behavior of Bone. *Phys. Med. Biol.* 28:1057-1066.

Moyle, D.D. and R.W. Bowden
1984 Fracture of Human Femoral Bone. *J. Biomechanics* 17:203-213.

Nagurka, M.L. and W.C. Hayes
1980 An Interactive Graphics Package for Calculating Cross-Sectional Properties of Complex Shapes. *J. Biomechanics* 13:59-64.

Neuman, W.F.
1980 Bone Material and Calcification Systems, In *Fundamental and Clinical Bone Physiology*, edited by M.R. Urist, pp. 83-107. J.B. Lippencott, Philadelphia.

Nicolini, C., F. Kendall, and W. Giaretti
1977 Objective Identification of Cell Cycle Phases and Subphases by Automated Image Analysis. *Biophys. J.* 19:163–176.

Nordin, B.E.C.
1983 Osteoporosis, with Particular Reference to the Menopause, In *The Osteoporotic Syndrome*, edited by L.V. Avioli, pp. 13–43. Grune and Stratton, New York.

Nordin, M. and V.H. Frankel
1980 Biomechanics of Whole Bones and Bone Tissue, In *Basic Biomechanics of the Skeletal System*, edited by V.H. Frankel and M. Nordin, pp. 15–60. Lea and Febiger, Philadelphia.

O'Conner, J.A., L.E. Lanyon, and H. MacFie
1982 The Influence of Strain Rate on Adaptive Bone Remodelling. *J. Biomechanics* 15:767–781.

Oxnard, C.E.
1971 Tensile Forces in Skeletal Structures. *J. Morphology* 134:425–436.

____
1975 *Uniqueness and Diversity in Human Evolution: Morphometric Studies of Australopithecines.* Univ. of Chicago Press, Chicago.

Parfitt, A.M.
1984a The Cellular Basis of Bone Remodeling: The Quantum Concept Reexamined in Light of Recent Advances in the Cell Biology of Bone. *Calcif. Tiss. Int.* 36 (Supp 1): S37–S45.

____
1984b Age-Related Structural Changes in Trabecular and Cortical Bone: Cellular Mechanisms and Biomechanical Consequences. *Calcif. Tiss. Int.* 36(Supp 1):S123–S128.

Paul, J.S.
1971 Load Actions on the Human Femur in Walking and Some Resultant Stresses. *Exp. Mech.* 11:121–125.

Perzigian, A.J.
1973 Osteoporotic Bone Loss in Two Prehistoric Indian Populations. *Am. J. Phys. Anthropol.* 39:87–96.

Phillips, H.B., S. Owen-Jones, and B. Chandler
1978 Quantitative Histology of Bone: A Computerized Method of Meauring the Total Mineral Content of Bones. *Calcif. Tiss. Res.* 26:85–89.

Pinto, M.R., J.P. Gorski, and P.J. Kelly
1984 Age-Related Changes in Composition and Ca ^{2} Binding Capacity of Canine Cortical Bone. *Orthop. Trans.* 8:294–295.

Plato, C.C., W.W. Greulich, R.M. Garruto, and R. Yanagihara
1984 Cortical Bone Loss and Measurements of the Second Metacarpal Bone. II. Hypodense Bone in Postwar Guamian Children. *Am. J. Phys. Anthropol.* 63:57–63.

Plato, C.C. and F.E. Purifoy
1982 Age, Sex and Bilateral Variability in Cortical Bone Loss and Measurements of the Second Metacarpal. *Growth* 46:100–112.

Popov, E.P.
1978 *Mechanics of Materials.* Prentice–Hall, Englewood Cliffs.

Quekett, J.
1849 On the Intimate Structure of Bone as Composing the Skeleton in the Four Great Classes of Animals, viz. Mammals, Birds, Reptiles and Fishes. *Trans. Royal Microscop. Soc. (London)* 2:46–58.

Reilly, D.T. and A.H. Burstein
1974 The Mechanical Properties of Cortical Bone. *J. Bone Jt. Surg.* 56(A):1001–1022.

Ries, W.L., J.K. Gong, and M.W. Sholley
1985 A Comparative Study of Osteoblasts: In Situ Versus Isolated Specimens. *Am. J. Anat.* 172:57–73.

Roesler, H.
1981 Some Historical Remarks on the Theory of Cancellous Bone Structure (Wolff's Law), In *Mechanical Properties of Bone*, AMD–Vol. 45, edited by S.C. Cowin, pp. 27–42. American Society of Mechanical Engineers, New York.

Rubin, C.T.
1984 Skeletal Strain and the Functional Significance of Bone Architecture. *Calcif. Tiss. Int.* 36(Supp 1):S11–S18.

Rubin, C.T. and L.E. Lanyon
1984 Dynamic Strain Similarity in Vertebrates – An Alternative to Allometric Limb Bone Scaling. *J. Theoret. Biol.* 107:321–327.

Ruff, C.B.
1984 Allometry Between Length and Cross–Sectional Dimensions of the Femur and Tibia in *Homo sapiens sapiens. Am. J. Phys. Anthropol.* 65:347–358.

Ruff, C.B. and W.C. Hayes
1982 Subperiosteal Expansion and Cortical Remodeling of the Human Femur and Tibia with Aging. *Science* 217:945–948.

________ 1983a Cross–Sectional Geometry of Pecos Pueblo Femora and Tibiae – A Biomechanical Investigation. I. Method and General Patterns of Variation. *Am. J. Phys. Anthropol.* 60:359–381.

________ 1983b Cross–Sectional Geometry of Pecos Pueblo Femora and Tibiae – A Biomechanical Investigation. II. Sex, Age and Side Differences. *Am. J. Phys. Anthropol.* 60:383–400.

________ 1984a Bone Mineral Content in the Lower Limb. *J. Bone Jt. Surg.* 66(A):1024–1031.

———— 1984b Age Changes in Geometry and Mineral Content of the Lower Limb Bones. *Ann. Biomed. Engr.* 12:573–584.

Ruff, C.B. and H.H. Jones
1981 Bilateral Asymmetry in Cortical Bone of the Humerus and Tibia – Sex and Age Factors. *Hum. Biol.* 53:69–86.

Ruff, C.B., C.S. Larsen, and W.C. Hayes
1984 Structural Changes in the Femur with the Transition to Agriculture on the Georgia Coast. *Am. J. Phys. Anthropol.* 64:125–136.

Rummel, R.J.
1970 *Applied Factor Analysis.* Northwestern University Press, Evanston.

Rybicki, E.F., F.A. Simonen, and E.B. Weis, Jr.
1972 On the Mathematical Analysis of Stress in the Human Femur. *J. Biomechanics* 5:203–215.

Saha, S. and W.C. Hayes
1977 Relations Between Tensile Impact Properties and Microstructure of Compact Bone. *Calcif. Tiss. Res.* 24:65–72.

Saunders, S.
1985 Surface and Cross-Sectional Comparisons of Bone Growth Remodeling. *Growth* 49:105–130.

Sawicki, W., J. Rowinski, and J. Abramczuk
1974 Image Analysis of Chromatin in Cells of Preimplantation Mouse Embryos. *J. Cell Biol.* 63:227–233.

Schaffler, M.B. and D.B. Burr
1984 Primate Cortical Bone Microstructure: Relationship to Locomotion. *Am. J. Phys. Anthropol.* 65:191–197.

Simon, M.R., K.R. Holmes, and A.M. Olsen
1984 The Effects of Quantified Amounts of Increased Intermittent Compressive Forces for 30 and 60 Days on the Growth of Limb Bones in the Rat. *Acta Anat.* 120:173–179.

———— 1985a Effects of Simulated Increases in Body Weight on the Growth of Limb Bones in Hypophysectomized Rats. *Acta Anat.* 121:1–6.

———— 1985b Bone Mineral Content of Limb Bones of Male Weanling Rats Subjected to 30 and 60 Days of Simulated Increases in Body Weight. *Acta Anat.* 121:7–11.

———— 1985c Effects of Simulated Increase in Body Weight from Birth on the Growth of Limb Bones in Rats. *Acta Anat.* 121:12–16.

Simonet, W.T. and P.J. Kelly
1984 A Comparison of Metabolic Activity in Cortical and Cancellous Bone Related to Age. *Orthop. Trans.* 8:295–296.

Singh, I.J. and D.L. Gunberg
1970 Estimation of Age at Death in Human Males from Quantitative Histology of Bone Fragments. *Am. J. Phys. Anthropol.* 33:373–382.

Smith, C.B. and D.A. Smith
1976 Relations Between Age, Mineral Density and Mechanical Properties of Human Femoral Compacta. *Acta Orthopaed. Scand.* 47:496–502.

Smith, Jr, E.L.
1971 *Bone Changes with Age and Physical Activity.* Unpublished Ph.D. dissertation, University of Wisconsin.

Smith, J.M. and W.S.S. Jee
1983 Automated Skeletal Histomorphometry, In *Bone Histomorphometry: Techniques and Interpretations*, edited by R.R. Recker, pp. 286–296. CRC Press, Boca Raton.

Smith, Jr., R.W. and R.R. Walker
1964 Femoral Expansion in Aging Women: Implications for Osteoporosis and Fractures. *Science* 145:156–157.

Sokal, R.R. and F.J. Rohlf
1969 *Biometry.* W.H. Freeman, San Francisco.

Sutton, R.A. and E.C. Cameron
1985 Osteoporosis: Prevention and Treatment. *B.C. Med. J.* 27:137–139.

Takahashi, H.
1982 An Examination of the Conformity of the Orientation of Bone Trabeculae to the Directions of Principal Stress in the Case of the Proximal End of the Femur. *J. Anthrop. Soc. Nippon* 90:53–60.

Thompson, D.D.
1979 The Core Technique in the Determination of Age at Death in Skeletons. *J. Forensic Sci.* 24:902–915.

____
1980 Age Changes in Bone Mineralization, Cortical Thickness, and Haversian Canal Area. *Calcif. Tiss. Int.* 31:5–11.

Treharne, R.W.
1981 Review of Wolff's Law and Its Proposed Means of Operation. *Orthopaed. Rev.* 10:35–47.

Van Gerven, D.P.
1973 Thickness and Area Measurements as Parameters of Skeletal Involution of the Humerus, Femur and Tibia. *J. Gerontology* 28:40–45.

Van Gerven, D.P. and G.J. Armelagos
1970 Cortical Involution in Prehistoric Mississippian Femora. *J. Gerontology* 25:20–22.

Vaughn, J.
1976 *The Physiology of Bone, 2nd ed.*. Clarendon Press, Oxford.

Villaneuva, A.R.
1976 Methods of Preparing and Interpreting Mineralized Sections of Bone, in *Bone Morphometry*, edited by Z.F.G. Jaworski, pp. 341–353. Univ. of Ottawa Press, Ottawa.

Vincentelli, R. and F.G. Evans
1971 Relations Among Mechanical Properties, Collegen Fibres and Calcification in Adult Human Cortical Bone. *J. Biomechanics* 4:193–201.

Vincentelli, R. and M. Grigorov
1985 The Effect of Haversian Remodeling of the Tensile Properties of Human Cortical Bone. *J. Biomechanics* 18:201–207.

Vose, G.P. and A. Engel
1973 Relationship of Radiographic Cortical Thickness Vs. Age in Thirteen Bones of the Hand. *J. Gerontology* 28:46–49.

Wainwright, S.A., W.D. Biggs, J.D. Currey and J.M. Gosline
1976 *Mechanical Design in Organisms.* J. Wiley, New York.

Wall, J.C., S.K. Chatterji, and J.W. Jeffery
1979 Age-Related Changes in the Density and Tensile Strength of Human Femoral Cortical Bone. *Calcif. Tiss. Int.* 27:105–108.

Welch, D.O.
1970 The Composite Structure of Bone and Its Response to Mechanical Stress. *Recent Adv. Engr. Sci.* 5:245–262.

Whedon, G.D.
1984 Disuse Osteoporosis: Physiological Aspects. *Calcif. Tiss. Int.* 36(Supp 1): S146–S150.

Woo, S.L.Y.
1981 The Relationships of Changes in Stress Levels on Long Bone Remodeling, In *Mechanical Properties of Bone,* AMD–Vol. 45, edited by S.C. Cowin, pp. 107–130. American Society of Mechanical Engineers, New York.